INDUCT DISSIPATIVE BAR-SILENCER DESIGN

by

Aaron Grey

A thesis submitted in
fulfilment of the requirements for the
Degree of Masters of Engineering

in the

Department of Mechanical Engineering
University of Canterbury
Christchurch, New Zealand

March, 2004

ABSTRACT

The aim of this project was to investigate the performance of bar-silencers in ventilation ducts, with and without mean flow. The goal of which was to determine a product which could be used on its own or in conjunction with current traditional methods for induct sound attenuation.

A literature review was conducted on induct sound attenuation and bar-silencers. A test facility was established in the Department of Mechanical Engineering, University of Canterbury. Modifications were made to an existing fan and duct rig to align it with ISO 7235 (1991) - Measurement procedures for ducted silencers - Insertion loss, flow noise and total pressure loss.

A number of bar-silencers were tested in the test facility to determine both their insertion loss and pressure loss characteristics. Bar-silencers which varied in thickness, (such as, triangular shaped silencers) were confirmed to have an insertion loss across a greater range of frequencies, but lower peak absorption than ducting lined on two sides.

It was found that the bar-silencers would not be a cost effective method of sound attenuation on their own, due to less effective noise absorption, higher material costs and higher pressure losses, than traditionally lined sections of ducting. However, the bar-silencers could be used in conjunction with traditional methods of sound attenuation to increase the attenuation or in low flow velocity ventilation exits where pressure losses are reduced.

ACKNOWLEDGMENTS

I would like to express my gratitude to my supervisors, Dr John Pearse and Professor Cliff Stevenson, whose expertise, understanding, and patience, added considerably to my graduate experience. Without their guidance and support, I would never have been able to complete the project on time.

Mr Mike Latimer and the crew at Latimer Acoustics, for supplying materials, friendly faces and advice on the testing program.

Also to my parents, who provided the item of greatest worth - opportunity. Thank you for standing by me through the many trials and decisions of my educational career.

Fellow students and friends in the Department, especially Andrew, who has made me laugh and kept me sane during the year. Lastly, I would like to thank Carmen for helping me make the decision to stay and complete a Masters.

TABLE OF CONTENTS

LIST OF FIGURES

LIST OF TABLES

NOMENCLATURE

Unless otherwise stated the symbols are defined as below.

V_a	*Air volume*
V_T	*Total volume of porous material*
ϕ	*Porosity, the volume fraction of the air volume (V_a) to the total volume of porous material (V_T)*
k or Γ	*Material structure constant*
σ	*Material resistance constant*
M	*Mass density of a material*
ρ'	*Mass density of the material which forms a porous structure*
D_h	*Dissipation of acoustical energy per unit volume*
ω	*Angular frequency*
κ_i	*Imaginary part of the complex compressibility constant*
Z_c	*Characteristic impedance*
ρ_0	*Density of air*
c_0	*Speed of sound*
f	*Frequency*
X	*Dimensionless parameter* $\left(=\frac{\rho_0 \cdot f}{\sigma}\right)$
U	*Average fluid flow velocity*
R	*Total normalized flow resistance*
γ	*Specific heat ratio* $(=C_p/C_v)$
L	*Absorber thickness*
λ	*Free field wavelength*
$p_i(\omega)$	*Complex amplitudes of sound*
$u(\omega)$	*Complex amplitude of the velocity for a given angular frequency (ω)*
γ_z and γ_y	*Lining propagation constants in the z and y-directions*
Z_y	*Lining characteristic impedance in the y-direction*
α_i	*Individual material absorption coefficients*

1

INTRODUCTION AND LITERATURE REVIEW

1.1 MOTIVATION

With an increasing number of both domestic and industrial buildings utilising air-conditioning systems, there is demand for cost-effective, easily installed and maintained systems for noise control. Most modern building codes include considerations for air-conditioning sound levels requiring both architects and engineers to achieve low noise levels while still delivering the heating and ventilation required. The induct sound reduction (attenuation) is directed towards minimising fan, fan motor and air-movement noise.

1.2 OBJECTIVE AND SCOPE

The primary objective of this investigation was to use realistic prediction methods, coupled with empirical data, to obtain a better understanding of the insertion loss of ‘bar-silencers’ with different cross sections in rectangular ducts. This study focuses on the development of

bar-silencers as a viable alternative for induct sound attenuation. The study considers three areas:

- The acoustic performance of bar-silencers in rectangular ducts with and without a mean fluid flow.

- The development of prediction techniques, which will express both the insertion, and pressure losses for bar-silencers.

- The development of design guidelines for the application of induct bar-silencers.

The duct rig used in the tests was constructed and tested to ISO 7235:1991.

1.3 LITERATURE REVIEW

The literature review identified and considered previous work on induct sound attenuation. This review provided background for this thesis and was carried out to gather knowledge on duct absorber theory as well as empirical duct attenuation data in order to ascertain the performance of existing absorber technologies. The survey considered the current methods of induct absorption, the absorbing medium, the effect of a mean fluid flow, bar-silencers and the performance of duct attenuators.

Noise sources in ducting systems usually originate from the fan and drive motor, generally for centrifugal fans (as used in the test rig for this thesis, see Chapter 2) the highest spectra levels are at lower frequencies (Sharland 1990). Secondary noise sources are generated by turbulence as the mean flow incurs obstacles such as bends, rough wall surfaces, grates and fittings. These secondary noise sources increase with increasing mean flow velocity. The noise generated has two general transmission paths as described by Sharland (1990), 'duct-borne', and 'flanking'. Duct-borne noise propagates with the fluid along the ducts, while flanking occurs when noise emanates from the ducting via mechanical vibration or breakout and returns to the duct downstream. Flanking transmission is an important phenomenon in a number of applications in building acoustics, and can be a limiting factor in the performance of duct silencers.

1.3.1 Types of induct attenuation

Years of research and investigation into induct noise attenuation in air-conditioning systems have led to many methods and theories. Currently there are three main groups of induct attenuation: passive isotropic (bulk reacting) / non-isotropic (locally reacting) liners, pod / splitter type absorbers, and active attenuators.

- Passive bulk / locally reacting liners are the widely accepted and implemented method of sound attenuation in ducting. They line part or the whole of a finite length of ducting (Figure 1.1). An added benefit of lining duct walls with material is the thermal insulation that it provides.

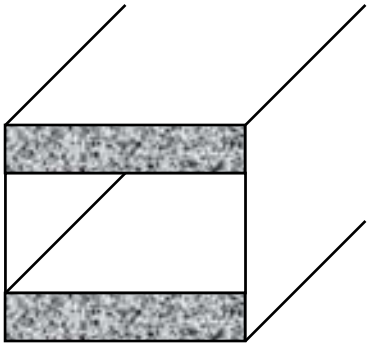

FIGURE 1.1: DUCT WITH TWO SIDES LINED WITH ABSORBING MATERIAL

A variety of materials are used as the absorbing medium. It is currently general practice in Australasia to use a porous absorber such as fibreglass, polyester or polymer based foam as the absorbing material.

- Pod / splitter type absorbers are surrounded by the mean fluid flow. Pod absorbers (Figure 1.2a) are centrally located circular bars of material running along the length of a circular duct. Splitters are one or more horizontally or vertically mounted flow dividers (Figure 1.2b).

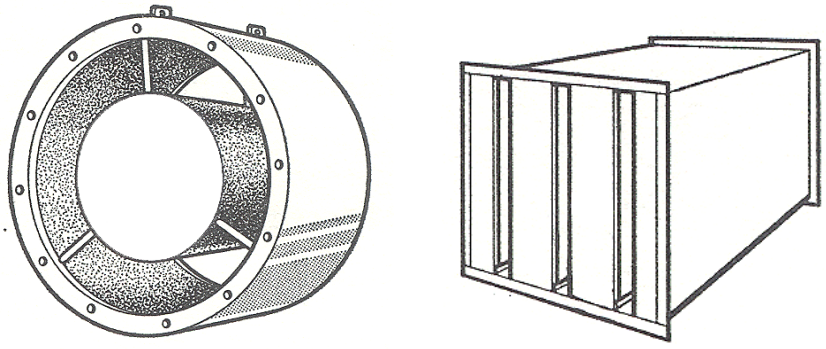

(A) (B)

FIGURE 1.2: POD ABSORBERS FOR CIRCULAR DUCTING (A), SPLITTERS FOR SQUARE / RECTANGULAR DUCTING (B)

These methods of duct absorbers provide greater attenuation than a purely lined section of duct due to the greater exposed area of absorbent. However, this comes at the price of flow resistance causing a greater pressure drop across the attenuating section. Pod and splitter absorbers may also be a source of noise within the duct as both produce turbulence, a source of noise. For this reason pods and splitters tend to be aerodynamically shaped to reduce both the drag and self generated noise. Both pod and splitter absorbers can be used in parallel with bulk and locally reacting duct liners and utilise the same absorbing medium.

- More recently, investigation and research has focused on active attenuators. This is due to the effectiveness of active attenuators at low frequencies in comparison to passive absorbers. First patented in 1934, active noise control systems are implemented by use of a microphone that detects the noise as it propagates down the duct. A digital signal processing (DSP) controller processes this microphone signal, determines a cancelling waveform and introduces this signal through a loudspeaker. A second microphone is used to apply either feedforward or feedback control for error correction. The attenuators show improved performance at lower frequencies (Kruger 2002) with attenuation of 12-20 dB between 40 Hz and 160 Hz (Goodman et al. 1992). With increased interest, the costs of such systems have dropped over the last decade from approximately 10,000 US$ to less than 1,500 US$ per system (Wise et al. 2000). However, these active attenuators introduce complexity, have increased installation requirements, and increased initial outlay and ongoing running costs compared to the more traditional attenuation methods.

1.3.2 Absorbing medium

Porous materials are the most common medium for attenuation in ducted systems. They consist of a network of interlocking air filled pores that allow the fluid to flow into a cellular structure where sound energy is converted into heat. Initially, there is the viscous loss as the sound waves propagate through the material. There is also the damping of the material. Damping refers to the capacity of the material to dissipate energy. Thicker materials generally show greater damping. Typical examples of porous absorbers are fibreglass, fibreboard, mineral wool, polyester and polymer based foams. They are primarily effective at mid to high frequencies.

Absorbing materials are either bulk reacting, meaning the absorption of an acoustic wave propagating through the material is independent of direction; or locally reacting, where the absorption is dependent on the direction. Fibrous absorbers are typically anisotropic (locally reacting) with the fibres in planes parallel to the surface of the material while the majority of foams are isotropic (bulk reacting). Non-isotropic behaviour can be due to the basic structure of the material or artificial such as with the use of partitions. In the case of duct linings, it was found that the optimum attenuation of the fundamental mode was achieved by non-isotropic absorbers with lower axial flow resistance which increased with increasing frequency (Kurze and Ver 1972).

The absorption characteristics of porous materials have been attributed to different properties of the material including flow resistance, porosity, mass density, heat

conductivity, and structure factor. Many of these are not independent parameters and influence each other greatly, however each has been considered individually below.

Porosity

Porosity (ϕ) is the volume fraction of the air volume V_a to the total volume of porous material V_T.

$$\phi = \frac{V_a}{V_T} \tag{1.1}$$

Only the volume of air which is not locked within the frame structure of the material must be considered in V_a. For example in foam materials, the voids (cells) can be open or closed. Although generally partially ignored as ϕ lies very close to unity for most fibrous and foam materials, ϕ does have an effect on the equations of continuity and motion (*Equations 1.2 and 1.3*) (Zwikker and Kosten 1949):

$$-\frac{\partial v}{\partial x} = \frac{\phi}{\rho_o} \cdot \frac{\delta \rho}{\delta p} \cdot \frac{\partial p}{\partial t} \tag{1.2}$$

$$-\frac{\partial p}{\partial x} = \frac{k}{\phi} \cdot \rho_o \cdot \frac{\partial v}{\partial t} \cdot \sigma \cdot v \tag{1.3}$$

where ϕ is porosity, ρ_0 is density of fluid medium (air), k is a structure constant and σ is a resistance constant. The resistance constant takes into account the viscosity of the fluid. For

the steady flow state the $\partial v/\partial t$ term cancels out, so that σ is defined as the ratio of pressure gradient and velocity of volume displacement.

Mass density

The mass density is the mass per unit volume of the material frame. It is related to the porosity through:

$$M = \rho'(1-\phi) \tag{1.4}$$

where M is the mass density of the material, ϕ is the porosity and ρ' is the mass density of the material which forms the porous structure. Only for a flexible material does the mass density have an effect, these effects are limited and can only be seen below 200 Hz where interaction between the sound waves and the material may induce oscillatory motions. Motion from the material will influence both the resistive and reactive part of the flow impedance and the structure factor of the material.

Structure factor

The structure factor (k or Γ), takes into consideration the pores and cavities that are perpendicular to the propagation direction of the travelling wave. It is a quantitative measure of the difficulty in accelerating the fluid within the porous material as opposed to in the free field. This is due to changes in flow direction, and viscous interaction forces. The structure factor can be accounted for in terms of an equivalent mass density of the fluid which is larger than the free field density by a factor typically between 1.2 and 2.0 (Ingard 1994).

Heat conductivity

Heat conduction has two effects on the absorption of a porous material. The first being power conversion from acoustic energy into heat which is described by the dissipation per unit volume:

$$D_h = \omega \cdot \kappa_i \cdot |p|^2 \tag{1.5}$$

where ω is the angular frequency $(\omega = 2\pi f)$ and κ_i is the imaginary part of the complex compressibility constant (Ingard, 1994). The second effect deals, more importantly, with the fact that compressibility will be isothermal. At sufficiently low frequencies, heat conduction makes the conditions within the material isothermal (as opposed to isentropic in free field) and thus increases the compressibility of the air with the material. This reduces the reactive part (dominant at low frequencies) of the input impedance, which increases the velocity amplitude and viscous dissipation.

Flow resistance

As stated, the absorption characteristics of porous materials have tried to be attributed to different properties of the material, the flow resistance is accepted as being the most significant factor. Delany and Bazley (1970) measured the complex wave number (k) and the characteristic impedance (Z_c) for a number of frequencies for a range of fibrous materials with porosity close to 1.0. They found that k and Z_c depend mainly on the angular frequency (ω) and on the flow resistivity (σ) of the material and proposed the following power law expressions to fit the measured data:

$$Z_c = \rho_0 \cdot c_0[1 + 0.0571 \cdot X^{-0.754} - j \cdot 0.087 \cdot X^{-0.732}] \tag{1.6}$$

$$k = \frac{\omega}{c_0}[1 + 0.0978 \cdot X^{-0.7} - j \cdot 0.189 \cdot X^{-0.595}] \tag{1.7}$$

where ρ_0 and c_0 are the density of air and the speed of sound respectively, X is a dimensionless parameter equal to:

$$X = \frac{\rho_0 \cdot f}{\sigma} \tag{1.8}$$

f being the frequency related to ω by $\omega = 2\pi f$. Delany and Bazley suggested limits for the validity of their laws in terms of the boundaries of X: $0.01 < X < 1.0$. Bies and Hansen (1979) later also presented that, for a porous material, the flow resistance was sufficient to typify its acoustical performance. The steady state flow resistance (σ) is defined as the ratio between the static pressure drop (ΔP) across the layer and the average velocity (U) of steady flow through the layer thickness (t).:

$$\sigma = -\frac{\Delta P}{U \cdot t} \tag{1.9}$$

The units of flow resistance are *rayl* [MKS rayls ($N \cdot s \cdot m^{-3}$) or ($N \cdot s \cdot m^{-4}$) per metre]. For a given porous material, the flow resistance can be considered independent of the flow speed only at sufficiently low speeds and generally increases with increasing flow velocity. Absorbers of different flow resistance obtained attenuation peaks at different frequencies, and thus an optimum flow resistance can only be found for particular frequency bands. This

was confirmed by a study into theoretical absorption by Ingard (1994) which gave an optimum value of the total normalized flow resistance by:

$$R = \frac{3}{\phi \cdot \gamma \cdot k \cdot L} \approx \frac{0.34}{\phi \cdot \left(L / \lambda \right)} \tag{1.10}$$

where ϕ is the porosity (value of 0.95 used), k ($= 2\pi f / c$) is the wave number, γ ($= C_p / C_v$) the specific heat ratio, L is the absorber thickness and λ is the free field wavelength. Ingard stated that this relationship was not consistent with the condition $R \cdot k \cdot L << 1$ so can only be used as a rough guide. He also stated that from an acoustical standpoint the absorption characteristics of a material are dominated by the thickness and flow resistance, with other factors of the material such as porosity, mass density and heat conductivity being less important. However some of these factors are dependent on each other. A more useful measure may be the (flow) impedance of the material, which combines the flow resistance and a structure factor of the material in an oscillatory flow such as in a sound wave. The impedance of material is defined as:

$$z_f(\omega) = \frac{[p_1(\omega) - p_2(\omega)]}{u(\omega)} \tag{1.11}$$

where $p_1(\omega)$ and $p_2(\omega)$ are the complex amplitudes of the sound on either side of the material and $u(\omega)$ is the complex amplitude of the velocity for a given angular frequency (ω). The oscillatory resistance increases slowly with frequency due to the frequency dependence of the viscous boundary layer thickness.

Facings

Thin facings can be applied to absorbers to modify or tune the attenuation characteristics of an absorbing material. In duct systems, coverings are generally either a thin metal sheet with an array of holes effectively producing a Helmholtz cavity absorber with a narrow band of peak absorption or a fabric covering, creating a multi-layered absorber. These facings are also used to protect ducted airflow from being contaminated with fibre particles from the bulk materials such as fibreglass where there are health regulations or user demands.

1.3.3 Fluid flow

The velocity of a wave propagating in a moving medium remains relative to that medium. Therefore, relative to a stationary frame of reference, the wave travels at:

$$b = U + a \tag{1.12}$$

where, b is the absolute velocity of the wave; U is the velocity of the medium and a is the relative velocity between the wave and medium (Munjal 1987). The mean flow not only affects the propagation of waves by convection but also by a refractive phenomenon. At the boundary layer of a flow, the free stream velocity decreases to zero in a short distance. As a result of the variation in wave speed through the boundary layer, refraction will occur. The sound will be refracted towards the boundary layer if the sound wave is travelling with the mean fluid flow or alternatively away if against the flow. As the waves are refracted the angle of incidence at which the waves interact with the absorbing medium will change, since the acoustic absorption coefficient generally depends on the angle of incidence the

flow will affect the absorption (Ingard 1994). If the sound propagates with the mean flow, the time the sound is exposed to any absorbent is reduced and visa-versa.

This refractive phenomenon was investigated in a mathematical study of acoustic plane waves propagating with a fluid flow through a duct (Pridmore-Brown 1958). Considering cases where the shear layer had a constant velocity gradient, and where the shear layer was turbulent by using a $^{1}/_{7}^{th}$ power law relationship. Pridmore-Brown showed that plane waves are diffracted by the velocity profile that is created at the boundary layer of a wall; waves tended to be diffracted towards the walls (or absorbing medium). This effect was more prominent at higher frequencies. He used his findings to estimate the effect of fluid flow on the sound attenuation in a duct with absorbing material on the side walls. It showed the effect of flow to increase attenuation at higher frequencies but to diminish that of lower frequencies.

Empirical data on ducts with two sides lined has shown that if the propagating wave is travelling with the mean flow then the attenuation at high frequencies will increase while lower frequency absorption will shift to the right and be reduced (Figure 1.3). This trend is reversed when the wave travels against the mean flow (Figure 1.4).

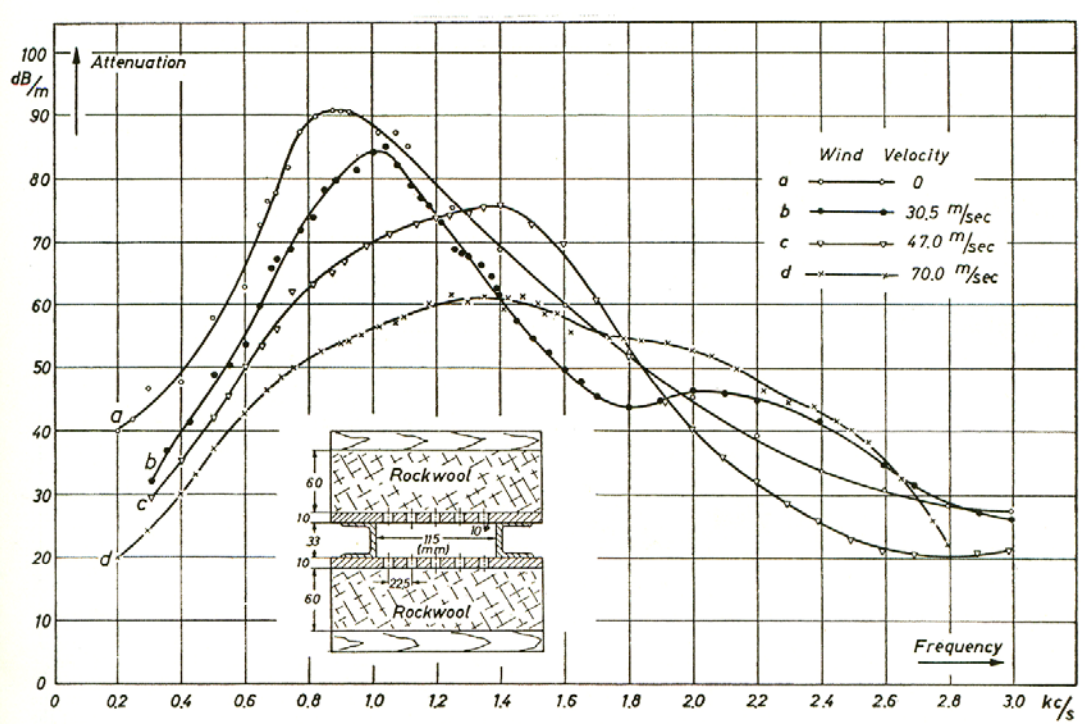

FIGURE 1.3: FORWARD-MOVING WAVES IN A DUCT LINED WITH ROCKWOOL OVER PERFORATED GYPSUM PANELS (MEYER ET AL. 1958)

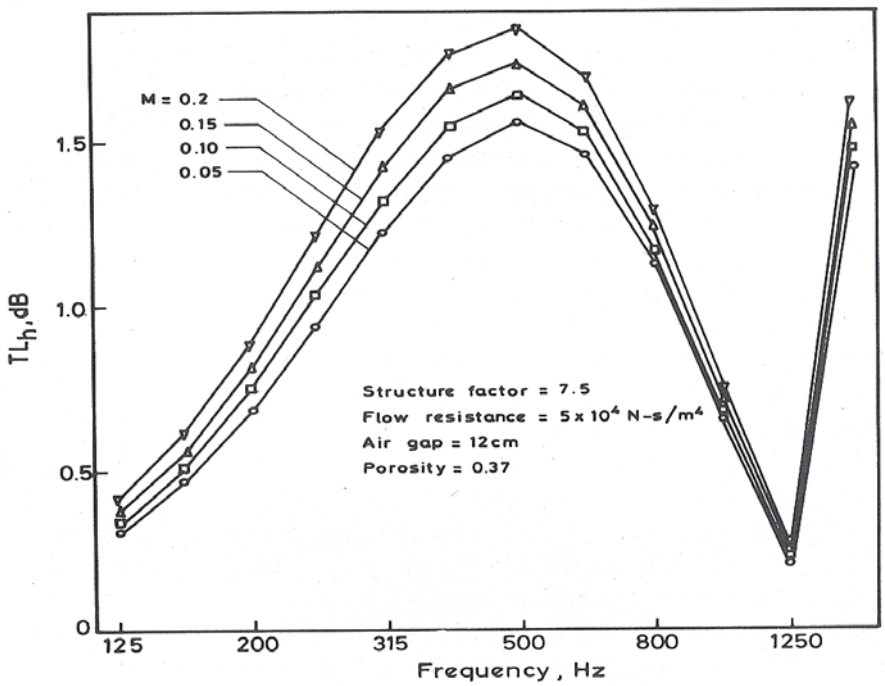

FIGURE 1.4: BACKWARDS-MOVING WAVES IN SQUARE DUCTS LINED WITH POROUS CERAMIC TILES, AT DIFFERENT VALUES OF MEAN-FLOW MACH NUMBER (M) (SHIRAHATTI 1985)

This effect has also been shown in splitter silencers by means of finite element computation (Cummings and Sormaz 1992), they also showed the variation in phase speed of the propagating wave travelling with or against the mean flow. Simulation by finite element methods and then confirmed by experiment (Cummings and Astley 1996) with bar-silencers again confirmed the effect of mean flow on attenuation.

The effects of the mean flow are not limited to the insertion loss of absorbers but also the generation of noise due to the mean flow. Any obstruction or fitting within the duct, which disturbs the flow, is capable of generating noise (ESDU-Engineering-Sciences-Data 1981). Even without fittings, surface-induced noise is generated by the fluid flowing over the duct walls although this noise source is usually negligible compared with noise induced by fittings. These sources of noise increase with increasing mean flow velocity.

1.3.4 Bar-silencers

The idea that square-section prisms or bars of absorbent could be mounted in an array over the cross-section of a duct (Figure 1.5) initially came from Nilsson and Söderqvist (1983).

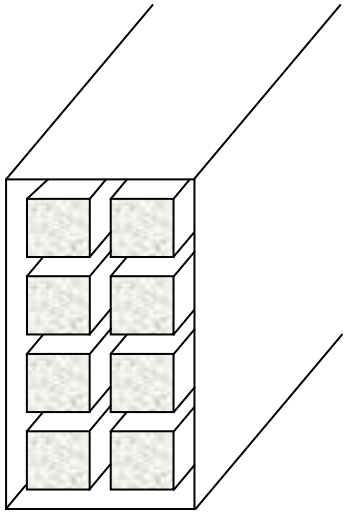

FIGURE 1.5: BAR SILENCER ARRAY IN RECTANGULAR DUCTING AS TESTED BY NILSSON AND SÖDERQVIST

They claimed the bar-absorbers had greater attenuation at both low and high frequencies then that of an equivalent splitter silencer (Figure 1.6). Attributing the high performance of the silencers to:

- *A constriction effect:* At low frequencies, the sound field in the silencer induces cylindrical waves within the silencers. As the sound penetrates each bar, it has to travel through gradually decreasing cylindrical areas, causing the particle velocity to decrease and sound pressure to increase. If the sound-absorbing material is optimised to utilize this effect, then a considerable increase in low-frequency attenuation will result.

- *A diagonal effect:* Sound waves enter the absorbing material via the corners, thus the acoustically effective thickness of the material then becomes ~20% greater than in a splitter-type silencer with the same baffle width.

- *A slot effect:* The absorber geometry results in shorter distances between sound-absorbing surfaces and a greater area of sound-absorbing material exposed to the sound field. This results in better attenuation results, particularly at higher frequencies.

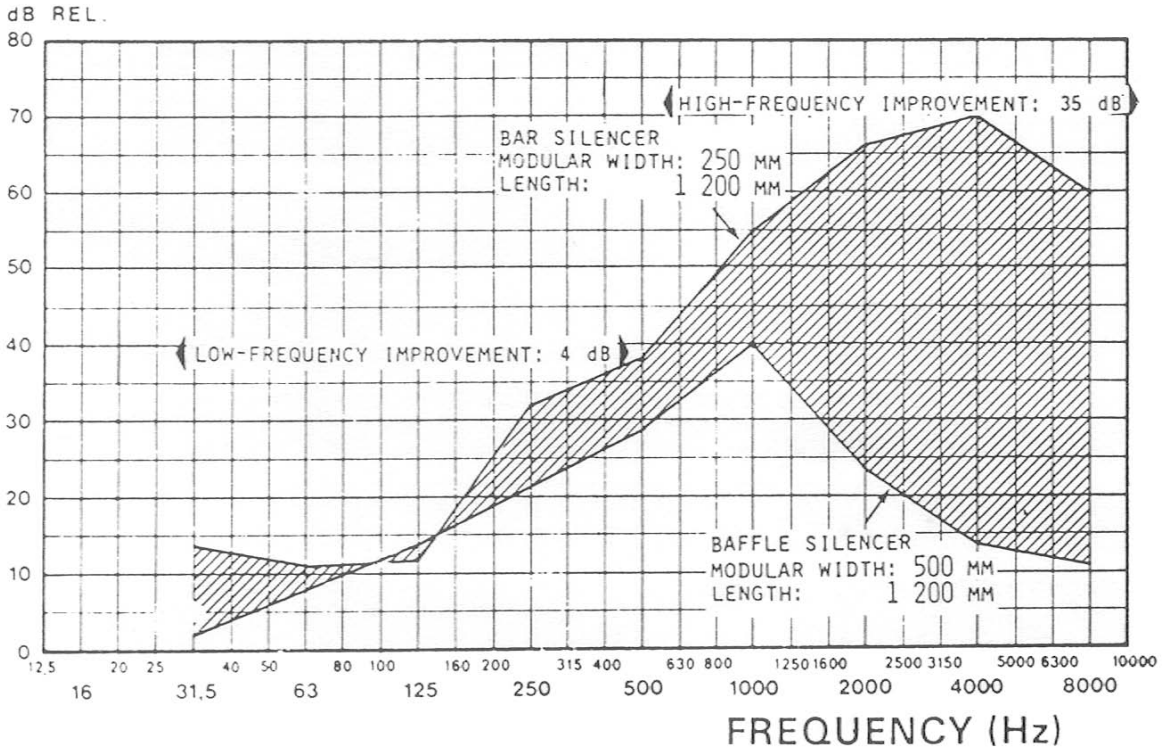

FIGURE 1.6: BAR AND BAFFLE SILENCER. A COMPARISON IN TRANSMISSION LOSS (NILSSON AND SODERQUIST 1983)

Cummings and Astley (1996) later modelled the square-section bar-silencers not only to better understand the physics but to enable a finite element computer simulation to be developed. They suggested that Nilsson and Söderqvists 'equivalent' baffle silencers may not have been so equivalent, given the geometries shown in the publication (Nilsson and Soderquist 1983). The work by Cummings and Astley could neither verify nor refute the assertion that the bar silencers performed better at all frequencies. However their results showed that bar-silencers tend to have better attenuating performance, in the critical low frequencies below ~100Hz, than that of an equivalent splitter silencer. Their finite element model showed good correlation with their own experimental data based on the least attenuated mode with and without a mean fluid flow. It was stated that lined ducts however did show greater attenuation in the mid to high frequencies. Cummings and Astley discussed the three (3) attributes cited by Nilsson and Söderqvist as reasons for the improved performance, by looking at the pressure contours for the least attenuated mode in a bar-silencer at different frequencies. The modelling of the absorbers only showed what could be argued to be these effects at a few frequencies.

Recently, Pettersson (2002) compared five single melamine resin foam bar-silencers of differently shaped cross-sections (triangle, circle and three square bar-silencers with varying amounts of foil facings applied (Figure 1.7)). A constant volume of material equal to that of two (2) 25 mm duct wall linings was used. He found that the foil facings reduced the attenuating performance at all frequencies. Of interest, Pettersson found that the unfaced triangle bar-silencers performed better than the other bar-silencers, this was attributed to the varying cross-sectional area. This triangle absorber had significantly higher

insertion loss at higher frequencies (1 kHz – 5 kHz) and comparable insertion loss below 1 kHz than that of two sides of ducting lined with 25mm of the same material.

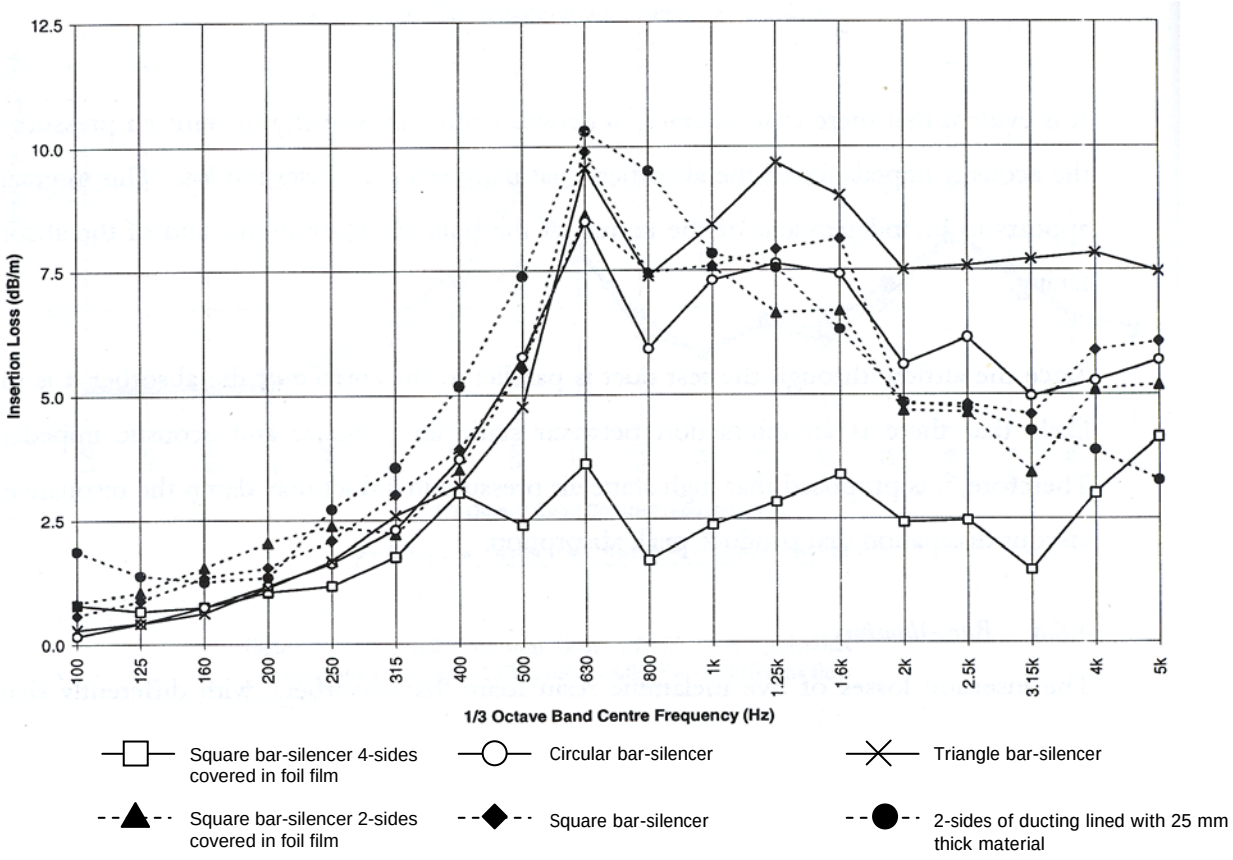

FIGURE 1.7: INSERTION LOSS OF VARIOUS BAR-SILENCERS AND EQUIVALENT LINED DUCTING OF MELAMINE RESIN FOAM (PETTERSSON 2002)

Lamatherm is a building services company based in the United Kingdom who specialise in fire, thermal and acoustic materials. They currently offer two bar-silencer products, SoundPAC CDI for circular ducts and SoundPAC RDI for rectangular ducts, these products come in the form shown in Figure 1.8.

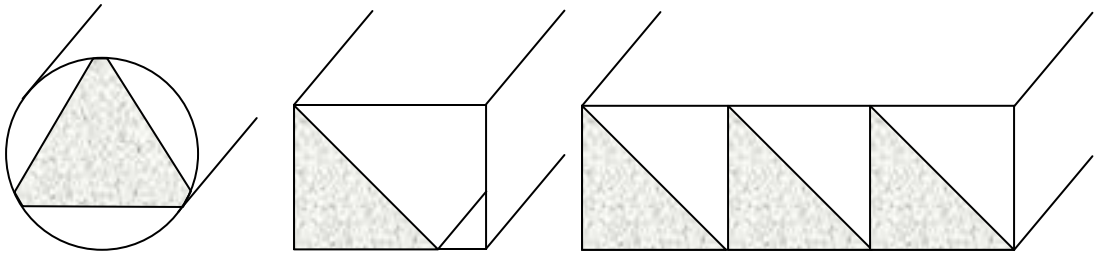

(A) (B) (C)

FIGURE 1.8: LAMATHERM 'SOUNDPAC' BAR-SILENCER SOLUTIONS; (A) CDI FOR CIRCULAR DUCTS (B) RDI FOR RECTANGULAR DUCTS (C) RECOMMENDED INSTALLATION FOR LARGER DUCT SIZES

Lamatherm show an average insertion loss for a single CDI and RDI bar-silencer in a 'common' range of duct sizes. No flow velocity was specified for the insertion loss and it is consequently difficult to assess the performance of these products.

1.3.5 Attenuator performance

Theoretical and empirical prediction methods often vary from actual attenuator performance.

Absorber thickness

It is commonly assumed that a thick lining will give more attenuation than a thinner one because for a given airway width and lining, more of the sound wave will be travelling in the lining. However, depending upon the airflow resistivity of the lining material, attenuation can reach a point where further increase of lining thickness yields no further benefit. Wassilieff (1988) looked at his own modified version (Wassilieff 1987) of Kurze and Ver's (1972) solution of the wave equation (*Equation 1.13*) for a duct lined on two

opposite sides for a locally reacting sound absorbing material, corrected for frequency dependence:

$$\sqrt{(\gamma l)^2+(k l)^2}\tan\sqrt{(\gamma l)^2+(k l)^2}=\frac{-\rho c k}{Z_y\gamma_z}\sqrt{(\gamma l)^2-(\gamma_z l)^2}\tan\left[\frac{\gamma_y}{\gamma_z}\frac{d}{e}\sqrt{(\gamma l)^2-(\gamma_z l)^2}\right] \tag{1.13}$$

where *2l* is the duct airway width, *d* the lining thickness, γ the duct propagation constant with γ_z and γ_y the lining propagation constants in the z and y-directions, Z_y the lining characteristic impedance in the y-direction, *k* (=2π/λ) the wave number, ρ the density of the fluid and *c* the speed of sound in the fluid. By considering the least attenuated mode, Equation 1.13 was solved to obtain the attenuation and showed good agreement with the measured experimental results. Wassilieff (1988) concluded that for a given duct airway width and lining flow resistivity, there is a maximum useful thickness, beyond which there is no further increase in attenuation. He presented design curves in which the material's flow resistivity and duct geometry would be sufficient to determine the attenuation in the ducting. Cummings (1976) also touches upon this 'law of diminishing returns' in the case of a bulk reacting material. These effects are of interest for bar-silencers as some cross-sectional shapes will result in very thick sections, which may result in no additional attenuation.

End effects

At any discontinuity in a pipe or section of ducting, there is a 'jump' in the characteristic impedance (ρc). Associated with this change in impedance is a reflection of sound. The reflection is known to be a function of the frequency, mean flow velocity and the change in

area. Sharland (1972), developed a general design chart (see Figure 1.9) for attenuation due to an open end reflection.

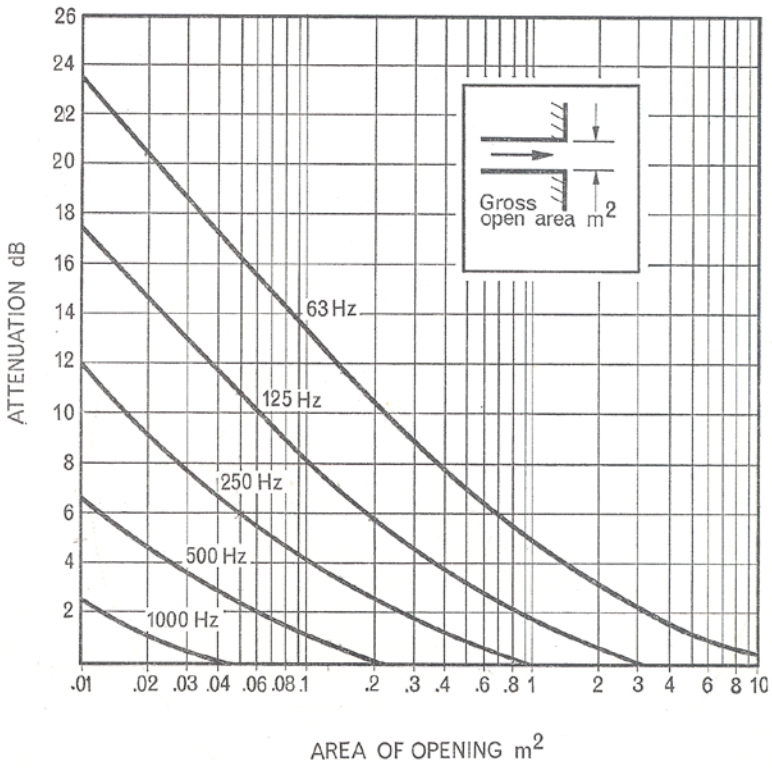

FIGURE 1.9: ATTENUATION DUE TO REFLECTION AT AN OPEN AREA

The effects of sound reflection and absorption due to changes in area in circular ducts both with and without a mean flow have been studied and models developed. Early one-dimensional models assumed an immediate expansion of the mean flow field directly after the area expansion; showing that as the Mach number increased, the reflection of any given frequency increased. The theoretical model only followed the experimental data for low Mach numbers. Cummings (1975) then assumed that scattering occurs in a region where the flow has not yet expanded which followed more closely to experimental data for higher

Mach numbers; he later concluded (Cummings and Haddad 1977) that the presence of entropy waves could be neglected from his earlier model. Peat (1988) used both an analytical frequency-dependent solution and a finite element method of finding the impedance of sound waves due to a change in area. Again, with the mean flow expanding directly after the expansion in area he concluded that the reflection coefficient was Mach number dependent.

These reflection effects are relevant due to the change in cross-sectional area directly before and after the bar-silencer as well as end reflections due to the end anechoic termination (see Chapter 2: Test facilities).

Installation effects

The effects on attenuation vary dramatically on the installation methods of the fan, ducting system and the chosen attenuator (Dumicich 1997). The amount of flanking and breakout noise varies with duct stiffness, type and size. It is difficult to account for the effects in theoretical models and specification sheets. Methods of fixing have also been seen to alter the way duct linings perform (Pettersson 2002). These and other installation variations can effect the desired attenuation.

Design charts

The performance of attenuators in ducting systems with a mean flow can be very complex and difficult to solve theoretically. Graphical methods tend to work only for simple locally reacting linings while iterative and finite element methods require much computational

power. With each fan and ducting system having is own characteristic sound generation, it is beneficial for practicing architects and engineers to use design charts. Often these charts show both theoretical and experimental attenuation over a wide range of frequencies allowing the user to select appropriate absorbers. As a result, architects and engineers use design curves as a quick and easy evaluation tool for many situations.

Examples of these design charts include duct acoustic linings locally available in New Zealand (Wassilieff 1985) , showing experimental attenuation against frequency for a range of rectangular duct sizes. Mechel (1987) published theoretical design charts for sound absorbing layers at various angles of incidence for both monolayer and multilayer absorbers. Finally, a wide range of experimental and theoretical design curves were produced for rectangular splitter silencers by Ramakrishnan (1992). These types of design charts continue to be used and are generally the best way to convey findings to those who will be implementing the methods of sound attenuation.

Frommhold and Mechel (1990) developed a series of simplified methods for the calculation of attenuation in lined ducts (circular and rectangular). These methods compared well with empirical data. They developed algebraic equations for engineering purposes, as they require little computational effort and could be easily solved.

1.4 CHAPTER SUMMARY

This chapter outlined the current duct attenuation technology; that of passive duct linings, splitter/baffle absorbers, active and reactive attenuators. A brief discussion of previous research into porous absorbing mediums, effects of fluid flow on attenuation, and the performance of attenuators was presented as well as a background into bar-silencers. The distinguishing feature of this investigation was the relatively good performance of the triangular-section bar-silencer shown by Pettersson (2002).

This research explores the performance of noise attenuating bar-silencers in ducting. The potential of the bar-silencer in industry is high, given they have shown performance comparable with current established methods of noise attenuation. If bar-silencers perform competitively, are cost-effective and practically applicable, it is perceived that design guides and recommendations will be established for new and retrofit applications.

1.5 REFERENCES

Bies, D.A., and C.H. Hansen. 1979. "Flow resistance information for acoustical design." *Applied Acoustics* 13: 357-391.

Cummings, A. 1975. "Sound transmission at sudden area expansions in circular ducts, with superimposed mean flow." *Journal of Sound and Vibration* 38: 149-155.

Cummings, A. 1976. "Sound attenuation in ducts lined on two opposite walls with porous material, with some applications to splitters." *Journal of Sound and Vibration* 49: 9-35.

Cummings, A., and R.J. Astley. 1996. "Finite element computation of attenuation in bar-silencers and comparisons with measured data." *Journal of Sound and Vibration* 196: 351-369.

Cummings, A., and H. Haddad. 1977. "Sudden area changes in flow ducts: further thoughts." *Journal of Sound and Vibration* 54: 611-612.

Cummings, A., and N. Sormaz. 1992. "Acoustic attenuation in dissipative splitter silencers containing mean fluid flow." *Journal of Sound and Vibration* 168(2): 209-227.

Delany, M.E., and E.N. Bazley. 1970. "Acoustical properties of fibrous absorbent materials." *Applied Acoustics* 3: 105-116.

Dumicih, K. 1997 "Fan Acoustics: Why what you see is not what you get."

ESDU-Engineering-Sciences-Data. 1981. "Noise in air-conditioning systems."

Frommhold, W., and F.P. Mechel. 1990. "Simplified methods to calculate the attenuation of silencers." *Journal of Sound and Vibration* 141(1): 103-125.

Goodman, S., K. Burlage, S. Dineen, S. Austin, and S. Wise. 1992. "Using active noise control for recording studio HVAC system silencing." in *93rd Convention of the Audio Engineering Society*. San Francisco.

Ingard, U. 1994. *Notes on sound absorption technology*: Noise Control Foundation.

Kruger, J.J. 2002. "The calculation of actively absorbing silencers in rectangular ducts." *Journal of Sound and Vibration* 257: 887-902.

Kurze, U.J., and I.L. Vér. 1972. "Sound attenuation in ducts lined with non-isotropic material." *Journal of Sound and Vibration* 24(2): 177-187.

Meyer, E., F. Mechel, and G Kurtze. 1958 "Experiments on the influence of flow on sound attenuation in absorbing ducts." *The Journal of the Acoustical Society of America 30(3): 165-174*

Mechel, F.P. 1987. "Design charts for sound absorber layers." *Journal of Acoustical Society of America* 83: 1002-1011.

Munjal, M.L. 1987. *Acoustics of ducts and mufflers*. Canada: Wiley-Interscience.

Nilsson, N-A., and S. Soderquist. 1983. "The bar silencer-improving attenuation by constricted two-dimensional wave propagation." *Proceedings of Internoise 83*: 1-4.

Peat, K.S. 1988. "The acoustical impedance at discontinuities of ducts in the presence of a mean flow." *Journal of Sound and Vibration* 127: 123-132.

Pettersson, M.J. 2002. *Duct absorber design*. A thesis submitted in partial fulfilment of the requirements for a Masters of Engineering degree in the Department of Mechanical Engineering, University of Canterbury.

Pridmore-Brown, D.C. 1958. "Sound propagation in a fluid through an attenuating duct." *Journal of Fluid Mechanics* 4: 393-406.

Ramakrishnan, R. 1992. "Design Curves for Rectangular Splitter Silencers." *Applied Acoustics* 35: 1-24.

Sharland, I. 1972. *Woods practical guide to noise control*: Butterworth-Heinemann.

Shirahatti, U.S. 1985. "Acoustic characterization of porous ceramic tiles." Ban galore: Indian Institute of Science.

Wassilieff, C. 1985. "Performance of duct acoustic lining available in New Zealand." *The Institution of Professional Engineer New Zealand* 12: 73-82.

Wassilieff, C. 1987. "Experimental verification of duct attenuation models with bulk reacting linings." *Journal of Sound and Vibration* 114: 239-251.

Wassilieff, C. 1988. "Predicting sound attenuation in absorber-lined ducts." *Australian Refrigeration, Air Conditioning and Heating*: 30-33.

Wise, S., J.-F. Nouvel, and V. Delemotte. 2000. "The first 1000 active duct silencers installed in HVAC systems - A summary of applications, successes, and lessons learned." *Proceedings of Internoise 2000*. Nice, France.

Zwikker, C., and C.W. Kosten. 1949. *Sound absorbing materials*. New York: Elsevier.

2

TEST FACILITIES

2.1 INTRODUCTION

This chapter presents an overview of the test facilities including the test rig, measuring equipment, test room, calibration and the methodology used for obtaining the results presented in this thesis. The test rig replicates typical industrial ducting and enabled the insertion loss of ducted silencers to be measured with or without a mean flow. The associated pressure losses could also be measured within the duct.

An existing 540 x 300 mm duct test facility was modified so that it conformed entirely to ISO 7235:1991 – ‘Acoustics – Measurement procedures for ducted silencers – Insertion loss, flow noise and total pressure loss’. In addition to this, a 270 x 300 mm facility was designed and commissioned. By meeting the requirements of the ISO standard, confidence was obtained in the performance of the test facilities, allowing comparison with other test facilities.

2.2 TEST ROOM

The room housing the test facility was located in the laboratory wing of the Department of Mechanical Engineering, University of Canterbury. The room was acoustically treated to reduce the noise field surrounding the test facility. The walls of the room were lined with sound absorbing material (50 mm Acoustop, a polyurethane acoustic foam) glued to 50 mm battens, creating a 50 mm cavity behind the absorbing material. The floor of the room was covered in cut-pile carpet on top of foam underlay. Absorbers constructed of a closed-cell low-density polyethylene foam (Quash), were suspended from the ceiling above the test facility. Quash has a self-supporting structure which allowed the sheets of material to be hung from wires along the ceiling as shown in Figure 2.1(A) and 2.1(B).

(A) (B)

FIGURE 2.1: QUASH HANGING ABSORBERS AND FIXING METHOD

2.2.1 Quash Hanging Absorbers

An investigation of the effectiveness of the hanging absorbers was undertaken. From the measured room parameters (Table 2.1), material dimensions (Table 2.2) and measured absorption coefficients (Table 2.3) predicted reverberation times were calculated and compared with the actual measured reverberation times before and after the installation of

the hanging absorbers. The Quash sheets were distributed evenly throughout the test room in a cell pattern shown in Figure 2.2.

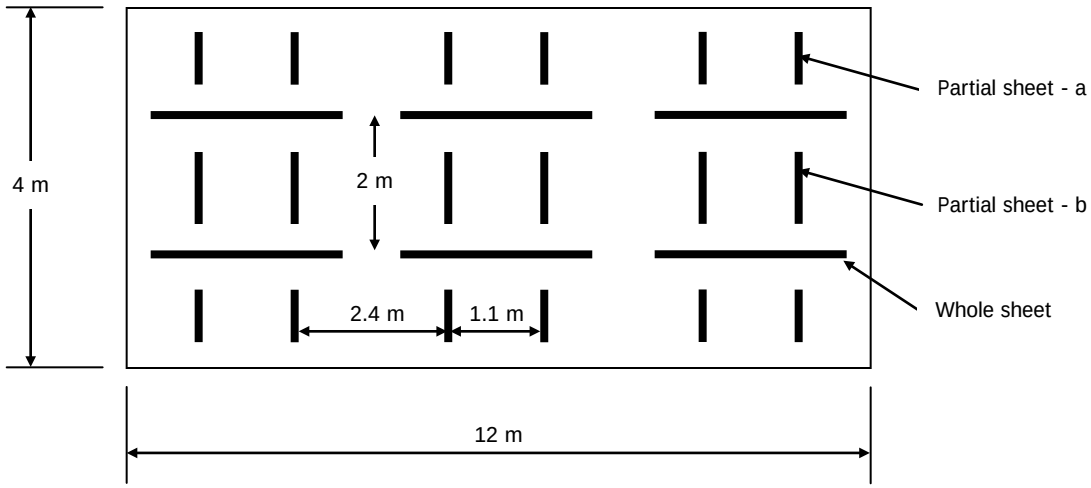

FIGURE 2.2: HANGING ABSORBER DISTRIBUTION IN TEST ROOM

TABLE 2.1: TEST ROOM PARAMETERS

	Test Room
Total surface area (m^2)	289
Total surface area (with Hanging absorbers) (m^2)	329
Room volume (m^3)	178

TABLE 2.2: DETAILS OF QUASH ABSORBERS

Thickness (mm)	30
Density (kg m^{-3})	32
Area of Quash sheets	
Whole sheet (m^2)	2.8
Partial sheet – a (m^2)	1.1
Partial sheet – b (m^2)	1.7
Total installed area (m^2)	40.2

Sabine Prediction

The Sabine equation was used for predicting the reverberation times (T_{60}) before and after the introduction of the Quash hanging absorbers:

$$T_{60} = \frac{55.25\,V}{c\,S\,\ddot{\alpha}} \tag{2.1}$$

where V is the volume of the room, c is the speed of sound in air (343 ms^{-1}), S is the total surface area of the room and $\ddot{\alpha}$ is the average absorption coefficient for the room, calculated from:

$$\ddot{\alpha} = \frac{\alpha_1 S_1 + \alpha_2 S_2 + ... + \alpha_n S_n}{S} \tag{2.2}$$

where α_i are the individual absorption coefficients for each surface, S_i, and S is the total surface area of the room.

The decay times were measured for two different speaker positions with four microphone positions being used for each speaker location. Two reverberation decays were measured at each microphone position.

TABLE 2.3: ABSORPTION COEFFICIENTS USED IN PREDICTED REVERBERATION TIMES

		Floor (Foam-backed carpet)	Two walls (Foam spaced from wall)	Ceiling (Painted concrete)	Two walls (painted concrete block)	Quash	Windows
Area (m^2)		**48**	**43.2**	**48**	**141.6**	**40.2**	**8**
$^1/_3$ Octave Band Centre Frequency (Hz)	*100*	0.03	0.27	0.01	0.01	0.13	0.06
	125	0.04	0.35	0.01	0.01	0.17	0.06
	160	0.03	0.43	0.01	0.01	0.13	0.05
	200	0.06	0.42	0.01	0.01	0.16	0.05
	250	0.08	0.63	0.01	0.01	0.16	0.04
	315	0.10	0.82	0.01	0.01	0.20	0.04
	400	0.11	0.94	0.01	0.01	0.23	0.03
	500	0.18	0.92	0.01	0.01	0.40	0.02
	630	0.25	0.88	0.01	0.01	0.60	0.03
	800	0.35	0.84	0.02	0.02	0.97	0.03
	1000	0.46	0.83	0.02	0.02	1.10	0.03
	1250	0.57	0.85	0.02	0.02	0.80	0.02
	1600	0.57	0.87	0.02	0.02	0.68	0.02
	2000	0.57	0.80	0.03	0.03	0.94	0.02
	2500	0.65	0.85	0.03	0.03	0.83	0.02
	3150	0.68	0.82	0.04	0.04	0.80	0.02
	4000	0.65	0.79	0.04	0.04	0.88	0.02
	5000	0.65	0.84	0.05	0.05	1.02	0.01
	6300	0.60	0.82	0.08	0.08	0.94	0.01
	8000	0.58	0.79	0.11	0.11	0.92	0.01

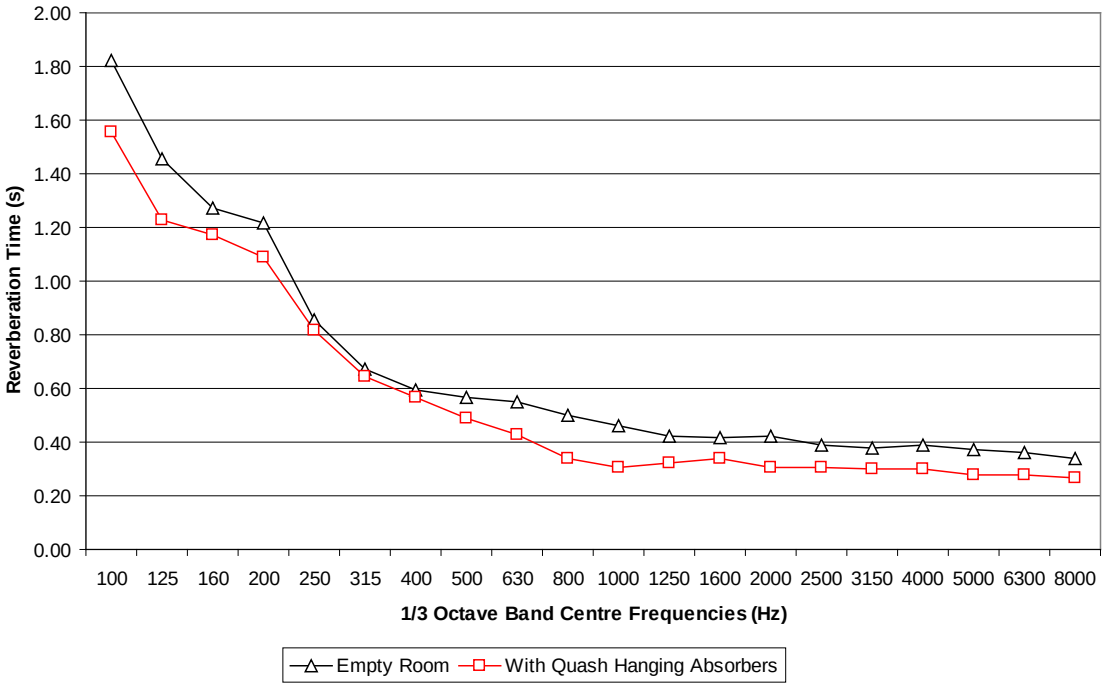

FIGURE 2.3: SABINE PREDICTED REVERBERATION TIMES

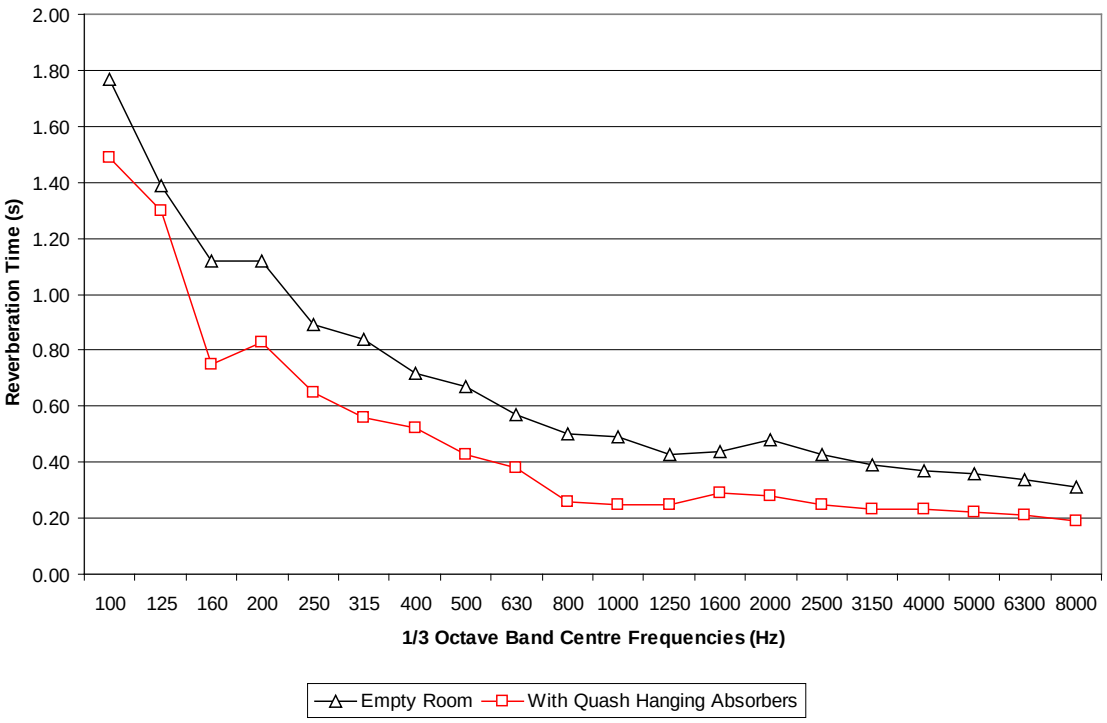

FIGURE 2.4: MEASURED REVERBERATION TIMES

The 'Empty Room' described in Figures 2.3 and 2.4 above indicate the test room without the hanging absorbers. The predicted reverberation times in Figure 2.3 were seen to under predict the effectiveness of the Quash hanging absorbers, with Figure 2.4 showing much higher measured sound absorption values for the installed hanging absorbers.

Effect of Hanging Absorber Spacing

The effect of increasing the spacing between Quash hanging absorbers was evaluated in a reverberation room. Four sheets (1.55 m x 1.1 m) were hung from the wires across the room with spacing of 0, 500 mm, 1000 mm and 1500 mm. The results in Figure 2.5 show that as the spacing between the sheets increases, the material absorbs more sound.

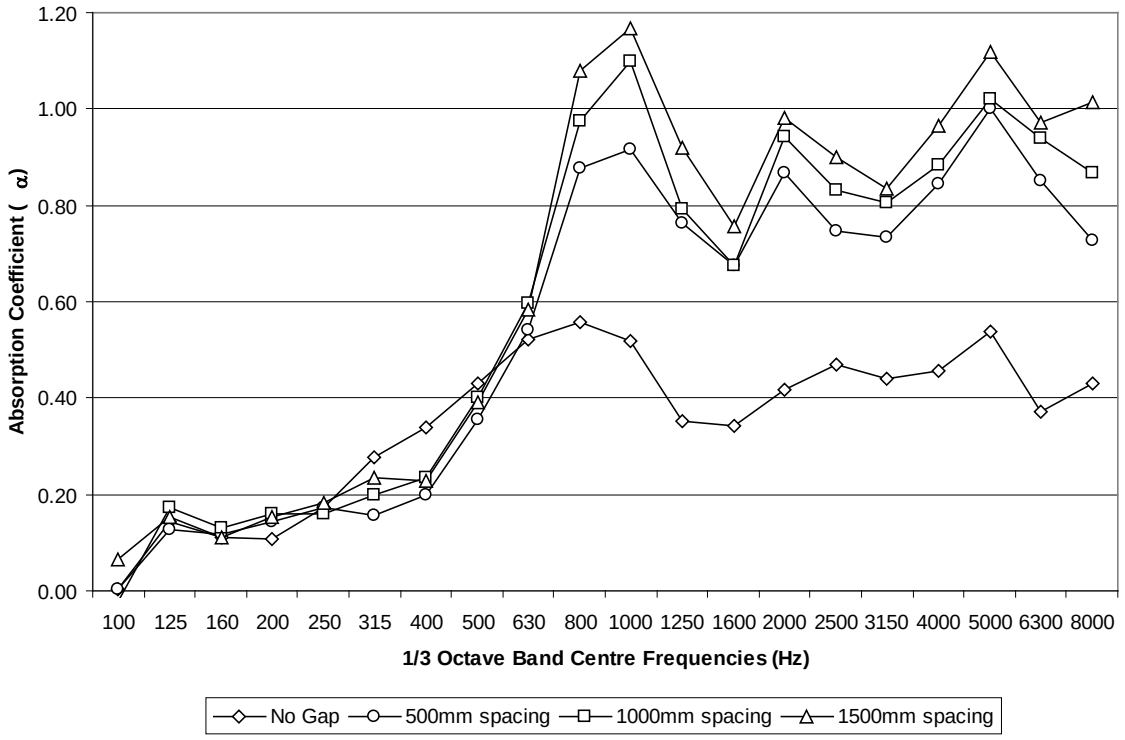

FIGURE 2.5: EFFECT OF ABSORBER SPACING

Effect of Number of Absorbers

The effect of the number of Quash hanging absorbers was also evaluated in the reverberation room. Single sheets of Quash (1.55 m x 1.1 m) were added to the room in increments until a total of six sheets were suspended. The distance between the sheets was kept at a constant 1 metre. The results in Figure 2.6 illustrate that the absorption per sheet was reduced with an increasing number of sheets. This was attributed to the change in acoustic environment in the reverberation room as more sheets were added.

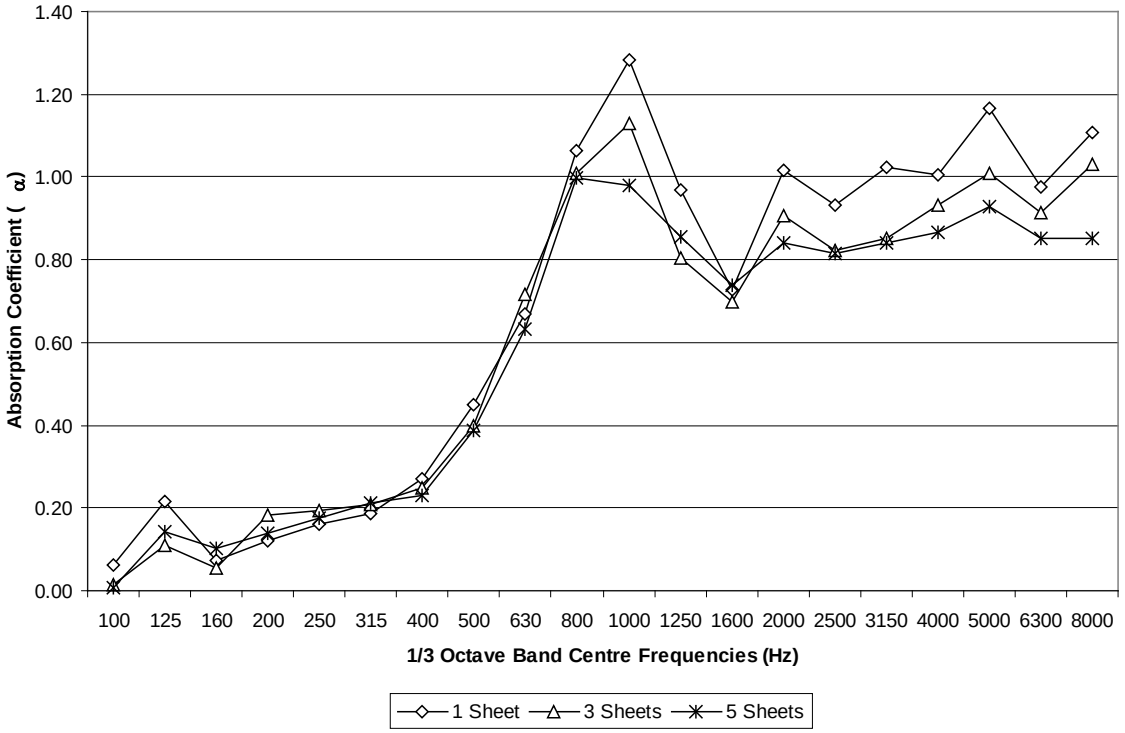

FIGURE 2.6: EFFECT OF NUMBER OF HANGING ABSORBERS

2.3 TEST APPARATUS

The original test facility was designed and built by Pettersson (2002), to be in accordance with ISO 7235 (1991) for use with the substitution method for determining the insertion loss of ducted silencers. The test facility was reassembled inside the test room and alterations made to meet the ISO standard.

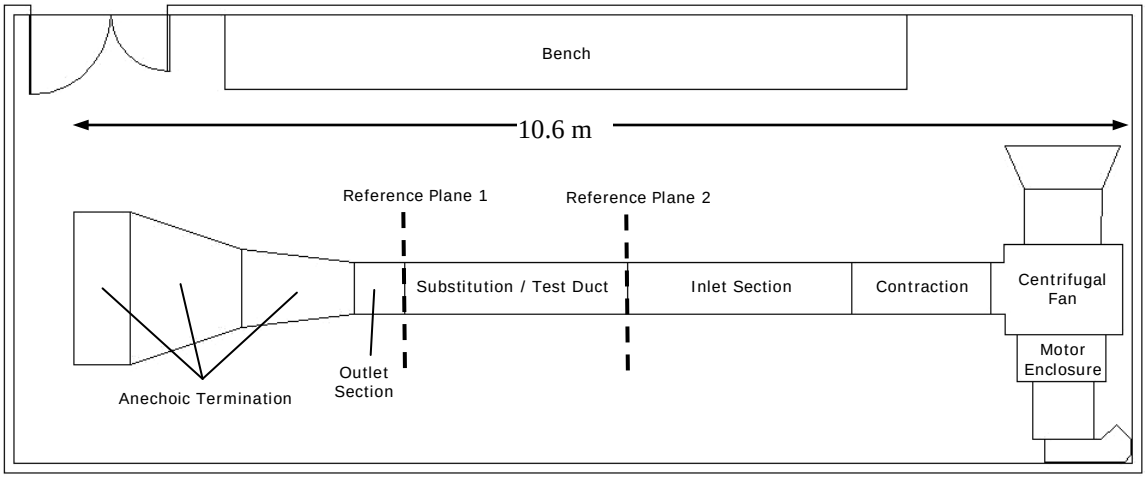

FIGURE 2.7: SCHEMATIC LAYOUT OF TEST RIG AND ROOM

The facility consisted of a centrifugal fan driven by a three-phase 15 HP motor. A speaker unit was mounted in the inspection window above the fan. The flow from the fan enters a contraction before the inlet section, passes through the test/substitution section and exits through an acoustic termination.

The original test rig consisted of rectangular ducts 540 mm x 300 mm. To increase the parameters available for study in the test program and to achieve more understanding of how shape, size, and scale of the duct affect absorption, another set of 270 mm x 300 mm ducts were constructed.

2.3.1 Centrifugal fan unit

The centrifugal fan was supplied by Taylors Ltd. (Christchurch, New Zealand). The fan had an impeller diameter of 690 mm consisting of 11 backwards inclined laminar (straight) blades. The volume flow rate was controlled by a variable speed AC drive unit connected to the 15 HP three-phase motor. The fan and drive motor could obtain a maximum volume flow rate of 4.125 m^3s^{-1}. Figure 2.8 shows the sound pressure levels measured outside of the ducting, at 1 m from the motor at maximum flow rate. The fan inlet duct was lined with 50 mm polyether polyurethane foam to attenuate noise entering and leaving the duct sections via the fan unit, thus reducing the amount of break-in noise.

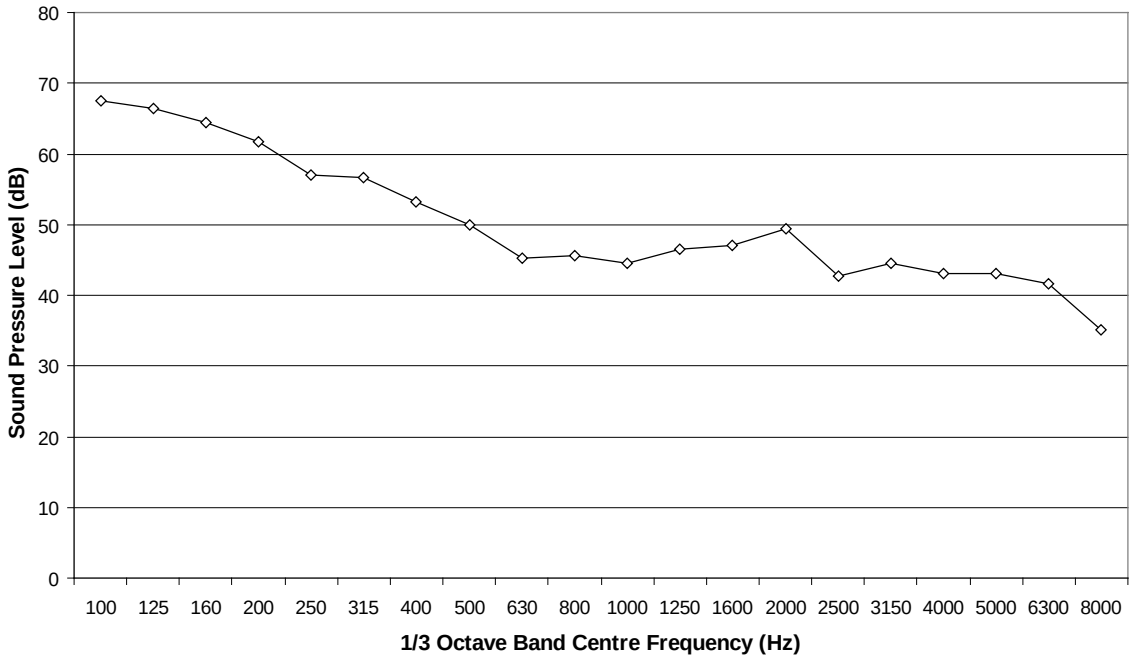

FIGURE 2.8: SOUND LEVELS OF CENTRIFUGAL FAN UNIT AT MAXIMUM FLOW RATE

A motor enclosure was used to attenuate the noise produced by the three-phase motor. The enclosure encompassed the drive motor and coupling and was altered to fit the new room size constraints. The motor enclosure layout and manufacturing drawings are shown in Appendix 1.

2.3.2 Transition

The 540 mm x 300 mm duct utilizes a transition section, this transition section changes the cross-sectional area from that of the centrifugal fan outlet to the cross-sectional area of the inlet duct section. The contracting transition section was redesigned (Appendix 2.2) and constructed to be in accordance with ISO 7235 §5.1.5 (1991). The standard called for a maximum wall angle of 15^{o} in the transition with the minimum length of the transition determined by Equation 2.3.

$$\frac{l_{\min}}{l_0} = \frac{A_{\text{large}}}{A_{\text{small}}} - 1 \tag{2.3}$$

Where l_{min} is the minimum length of the transition section, l_0 = 1 metre, A_{large} and A_{small} are the cross-sectional areas of the ends of the transition. The resulting minimum allowable length of the transition section was 1.42 m. The redesigned contraction was 1.5 m long.

The 270 mm x 300 mm ducts used a reconfigured centrifugal fan mount, eliminating the need for a transition. This resulted in a lower maximum flow rate.

2.3.3 Noise source

The noise source was generated at the fan end of the test apparatus, with a Philips AD8066 8Ω loudspeaker mounted in the inspection window on top of the centrifugal fan casing. Tonal and pink noise signals were generated by a Neutrik Minirator type MR1 audio generator in order to have a constant, stable and repeatable noise source. This signal was fed through a Sony F210 100W power amplifier before being fed to the loudspeaker. The external noise source was used to give a constant sound power in each $^1/_3$ octave band.

2.3.4 Noise reception

The sound field was measured using a type 1, Brüel and Kjær (B&K) 2260 Investigator, loaded with B&K BZ7204 Building Acoustics software package. The B&K 2260 was connected to two B&K type 4189 condenser microphones. The sound field was measured at two planes of reference, one before the test / substitution duct section and one after (see Figure 2.7). For the 540 mm x 300 mm duct, the sound field was measured at five microphone positions as seen in Figure 2.9. Each microphone was placed inside an aerodynamic holder and used B&K type UA0386 nose cones to reduce flow noise.

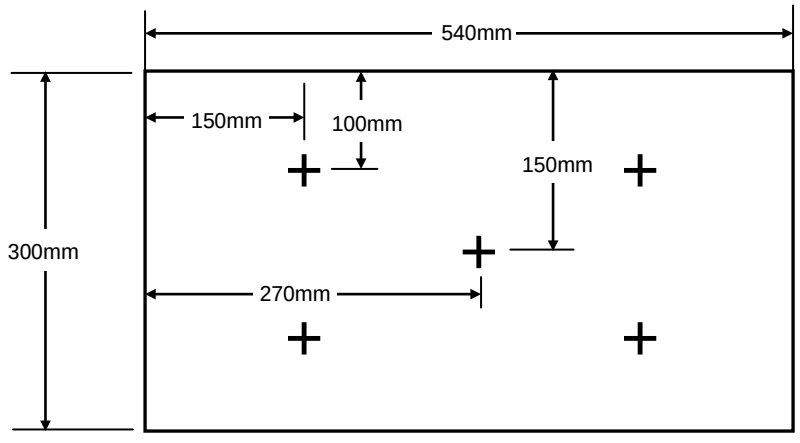

FIGURE 2.9: 540 MM X 300 MM DUCT SOUND FIELD MEASUREMENT POSITIONS

The sound field for the 270 mm x 300 mm duct was measured at four microphone positions as seen in Figure 2.10. For each measurement the microphone was placed inside an aerodynamic holder.

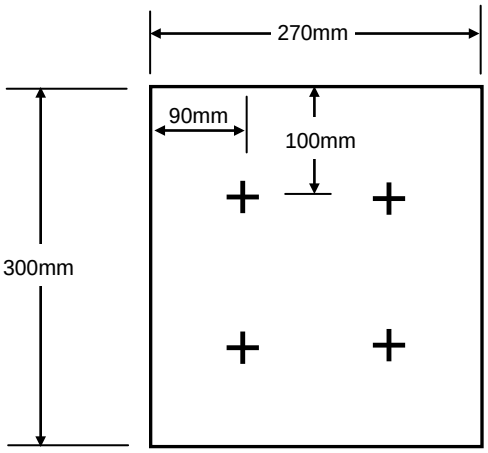

FIGURE 2.10: 270 MM X 300 MM DUCT SOUND FIELD MEASUREMENT POSITIONS

2.3.5 Flow measurement

Two arrays of four Pitot rakes (Figure 2.11(A)) were used to determine the volume flow rate and velocity profiles along the ducting. A set of four static pressure points, two at each reference plane, enabled the dynamic pressure to be determined from the total pressure. The arrays were positioned at the upstream and downstream boundaries of the test / substitution section. A pressure transducer (Figure 2.11(B)) and computer controlled scanner enabled the 42 pressures to be measured in approximately 90 seconds, reducing the effects of variations in the flow during measurement.

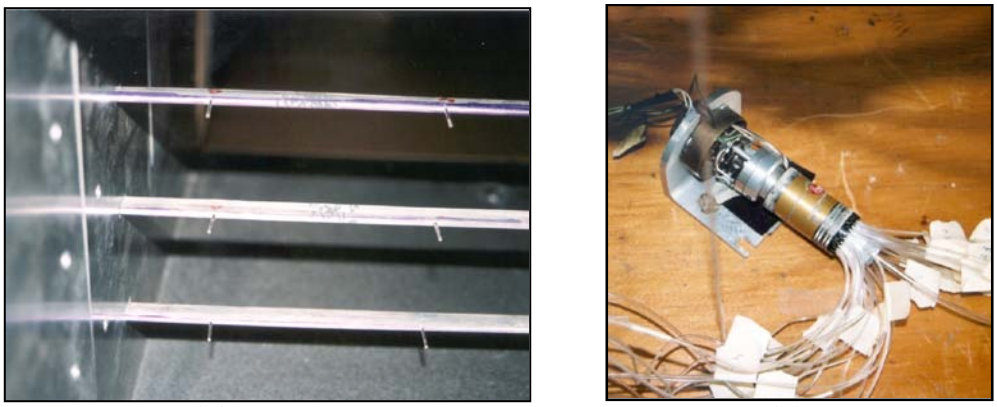

(A) (B)

FIGURE 2.11: FLOW MEASUREMENT EQUIPMENT, PITOT ARRAY (A) AND SCANNING EQUIPMENT (B)

2.3.6 Ducting

ISO 7235 (1991) describes the requirements for the ducting sections. It states (ISO 7235:1991 §5.1.4.2) that the duct must be as long as half the wavelength of the lowest centre frequency of interest. It was considered sufficient to measure the frequencies between 100 Hz and 8000 Hz. The half wavelength of 100 Hz is 1.72 m, which is within the 2.4 m long duct sections. The standard (ISO 7235 §5.1.4.2) also requires that the duct length not be less than four times the maximum duct cross-dimension. In the case of measurements with a mean flow, the upstream and downstream sections shall be straight for a minimum length of five times the equivalent circular duct diameter (d_e), where d_e is given by Equation 2.4.

$$d_e = \sqrt{\frac{4s}{\pi}} \tag{2.4}$$

where s is the cross-sectional area of the ducting. For the larger 540 mm x 300 mm ducts, this gave an equivalent circular ducting diameter of 0.454 m. The current test rig therefore

has more then the required 2.27 m of straight ducting required either side of the test / substitution duct section. For the 270 mm x 300 mm ducts, Equation 2.4 gave a circular ducting diameter of 0.321 m. The 2.4 m ducts are again longer than the 1.6 m lengths required by ISO 7235.

The ducting sections were constructed from 18 gauge steel. In the case of the 540 mm x 300 mm ducts, four test sections were used. Three sections allowed a constant airflow cross-section, one with 25 mm thick absorbers lining 4 sides, another with 25 mm thick absorbers lining only the top and bottom sides of the duct and the other with a varying cross-section from 0 mm to 50 mm thick absorbers. Finally the substitution duct doubled as a test section for bar-silencers. The four sections can be seen schematically in Figure 2.12.

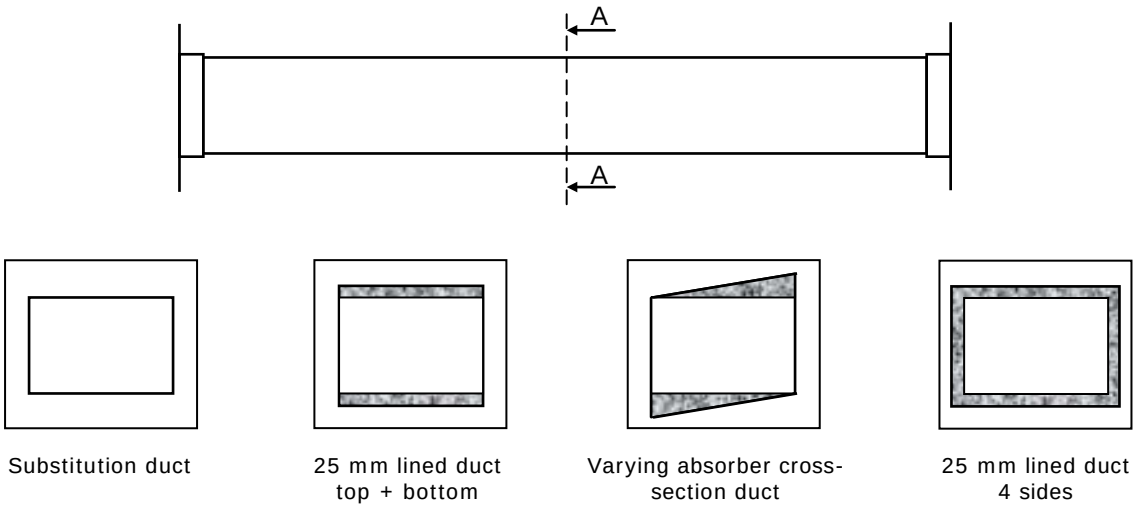

FIGURE 2.12: SCHEMATIC OF 540 MM X 300 MM DUCT TEST SECTION CONFIGURATIONS

For the case of the 270 mm x 300 mm ducts, three test sections were used. All three sections allowed a constant airflow cross-section, one with 25 mm thick absorbers lining 4

sides, one with 25 mm thick absorbers lining the top and bottom sides of the duct and lastly the substitution duct doubled as a test section for the bar-silencers. The three sections can be seen schematically in Figure 2.13.

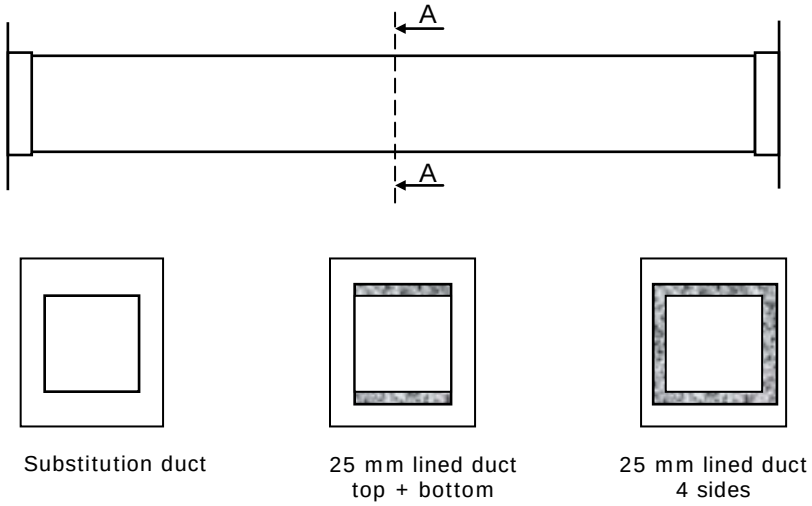

FIGURE 2.13: SCHEMATIC OF 270 MM X 300 MM DUCT TEST SECTION CONFIGURATIONS

2.3.7 Anechoic Termination

The anechoic termination situated at the end of the Outlet Section was designed to attenuate the plane wave reflections at the outlet and hence prevent standing waves in the rig.

2.4 CALIBRATION

The test facility was tested and calibrated to verify it met the requirements of ISO 7235 (1991). Modifications were made to any sections of the test facility which did not meet the specifications of the ISO standard.

Break-in Noise

Break-in noise is generated sound taking an alternative path from the sound source to the microphone other than that of duct-borne noise. Flanking paths limit the effective insertion loss in a ducting system. ISO 7235 Annex C (1991) describes both the performance requirements and the testing procedure for determining the break-in-noise. It is required that the Sound Pressure Level (SPL) of noise entering the test duct sections be at least 10 dB above the sound entering the test ducts via break-in when measured with a transmission barrier in place.

A 30 mm thick chipboard transmission barrier as described in ISO 7235 Annex C §C.2.2 (1991) was inserted between the transition / settling section and the inlet duct. The sound pressure levels were measured at reference plane 2 (Figure 2.7), with and without, the transmission barrier in place.

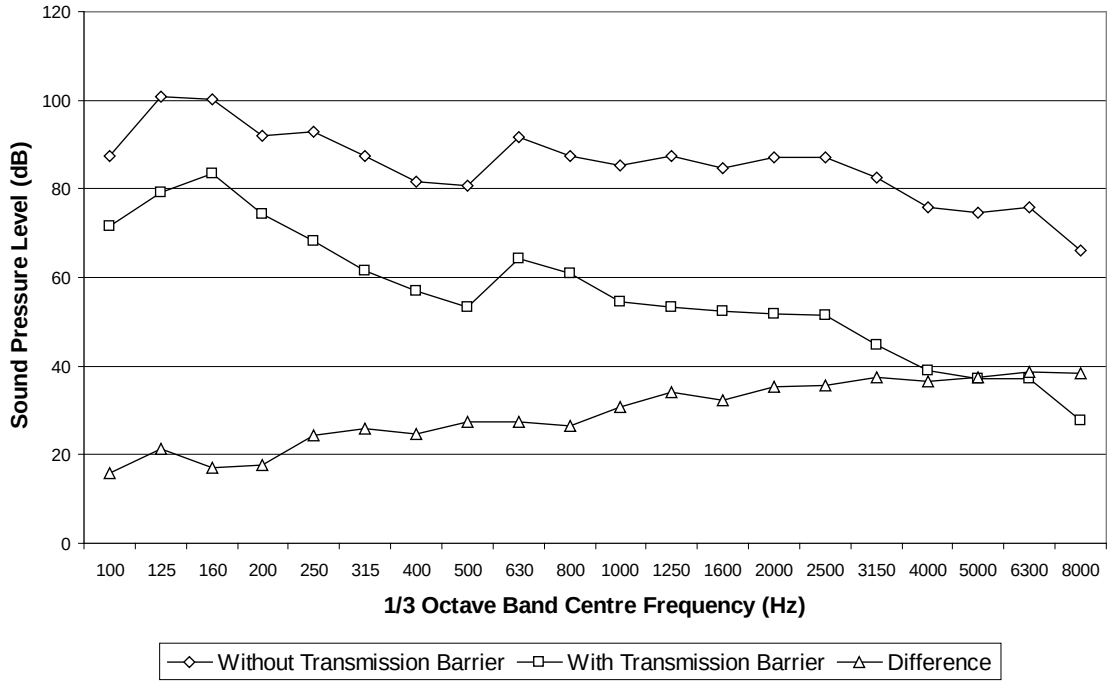

FIGURE 2.14: LIMITING INSERTION LOSS DUE TO BREAK-IN NOISE VIA FLANKING PATHS FOR 540 MM X 300 MM DUCT

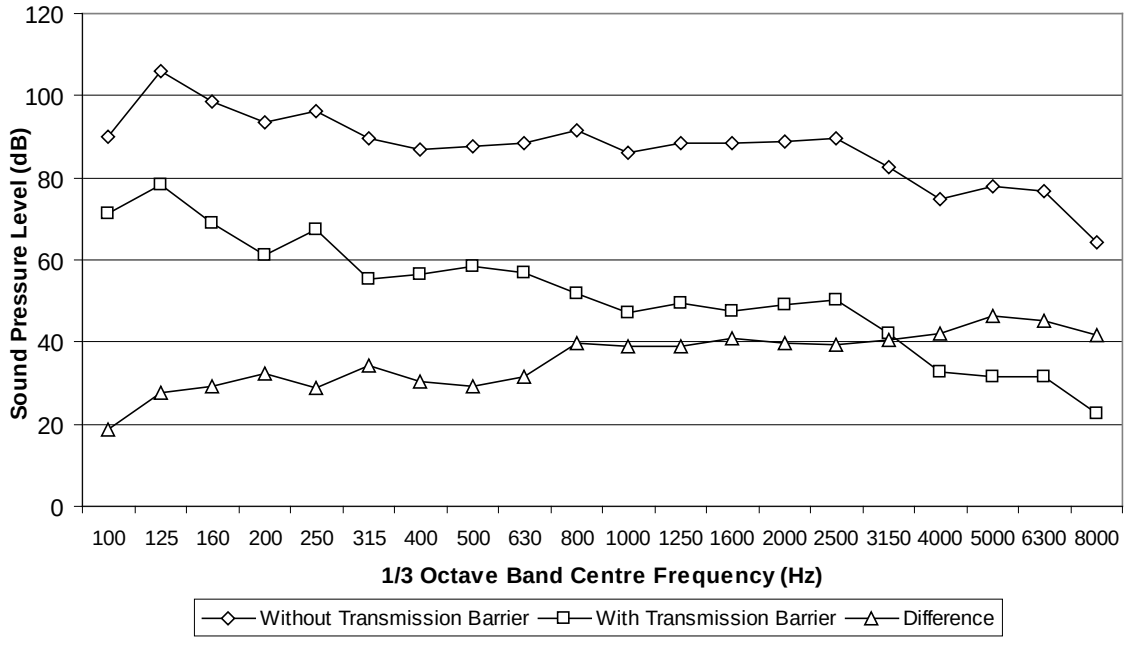

FIGURE 2.15: LIMITING INSERTION LOSS DUE TO BREAK-IN NOISE VIA FLANKING PATHS FOR 270 MM X 300 MM DUCT

The minimum difference for the 540 x 300 mm duct (Figure 2.14) was 16 dB, while for the 270 x 300 mm duct (Figure 2.15) the minimum difference was 19 dB, both of which were above the minimum 10 dB difference required. The SPL in the test ducts while the transmission barrier is in place was due to:

- Noise propagating through the chipboard barrier.
- Structure-borne noise emanating from the duct walls.
- Air-borne noise in the room entering through the duct walls.
- Air-borne noise propagating from the room into the duct by way of the anechoic termination.

Flow measurements

Due to the nature of duct absorbers and bar-silencers there is an associated pressure loss across the absorber. Using the Pitot rakes described in Section 2.3.5 and two pairs of static pressure taps at each reference plane, velocity profiles as well as pressure losses could be calculated. Each Pitot tube was connected to a pressure transducer creating a voltage (V). The pressure (P) was obtained from the calibration data for the transducer:

$$P = mV + c \tag{2.5}$$

These individual pressures were converted (Equation 2.6) into velocities (v) to give either a velocity profile over the reference planes or a mean flow velocity from which the flow rate were calculated.

$$v = \left(\frac{2P}{\rho} \right)^{1/2} \tag{2.6}$$

The effects of the mean flow on insertion loss were investigated. For these measurements, the signal to noise ratio of the microphones in the flow would have to be high. The microphones were held in aerodynamic holders to reduce the self-induced noise as the mean flow passed the microphone. With the microphones held in place, pink noise was generated at the fan unit. For mean airflow velocities of 0, 5 ms^{-1}, 10 ms^{-1}, 15 ms^{-1}, 20 ms^{-1} and 25 ms^{-1} the SPL levels were measured. An example of the effects of the mean flow on the SPL measurements can be seen in Figure 2.16.

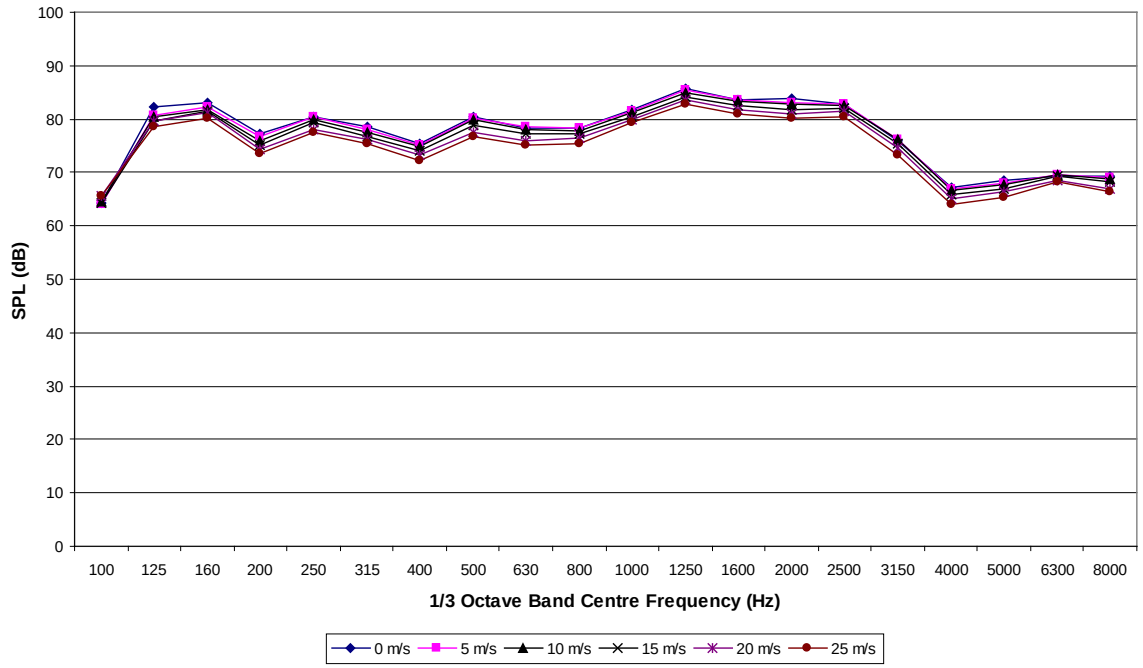

FIGURE 2.16: EFFECTS OF VARYING MEAN FLOW ON SPL MEASUREMENTS FOR 540 MM X 300 MM DUCT

The results showed that the effects of the mean flow on the microphones were limited. As the mean flow increased, the measured sound pressure levels decreased by up to 1 dB per 5

ms^{-1} increase in flow velocity. This effect was seen across all frequencies and there appeared to be no self-induced noise at any frequency.

Internal noise field uniformity

The sound field in both substitution ducts were tested to ensure that there was no significant variations in the noise field before the duct silencers were employed. Pink noise was generated at the fan unit and $^1/_3$ octave band centre frequency measurements recorded at each microphone position. The measurements can be seen in Appendix 4. The results showed the maximum variation in sound pressure level to be 1.8 dB for the 540 x 300 mm duct and 1.6 dB for the 270 x 300 mm duct.

Due to the nature of bar-silencers creating a blockage in the ducting and absorbing more sound in particular regions of the ducting, a number of measurement points (Figure 2.9 and Figure 2.10) were taken at each reference plane. By taking a number of measurement points, any variations or irregularities in the noise field was reduced. A spatial average of the points at each plane was taken to obtain the SPL at that point (see Methodology §2.5).

Anechoic Termination

The purpose of the anechoic termination was to attenuate the plane wave reflections at the outlet as well as preventing standing waves in the test rig. The effectiveness of the termination is determined by a Pressure wave Reflection Coefficient (PRC) measured at $^1/_3$ octave band centre frequencies below a described cut-off frequency. The PRC, r_a , is given by Equation 2.7.

$$r_a = \frac{10^{\Delta L/20} - 1}{10^{\Delta L/20} + 1} \tag{2.7}$$

where ΔL is the difference between the maximum and minimum sound pressure levels occurring in the duct as a result of the standing waves formed by the incident and the reflected plane waves at each $^1/_3$ octave band centre frequency of interest. The PRC values are measured below a plane wave cut off frequency (f_o):

$$f_0 = 0.586\frac{c}{d_e} \tag{2.8}$$

where c is the speed of sound (343 ms^{-1}) and d_e is the diameter of the throat of the termination (m) as calculated from Equation 2.4. For the 540 x 300 mm duct, this yields a $^1/_3$ octave band centre cut off frequency of 315 Hz, and 630 Hz for the 270 x 300 mm duct.

Pure tones at $^1/_3$ octave band centre frequencies from 50 Hz to the cut off frequency were generated inside the fan enclosure and a microphone traversed along the test duct. The variation in sound pressure level down the ducting had two components superimposed; the standing wave pattern and the insertion loss due to the substitution duct. The recorded data points for each $^1/_3$ octave band were fitted to the following curve:

$$SPL(x) = \underbrace{A\sin(\omega x + \phi)}_{\text{a}} + \underbrace{Bx}_{\text{b}} + C \tag{2.9}$$

Where part ‘a’ is the equation of the standing wave, consisting of: A the amplitude of the standing wave, ω the frequency and Φ is the phase. Part ‘b’ is the insertion loss of the duct, where B is the gradient of the insertion loss per metre with respect to length x. The variable ‘C’ is the dB offset due to the source SPL. Equation 2.9 part ‘a’ yields the true difference in maximum and minimum SPL for the standing wave; this was used in Equation 2.5 to calculate the PRC. The associated MATLAB script can be seen in Appendix 5. An example of the curve fitted data is shown in Figure 2.17. The data is for the anechoic termination as it was in original configuration (Pettersson, 2002).

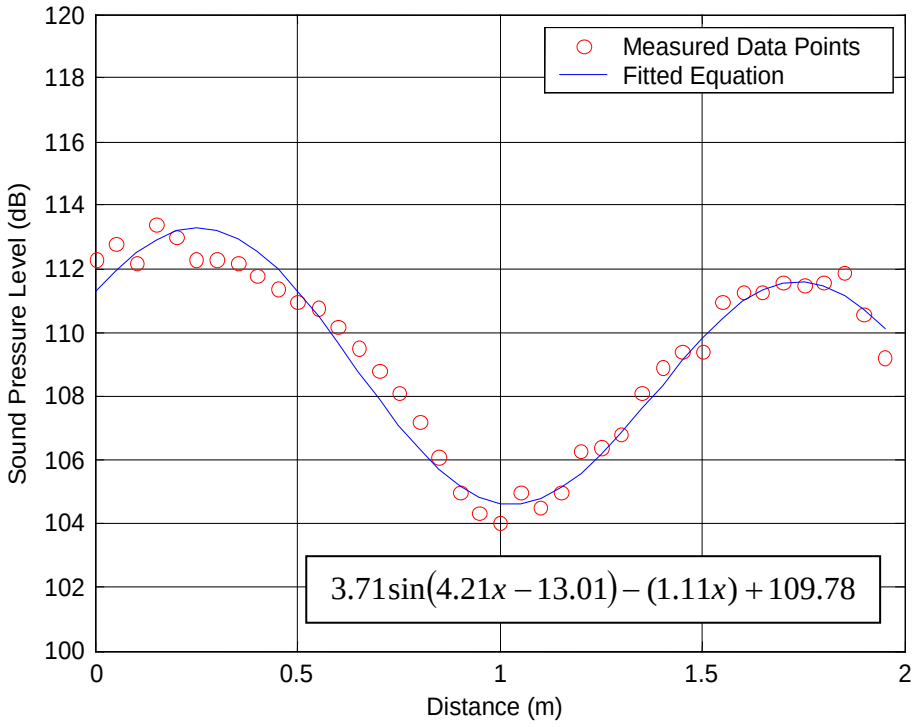

FIGURE 2.17: EXAMPLE CURVE FITTED SOUND PRESSURE LEVELS FOR THE 540 MM X 300 MM DUCT SYSTEM AT 125 HZ FOR THE ANECHOIC TERMINATION AS RECEIVED

The PRC values for the termination in its initial configuration were not within those outlined in ISO 7235 §5.1.6 (1991). In the case of the 540 x 300 mm duct system, standing waves of significant amplitude were seen at 125 Hz and 250 Hz, the PRC values for these frequencies as alterations were made can be seen in Table 2.4. Initially, a pyramid of acoustic foam was positioned at the exit of the termination (see Figure 2.18), this reduced the PRC, but not to within the limits outlined in the standard. With the pyramid still in place, 25 mm thick, acoustic foam was applied to the top and bottom final 2.8 m of the anechoic termination. Again, the resulting PRC values, although improved, were not within the standard requirements. Finally, the polyester filler in the termination was replaced with fibreglass, which has higher absorption coefficients. The combined effect of all three alterations reduced the PRC values for frequencies between 50 Hz – 315 Hz to within the ISO standard requirements.

TABLE 2.4: ANECHOIC TERMINATION PRESSURE REFLECTION COEFFICIENTS

	125 Hz *	**250 Hz ***
As received	0.42	0.39
With pyramid	0.29	0.22
With pyramid and 25 mm thick acoustic foam lining	0.19	0.08
With pyramid, 25 mm thick acoustic foam lining and fibreglass installed	0.13	0.09

* Under ISO 7235 (1991) the permissible PRC is 0.15 at 125 & 250 Hz (see Table 2.5)

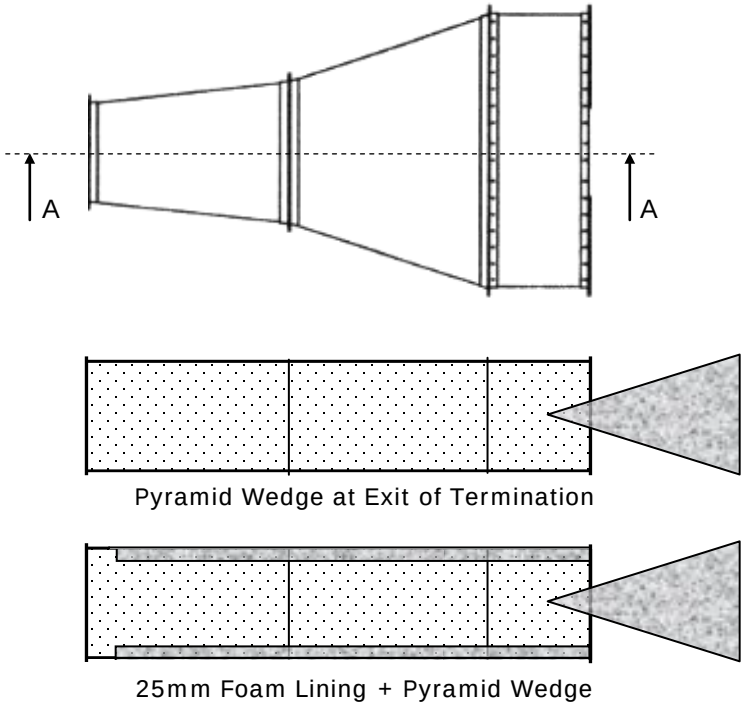

FIGURE 2.18: ALTERATIONS TO ANECHOIC TERMINATION

TABLE 2.5: FINAL PRC VALUES FOR THE ANECHOIC TERMINATION ATTACHED TO THE 540 MM X 300 MM DUCTS

$^1/_3$ Octave Band Centre Frequency (Hz)	**Permissible PRC in ISO 7235**	**PRC of Anechoic Termination**
50	0.40	0.36
63	0.35	0.32
80	0.30	0.26
100	0.25	0.06
125	0.15	0.13
160	0.15	0.11
200	0.15	0.12
250	0.15	0.09
315	0.15	0.07

TABLE 2.6: FINAL PRC VALUES FOR THE ANECHOIC TERMINATION ATTACHED TO THE 270 MM X 300 MM DUCTS

$^1/_3$ Octave Band Centre Frequency (Hz)	Permissible PRC in ISO 7235	PRC of Anechoic Termination
50	0.40	0.38
63	0.35	0.33
80	0.30	0.24
100	0.25	0.15
125	0.15	0.13
160	0.15	0.09
200	0.15	0.10
250	0.15	0.05
315	0.15	0.08
400	0.15	0.09
500	0.15	0.12
630	0.15	0.13

Table 2.5 and Table 2.6 show the final PRC values for the anechoic termination attached to the 540 x 300 mm and 270 x 300 mm duct systems respectively. All the PRC values are within those required by ISO 7235 (1991).

Substitution Duct Insertion Loss

The substitution ducts consisted of typical sheet metal ducting sections. As such, the duct section has an associated insertion loss due to breakout and duct wall vibration. Pink noise was generated in the fan unit and sound pressure levels were taken in the same manner described for determining the pressure reflection coefficients. This ensured that the SPL measurements at each reference plane were not influenced by standing waves in the test rig.

All frequencies were fitted to Equation 2.9. For cases where there were extremely low amplitudes or no standing waves the fitted curve returned wave amplitudes less than 0.01. This left coefficient ‘B’ which gives the resulting insertion loss per metre. The insertion loss of the substitution test sections are shown in Figure 2.19.

Vér (1978) explains the low frequency peak attenuation being due to a resonance phenomenon caused by the mass of the dynamically limp duct walls interacting with the stiffness of the enclosed air volume. Vér gives the resonance frequency (Hz) by Equation 2.10.

$$f_{res} = \frac{c}{2\pi}\sqrt{\frac{\rho}{\rho_s}\frac{P}{A}} \tag{2.10}$$

where c is the speed of sound, ρ is the density of the fluid medium, ρ_s is the mass per unit area of the duct wall, P is the perimeter and A is the cross-sectional area. The equations give a resonance frequency of ~65 Hz for the 540 x 300 mm duct and ~250 Hz for the 270 x 300 mm duct. It can be seen that the resonance frequencies are in reasonable agreements with the peak insertions losses shown in Figure 2.19.

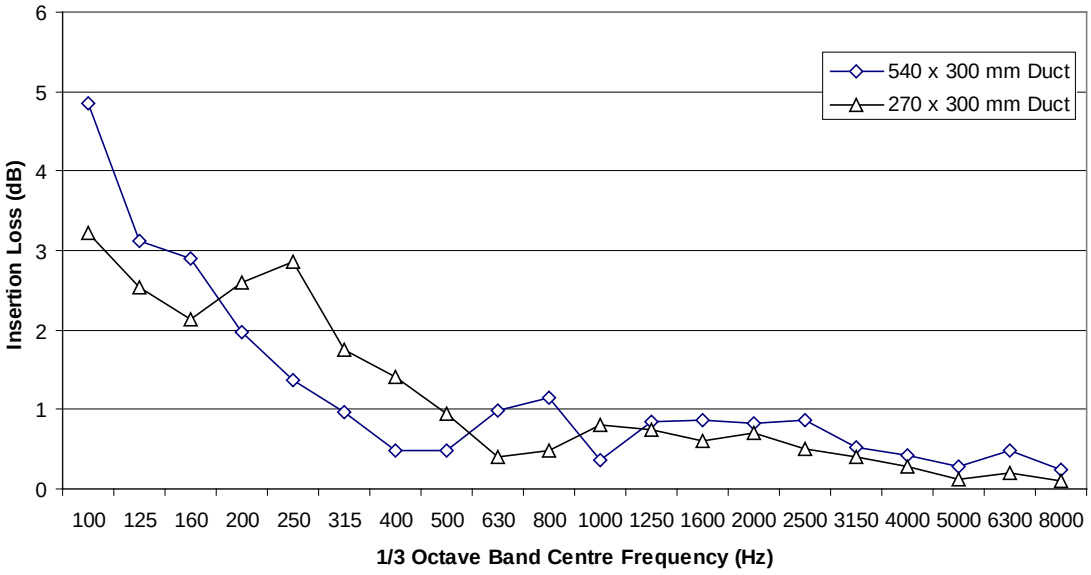

FIGURE 2.19: INSERTION LOSS OF THE SUBSTITUTION DUCTS

2.5 METHODOLOGY

The insertion loss (D) for a duct absorber at a given frequency was calculated by Equation 2.11.

$$D = \overline{L_{pb}} - \overline{L_{pa}} \tag{2.11}$$

where the insertion loss is the difference in the spatial averaged sound pressures before ($\overline{L}_{pb}$) and after ($\overline{L}_{pa}$) the duct absorber has been installed. This gives an insertion loss improvement on the substitution duct. Each spatial averaged sound pressure level was calculated from local sound pressure levels (L_{pi}). For each averaged SPL there were five

measurements for the 540 mm x 300 mm duct and four for the 270 mm x 300 mm duct, at the positions indicated in Figure 2.9 and Figure 2.10.

$$\overline{L}_p = 10\log\left[\frac{1}{n}\sum_{i=1}^{n}10^{0.1L_{pi}}\right] \tag{2.12}$$

Where *n* is the number of measurements. This was repeated for all frequencies of interest (100 Hz – 8000 Hz in 1/3 octave band centre frequencies). SPL readings were measured over 10 second intervals.

Procedure

Using the equipment that has been described in this chapter, pink noise was generated inside the fan housing at approximately 90 dB. The initial sound pressure measurements were taken at reference plane 2 with the substitution duct in place. Sound pressure measurements were recorded in $^1/_3$ octave bands. The substitution duct was replaced with the test specimen and with the same noise (SPL) being generated, the measurements were again recorded. From these two sets of measurements the insertion loss was calculated. The procedure was repeated for the flow rates required. For measurements with a mean flow, the dynamic and static pressures were recorded at reference planes 1 and 2. These pressure measurements were recorded in separate tests from the insertion loss measurements to avoid increased flow noise due to the pitot tubes.

Conventions

Insertion loss is recorded in ‘dB’. For the absorbers in this thesis the insertion loss is for duct silencers of 2.4 metres in length.

2.6 REFERENCES

ISO 7235. 1991 "Measurement procedures for ducted silencers - Insertion loss, flow noise and total pressure loss."

Pettersson, M.J. 2002. *Duct Absorber Design*, a thesis submitted in partial fulfilment of the requirement for a Masters of Engineering degree in the Department of Mechanical Engineering, University of Canterbury.

Vér, I.L. 1978. “A review of the attenuation of sound in straight lined and unlined ductwork of rectangular cross section.” ASHRAE Transactions 84: 122-149

3

EXPERIMENTAL RESULTS

3.1 SUMMARY

This chapter records the testing performed in the duct test facility described in Chapter 2. Various bar-silencers were tested experimentally, with the effect of position, shape, volume, length and duct size investigated. All bar-silencers were constructed of melamine foam for consistency (to minimise the number of variables). The insertion losses of the bar-silencers were compared with ducts lined on two and four sides.

Bar-silencers of varying cross-section (i.e. triangular) were confirmed to outperform other shaped silencers of the same cross-sectional area. These triangular bar-silencers tended to have lower peak insertion loss than the lined section of ducting but attenuated noise over a broader frequency range. Pressure losses due to the bar-silencers were measured at average mean flow velocities between 0 and 25 ms^{-1}. The bar-silencers were found to have significant pressure losses at higher flow rates, which restrict their application to situations where pressure losses are not an issue or where flow velocities are low.

3.2 CONVENTIONS

Schematic representations of each test were used in the key for insertion loss plots and data tables. The outside box represents the end flange of the ducting (Figure 3.1 (a)), while the inside box represents the duct walls (Figure 3.1 (b)). The location and shape of the absorbing material is shown by the shaded region. The bulk absorbing material is abbreviated on the lower right of the schematic (Figure 3.1 (c)); 'MEL' for Melamine foam resin; and 'FIBG' for fibreglass. For lined ducts, the thickness of the material in millimetres is positioned at upper right side of the schematic (Figure 3.1 (d)). For bar-silencers, the cross-sectional area is shown in the same position. Some materials have been tested with a facing, the facing type is presented above the material (Figure 3.1(e)) and attachment method shown by a '-B' for bonded or '-L' for loose-pinned. Facings include; 'TIS' for fibreglass tissue; and 'MET' for 137 g/m^2 metallic foil. These representations are not to scale. The bar-silencers and various duct absorber profiles are shown in Appendix 6.

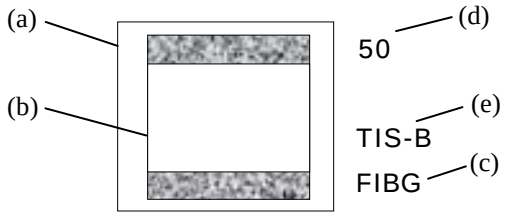

(A)

FIGURE 3.1: EXAMPLE REPRESENTATION

3.2.1 Convention Examples

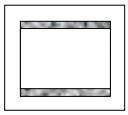

Represents a 25 mm thick lining of fibreglass on the top and bottom faces of the 540 mm x 300 mm ducting. The fibreglass has a tissue fabric bonded to the surface.

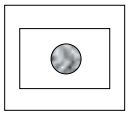

Represents a circular bar-silencer placed in the centre of the 540 mm x 300 mm duct. The circular bar-silencer has a cross sectional area of 27,000 mm^2 and is constructed of melamine foam.

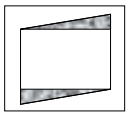

This is two melamine foam triangles giving a total cross-section of 27,000 mm^2. The triangles are positioned to leave an open area consistent with that of a straight unlined 540 mm x 300 mm duct.

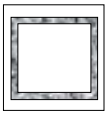

The smaller 270 mm x 300 mm duct lined on all four sides with 25 mm thick melamine foam.

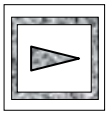

A 13,500 mm^2 cross-sectional melamine bar-silencer positioned centrally in a 270 mm x 300 mm duct lined on all four sides with 25 mm fibreglass.

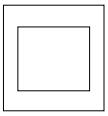

Represents the 270 mm x 300 mm substitution duct with no absorbing material.

3.3 FACILITY VERIFICATION

Traditional rectangular ducts in New Zealand and Australia are usually lined on all four sides. A mat faced fibreglass material, 'Siliner' is the most common product used. Manufactured by Tasman Insulation,

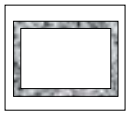

the performance of the product is given as random incidence sound absorption coefficients from reverberation room testing. A constant air flow open area was obtained by increasing duct size to accommodate the absorber thickness.

The measured insertion loss data for all linings and bar-silencers tested can be seen in Appendix 8.

3.3.1 Benchmark Test

In order to validate the insertion loss measurements obtained using the test facility, apart from conforming to the requirements of ISO 7235 (1991), a benchmark test was required to confirm the data produced. There was difficulty obtaining reliable (experimental) data on any common duct linings. 25 mm lined fibreglass (Siliner) was tested and compared to three semi-empirical prediction methods.

Sabine

Duct attenuation prediction in New Zealand has often relied upon the Sabine (1940) formula:

$$\text{Attenuation} = 1.05\frac{P}{A}\alpha^{1.4} \tag{3.1}$$

where P is the perimeter of duct lined with absorbent, A is the cross-sectional area of duct and α is the random incidence sound absorption coefficient of the lining for a given frequency. Although this formula is only valid for frequencies where the duct width is less than $^1/_{10}$ of the wavelength of the sound, it is commonly extended to cover the entire frequency range. The formula is known to under predict sound attenuation in ducts at most frequencies.

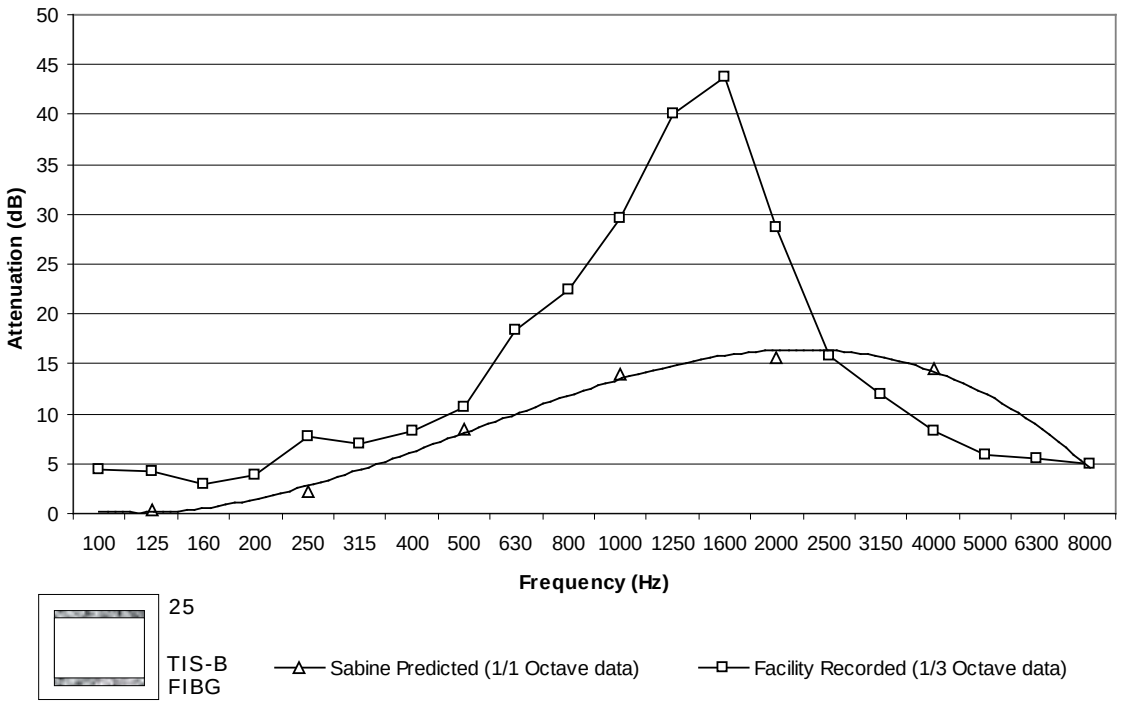

FIGURE 3.2: SABINE PREDICTED ATTENUATION DUE TO 25 MM SILINER

There are limited Sabine predicted points plotted, as the Sabine formula uses sound absorption coefficients, and the manufacturer's data was provided in octave bands. Figure 3.2 shows that the Sabine formula has considerably under predicted the insertion loss of the Siliner duct lining. Calculations and values are presented in Appendix 7 (A.7.1).

Wassilieff

Unlike the Sabine formula, Wassilieff (1985) prediction scheme utilizes design curves showing the characteristic attenuation of the fundamental mode for a particular frequency. There is a specific design curve for each material (brand and thickness) and duct size. Wassilieff's attenuation for square ducts at a given frequency is given by Equation 3.2.

$$\text{Attenuation} = (C \times \frac{l}{d}) + H \tag{3.2}$$

where C is the characteristic attenuation of the fundamental mode, l is the total continuous lined length of ducting, d is the duct width and H is the attenuation due to higher order modes. This equation can be extended for rectangular ducts, in this case the attenuation is assumed to be equal to the sum of half the attenuation due of square ducts of size equal to both the height and width of the rectangular ducting. This gives Equation 3.3:

$$\text{Attenuation} = \frac{1}{2}(C_a \times \frac{l}{d_a}) + \frac{1}{2}(C_b \times \frac{l}{d_b}) + H \tag{3.3}$$

where subscript a is the rectangular duct height and b is the rectangular duct width.

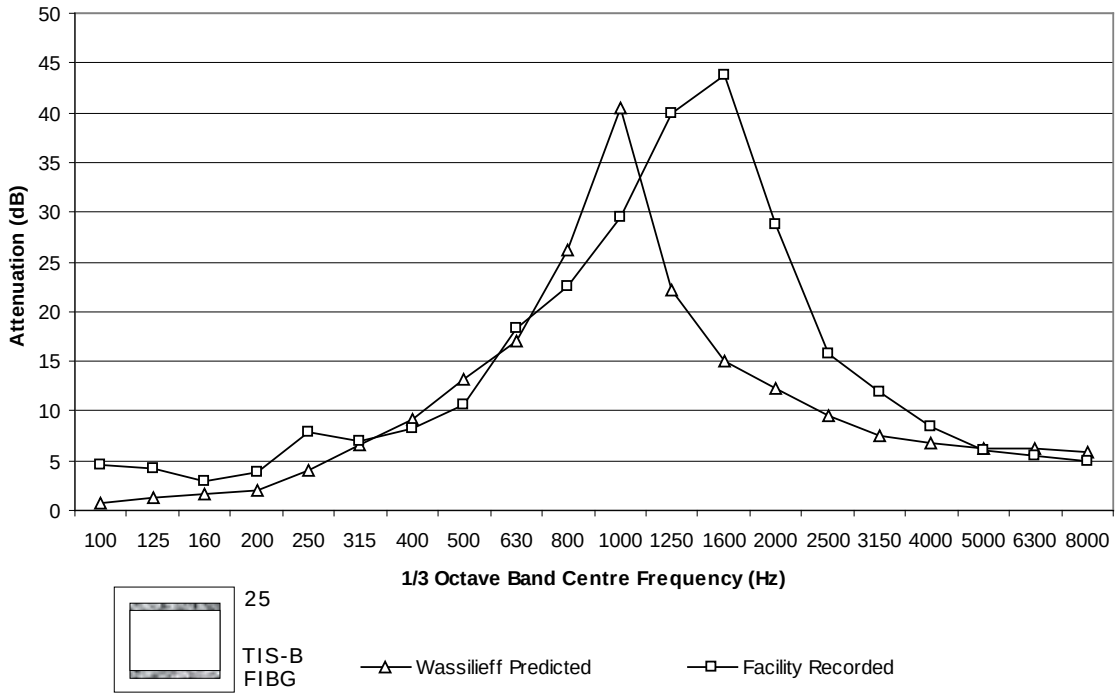

FIGURE 3.3: WASSILIEFF PREDICTED ATTENUATION DUE TO 25 MM SILINER

When compared to the measured results (Figure 3.3), the predicted curve has a peak absorption shifted two $^1/_3$ octave bands to the left. As the ducting was rectangular, Equation 3.3 was used. However, only the wider side of the ducting was lined, which means the predicted curve is obtained from half of a square 540 mm x 540 mm duct. The fact the ducting is rectangular, was effectively ignored, the resulting predicted curve was thus moved to the left. The curve has generally under predicted the absorption in all frequencies except for the peak absorption at 1000 Hz. Calculations and values are presented in Appendix 7 (A.7.2).

Vér

This method is a graphical method for porous materials, based on a dimensionless variable constructed from the perimeter of lined ducting, cross-sectional area and the length of straight lined ducting.

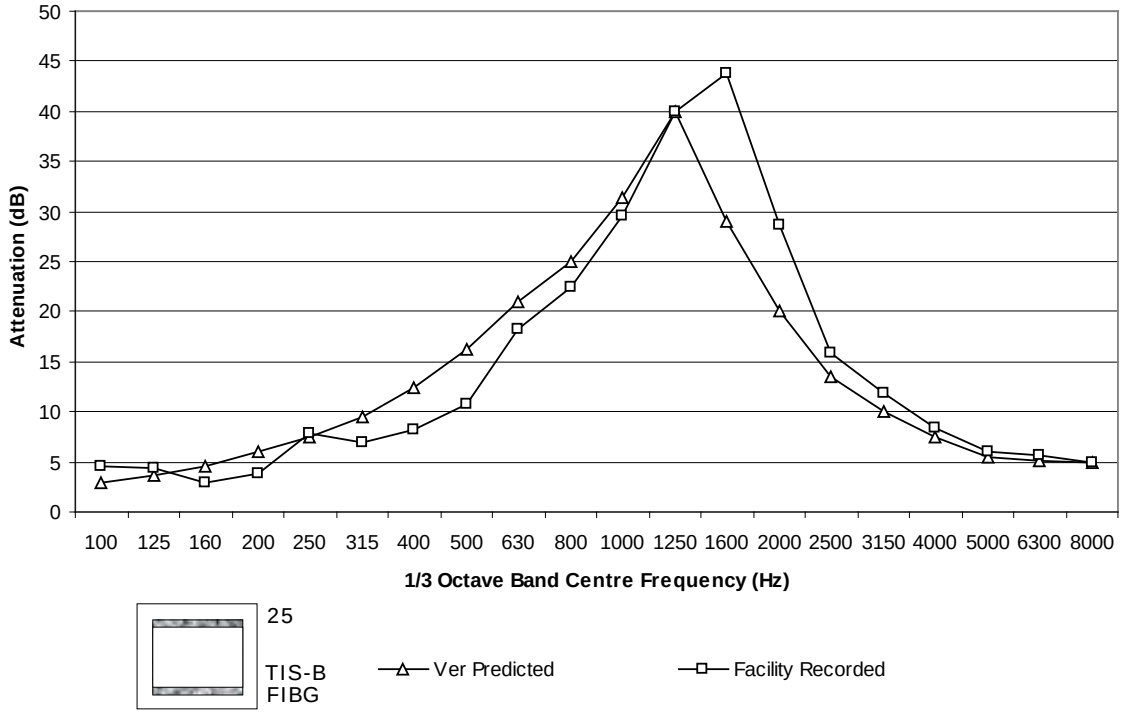

FIGURE 3.4: VÉR PREDICTED ATTENUATION DUE TO 25 MM SILINER

The Vér predicted attenuation due to the duct lining follows the actual measured data well both at low and high frequencies. The only discrepancy is at the peaks where the predicted attenuation has its peak $^{1}/_{3}$ octave lower, and slightly under predicts the actual attenuation. Calculations and values can be seen in Appendix 7 (A.7.3).

Although actual attenuation data for the Siliner in the same duct size was unobtainable, the Wassilieff and Veŕ prediction methods have shown similar trends. Wassilieff's method did

not take into account the shape of the duct, while the material properties in this work are likely to be different from Vér. Hence, actual data was always expected to deviate from these methods. With the test facility adhering to the ISO standard, and the results aligning with the more recent prediction methods, confidence in the results has been obtained.

3.3.2 Cross Modes

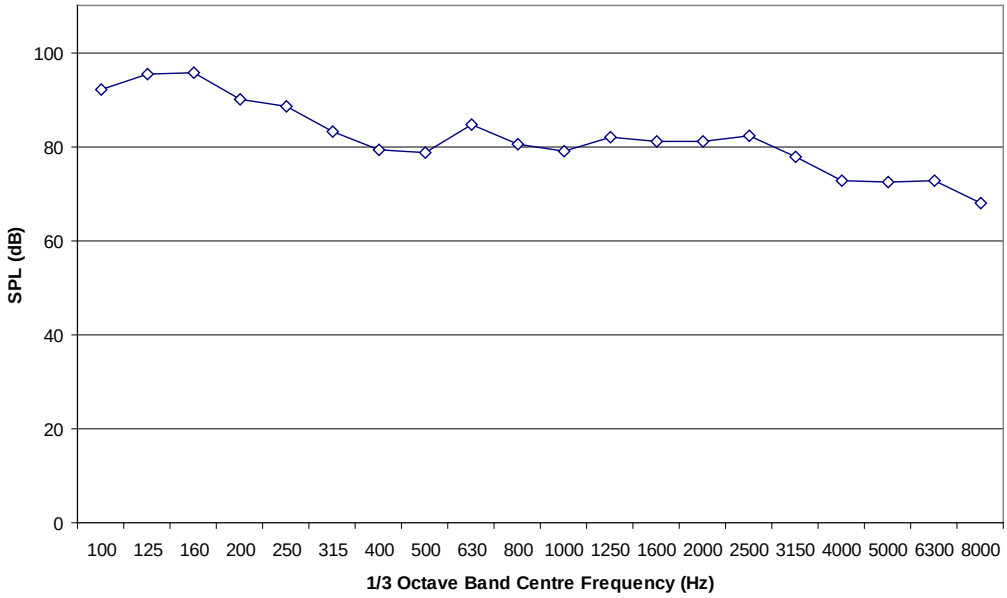

FIGURE 3.5: SPL VALUES IN THE 540 MM X 300 MM SUBSTITUTION DUCT

The SPL values presented in Figure 3.5 for the 540 mm x 300 mm duct show an increase at 630 Hz. This increase has been associated with wavelength cross-mode of equal length to the duct height. The 630 Hz frequency corresponds to a ½ wavelength of 0.29 m, approximately the same width as the test duct. This rise in SPL is not as marked in the presence of a test absorber, and hence the reported insertion loss data probably shows an increased insertion loss in the 630 Hz $^{1}/_{3}$ octave band centre frequency. As the ducting is rectangular, it could be expected the same phenomena would be seen at the ½ wavelength

corresponding to the duct width. This duct height (0.54 m) falls within the 315 Hz $^1/_3$ octave band centre frequency, but the increase in insertion loss is not as pronounced.

Both ½ wavelength cross-modes of the 270 mm x 300 mm duct lie within the 630 Hz $^1/_3$ octave band centre frequency. However, this band did not show significant evidence of the cross modes.

3.4 ABSORBER MATERIAL

Basotect melamine foam was used throughout the test procedures. Basotect is a light weight, open cell foam, which has a self-supporting structure allowing various shapes to be cut from bulk material. Made from melamine resin, a thermoset plastic from the aninoplastics group, the material has a density of 11 kgm^{-3}. Basotect is easy to work with, due to the absence of fibres and toxins. This also makes it ideal for situations where air-borne fibres are unacceptable, such as in hospitals and laboratories.

Basotect melamine foam has similar random incidence absorption coefficients as the traditional Siliner (fibreglass), with the fibreglass performing slightly better at most frequencies. This similar performance can be seen in Figure 3.6 for the insertion loss of 25 mm thick absorbers lining two sides of the ducting. The figure shows the two materials having a similar trend, with the fibreglass Siliner, having higher insertion losses than the Basotect melamine foam in low to mid frequencies below 2500 Hz. Only the melamine

foam was used for the construction of bar-silencers as fibreglass is not suitable for the bar-silencers, by keeping the material constant, other factors influencing the insertion loss could be experimentally identified.

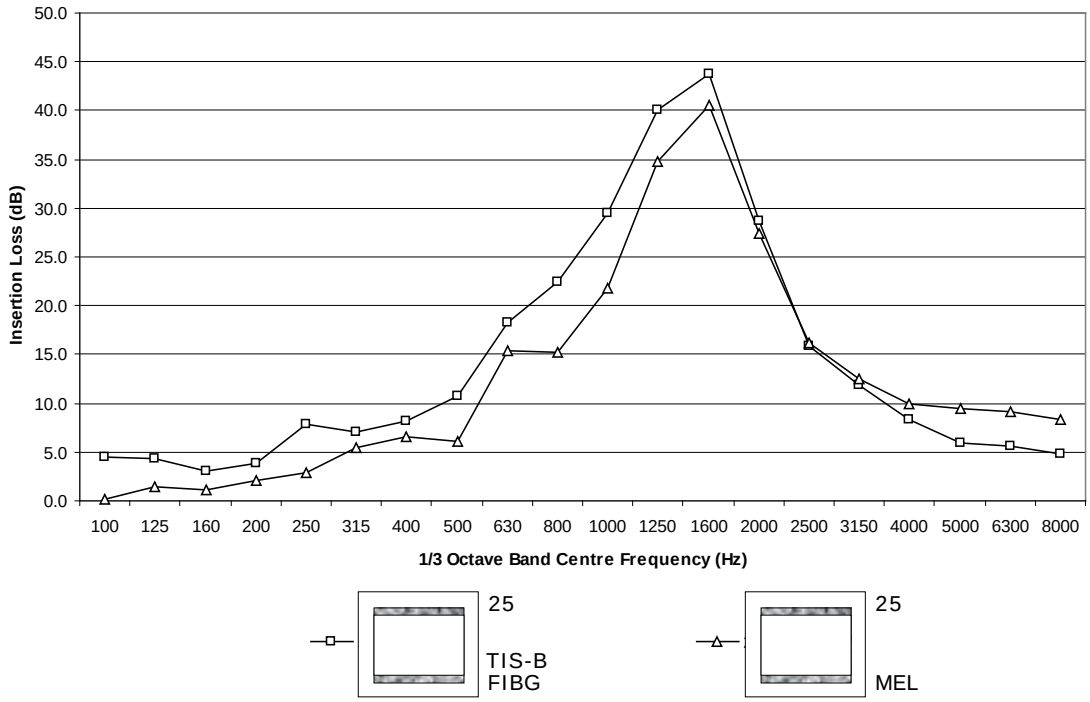

FIGURE 3.6: 25 MM LINING COMPARISON BETWEEN SILINER FIBREGLASS AND BASOTECT MELAMINE FOAM

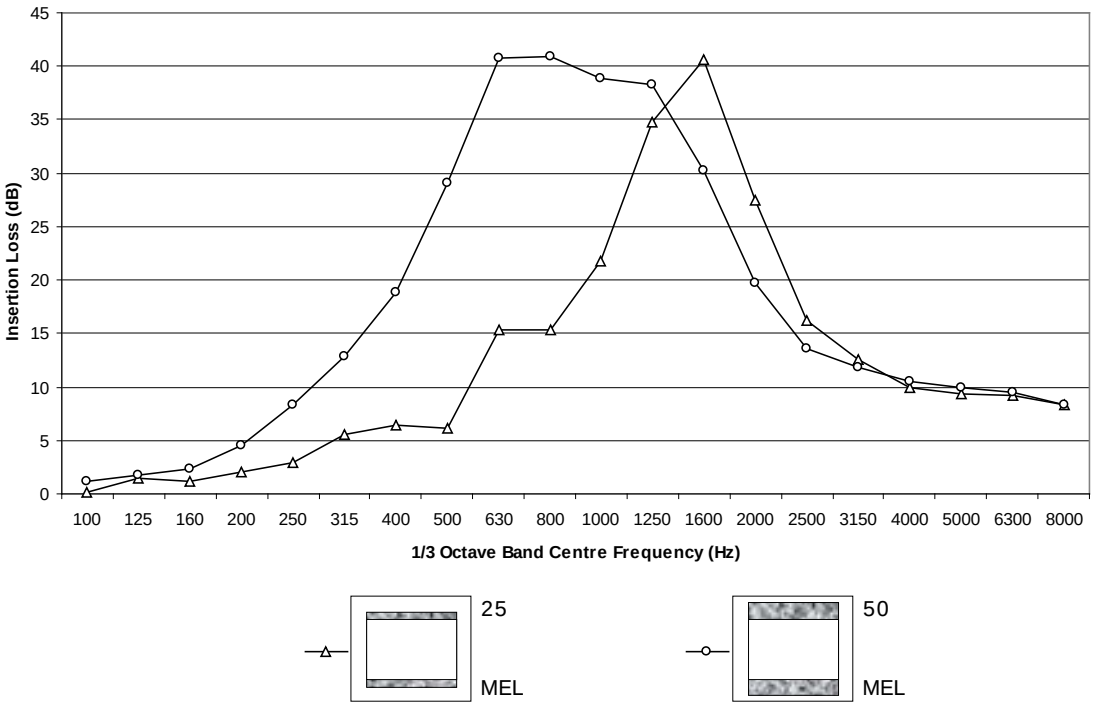

FIGURE 3.7: VARIATION IN LINING THICKNESS FOR MELAMINE FOAM

Two duct lining thicknesses were tested (Figure 3.7), and their insertion loss characteristics compared. Both configurations had a constant open area and the samples were fixed to the duct walls with pins. The 25 mm thick melamine foam was seen to have significant peak absorption in the 1600 Hz $^1/_3$ octave band. The thicker wall lining broadened the absorption and moved the peak towards lower frequencies, so that, the peak lay between the 630 and 1250 Hz $^1/_3$ octave bands. On both plots the insertion loss in the 630 Hz $^1/_3$ octave band was probably less than indicated above due to the higher order cross mode mentioned earlier. It would be expected that the peak absorption lay at the ¼ wavelength, which corresponds to the thickness of the duct linings. However, the peak absorption seems to be at half of this frequency, with ¼ wavelengths of 25 mm at 3400 Hz and 50 mm at 1700 Hz, while the peak absorption occurs at ~1600 Hz and ~800 Hz respectively.

3.5 BAR-SILENCER SHAPE

The effect of bar-silencer shape was the first factor to be investigated. Three different melamine shapes with a constant cross-sectional area of 27,000 mm^2 were tested. The tests were performed in the 540 mm x 300 mm substitution duct with no flow. The three shapes consisted of a square, isosceles triangle and a circle, all with a length of 2.4 m. The dimensions of each bar-silencer were such that each shape had the same volume of material, unless otherwise stated.

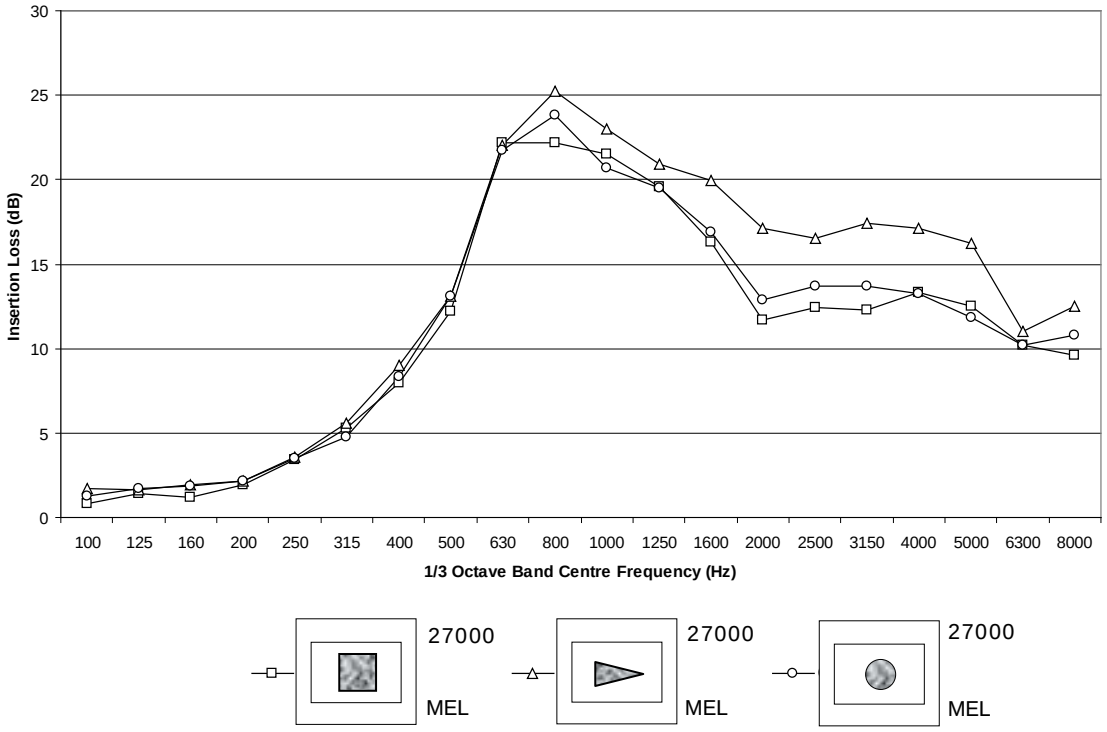

FIGURE 3.8: BAR-SILENCER TEST ON SHAPE

The measured results were comparable with previous experimental work done by Pettersson (2002) showing the same trends for the bar-silencers. The isosceles triangle was

seen to have a greater insertion loss above the 630 Hz $^1/_3$ octave band. It was initially thought that the higher insertion loss may have been a function of exposed surface area.

TABLE 3.1: BAR-SILENCER EXPOSED SURFACE AREA

Bar-Silencer Shape	**Area** m^2
Square	1.6
Isosceles Triangle	2.0
Circle	1.4

As can be seen from Figure 3.8, the circular bar-silencer outperformed the square silencer in the mid to high frequencies. However, the square bar-silencer had a greater surface area than that of the circular bar-silencer (Table 3.1). It was concluded that although possibly still a factor, the exposed surface area was not the dominating factor influencing the insertion loss.

Further shapes were not tested, as increasing the number of sides on a polygon past four, starts to approach the circular silencer in shape. Other abstract shapes were not tested as the number of shapes possible would be limitless.

The square bar-silencers have been previously investigated by both Nilsson and Söderquist (1983) and by Cummings and Astley (1996). Direct comparisons with their results were not possible. Nilsson and Söderqvist (1983) experimentally tested an array of bar-silencers, as opposed to a single silencer. Their bar-silencers were constructed from an unspecified

material. Cummings and Astley's 0.4 x 0.4 m bar-silencers were also arranged in an array and constructed of Rockwool, again making comparison difficult.

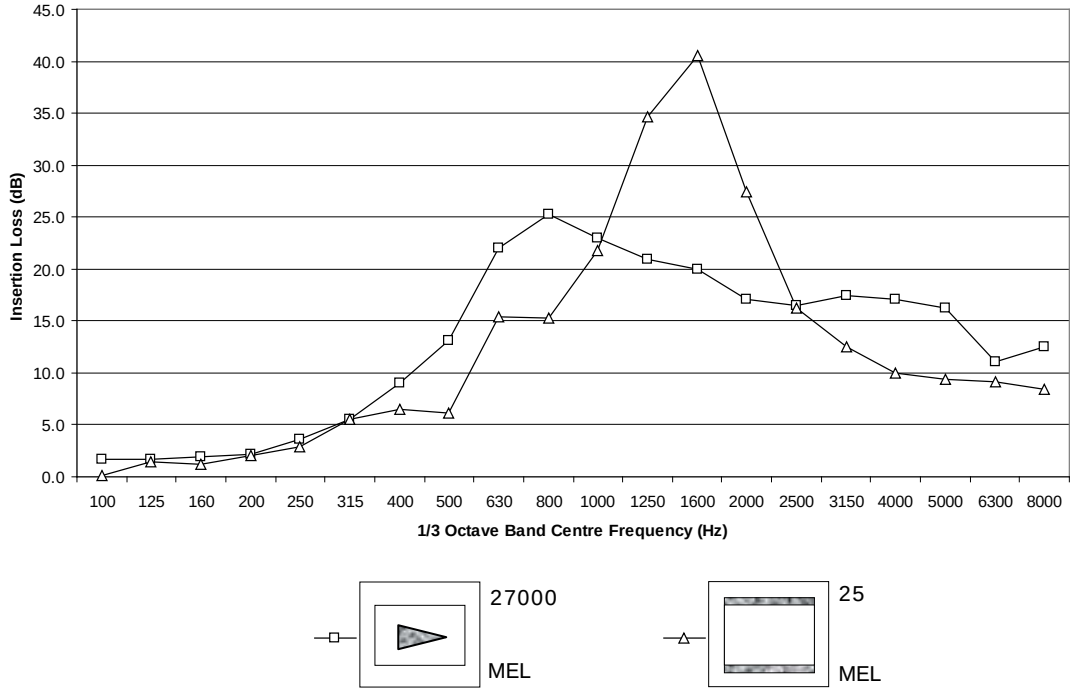

FIGURE 3.9: INSERTION LOSS COMPARISON OF 25 MM LINING AND ISOSCELES TRIANGLE

The duct lined with 25 mm on two sides corresponded to the same volume of material used for the bar-silencers of 27,000 mm^2 cross-sectional area. The isosceles triangular bar-silencer shows the peak absorption being shifted towards lower frequencies, while the 25 mm lining shows a larger peak (Figure 3.9). It was seen that the triangle bar-silencer showed an increased insertion loss both above and below the 1600 Hz peak shown by the 25 mm thick lined section. The 25 mm duct lining was pinned to the walls, it has been previous determined that linings 'pinned' to the duct walls acoustically outperform those 'bonded' (Pettersson, 2002). This improved performance may be the result in change of

boundary condition, in the way the lining interacts with the duct walls and how the duct walls vibrate.

3.6 EFFECT OF THICKNESS VARIATION

Conclusions from previous work on duct absorbers including bar-silencers (Pettersson 2002) indicated that an improvement in insertion loss of triangular bar-silencers over other shapes may have been due to a change in cross-section of the absorbing material. To experimentally test this hypothesis, two absorbers were tested, each absorber having the same volume of material as well as the same exposed area to the duct. One section consisted of 25 mm lined ducting on two sides, while the other section utilized an angled duct section where the absorbing material varied in thickness from 0 to 50 mm. The test was performed with no mean flow.

The wedge shaped absorbers (Figure 3.10) showed a lower peak insertion loss in the 1600 Hz $^{1}/_{3}$ octave band than the 25 mm lined section. This trend followed that of the results for the isosceles triangle shown in Figure 3.9 with a wider spectrum giving greater insertion loss above and below the peak.

The change in duct shape obviously changed the duct modes within the duct. How this affected the resulting measured insertion loss of the wedge absorbers was unclear. It is known that thicker materials move the peak absorption to the left and have increased lower

frequency absorption. This phenomenon is seen in both in random incidence sound absorption as tested in reverberation rooms and in duct insertion loss as seen in Figure 3.7.

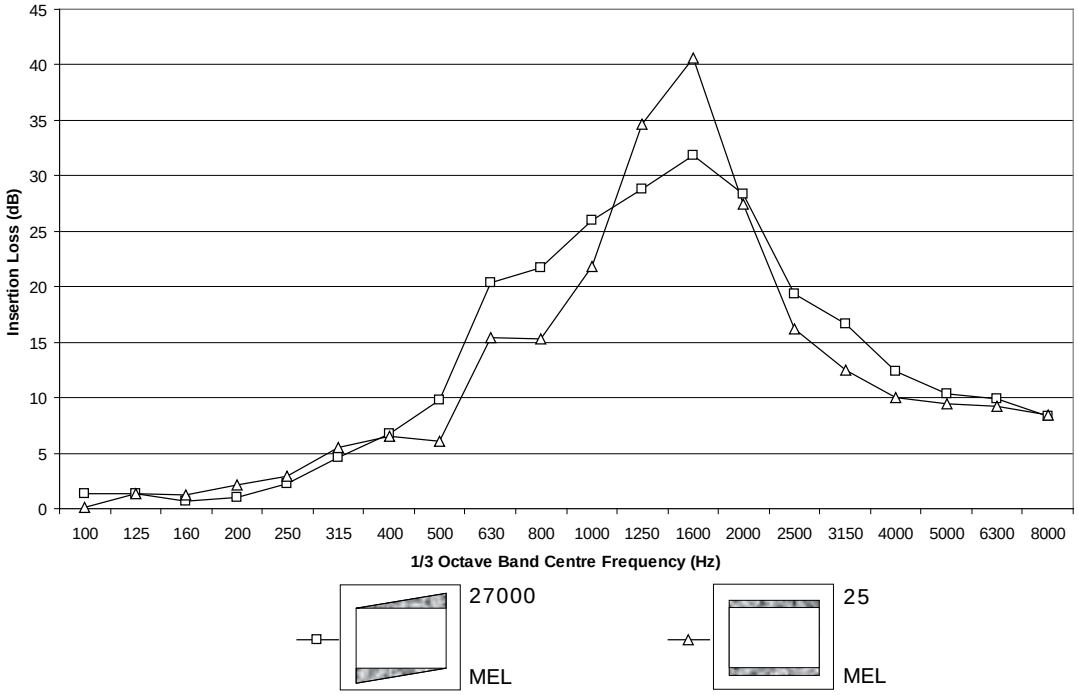

FIGURE 3.10: COMPARISON OF WEDGE SHAPED AND 25 MM THICK WALL LININGS

Reverberation room tests

The 25 mm and wedge shaped duct linings were tested in a reverberation room to assess their random incidence sound absorption characteristics. A number of tests performed by Parkinson (1999) on contoured foam absorbers concluded that although there are some slight variations, that the average thickness of the absorber was the dominant variable for absorber performance.

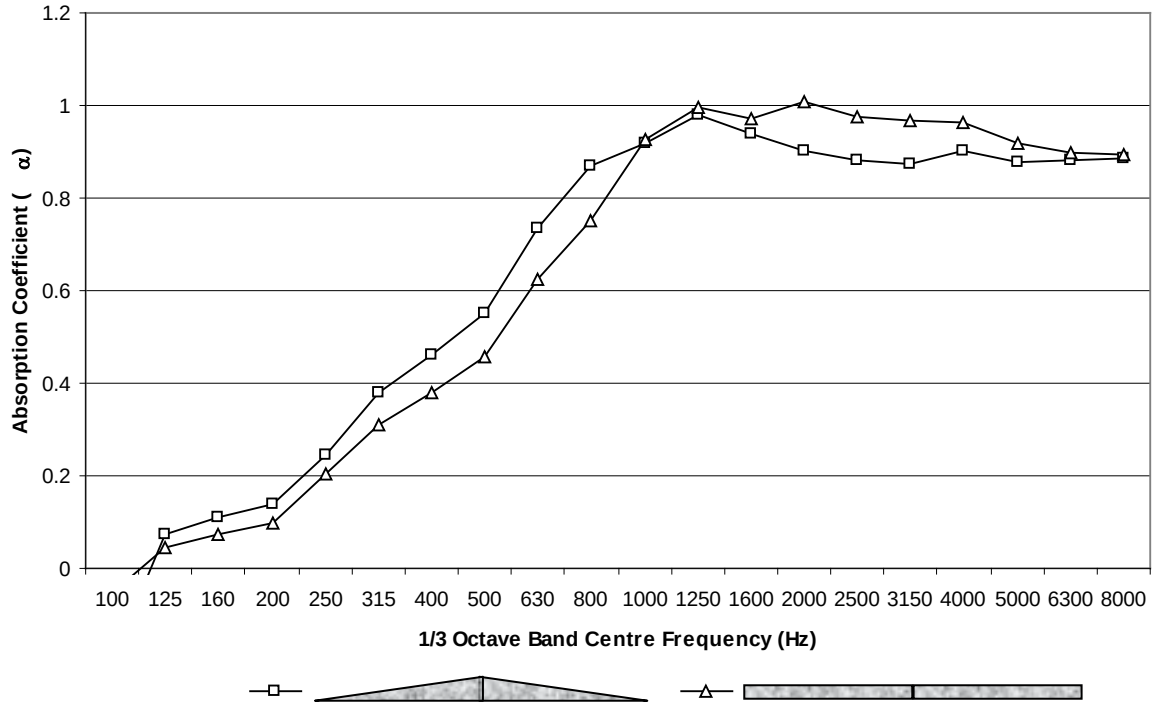

FIGURE 3.11: ABSORPTION COEFFICIENTS FOR WEDGE DUCT LININGS

To remove edge effects from the test specimens, medium density fibreboard (MDF) frames were used around the 25 mm samples and the wedge absorbers were placed 'back to back' (Figure 3.11). From the results, it can be seen that, the wedge lining had greater sound absorption at frequencies below 1000 Hz, while dropping below the sound absorption of the 25 mm thick lining above the 1000 Hz $^{1}/_{3}$ octave band centre frequency. This demonstrates that random incidence sound absorption is not necessarily related to duct attenuation. This is shown with the reversal of performance at high frequencies when the linings are placed in the duct. This trend at high frequencies in the reverberation room is contrary to that in the duct where the triangular linings at higher frequencies show improved absorption.

3.7 BAR-SILENCER POSITION

A smaller cross-sectional area (13,500 mm^2) equilateral triangle was used to investigate the effect on insertion loss due to position within the duct. The equilateral triangle was positioned in the middle, bottom centre and bottom left corner of the substitution duct. All tests were measured in the absence of a mean flow.

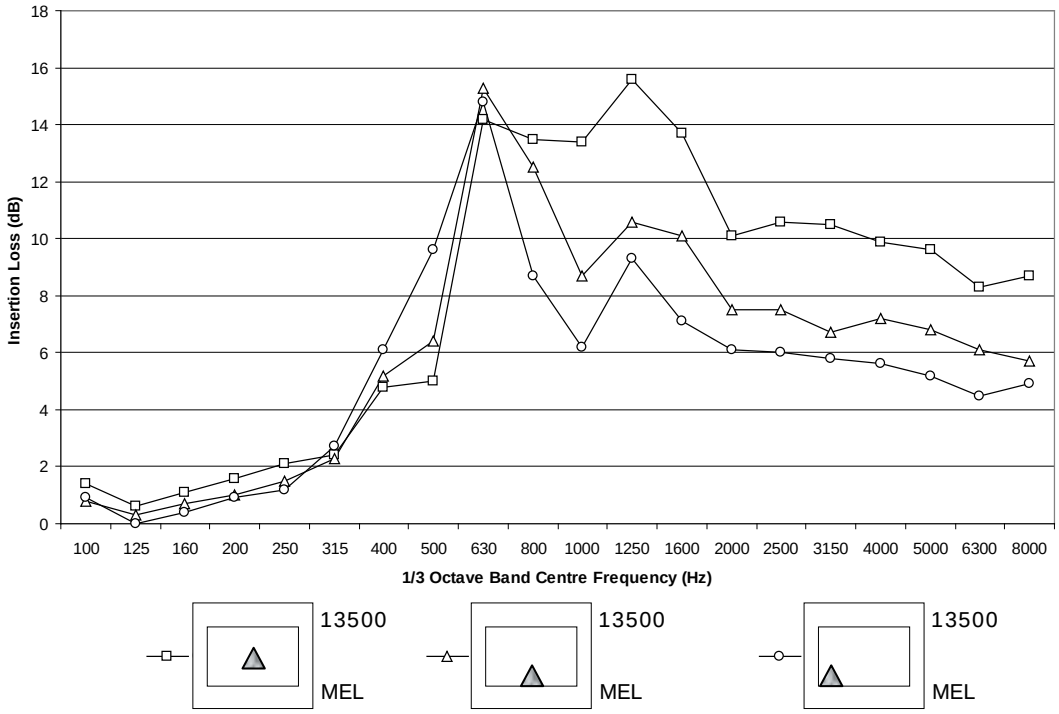

FIGURE 3.12: VARIATION OF EQUILATERAL TRIANGLE POSITION IN SUBSTITUTION DUCT

The results (Figure 3.12) showed that as the bar-silencer was moved away from the centre of the duct, the insertion loss, especially in the higher frequencies, was reduced. This result was expected as the absorbing material has less 'contact' with the noise field. There appears to be discrepancy in the measured results in the 630 Hz and possibly 1250 Hz $^1/_3$

octave bands. The cause of these phenomenon was unclear, although the two discrepancies again corresponded to the cross-modes of equal length to that of the duct height and width respectively.

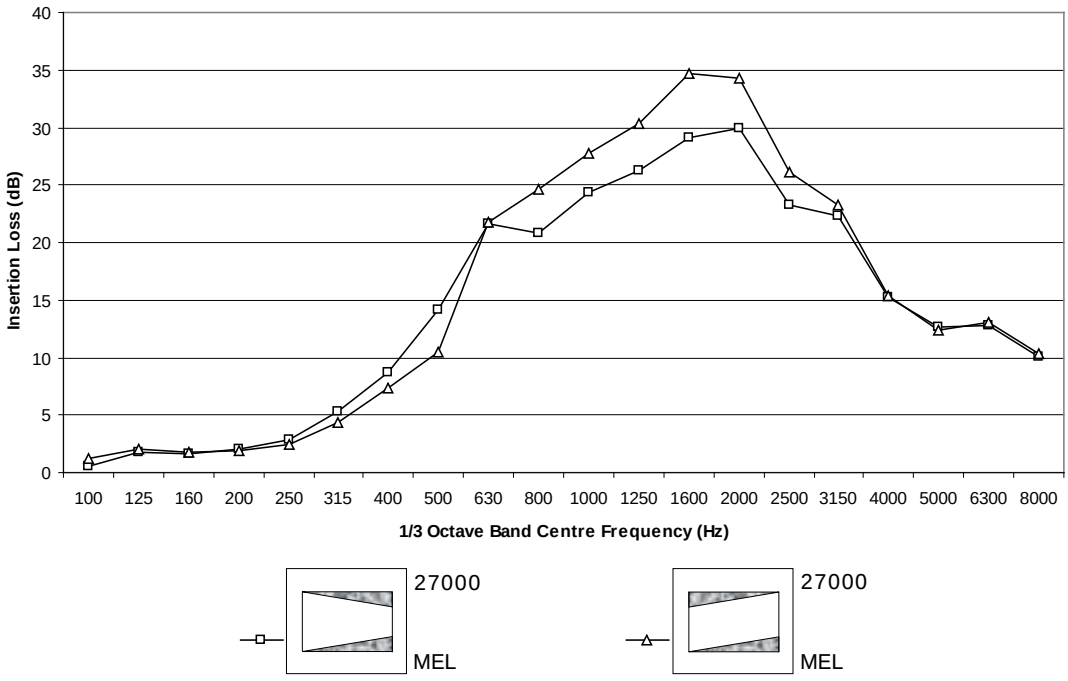

FIGURE 3.13: EFFECT OF WEDGE SHAPED ABSORBER ORIENTATION

Using the same wedge absorbers as in Figure 3.10, the effect of absorber orientation inside the substitution duct was investigated. Figure 3.13 shows that the system with the thicker sections at alternate sides of the substitution duct had greater insertion loss in mid frequencies. For the system with the thicker sections arranged along the same side of the ducting, it was thought that the sound was 'beaming' down the left hand side of the duct. This was confirmed by the SPL measurements at the exit end of the absorbers with the wedge absorbers installed, showing (Figure 3.14) an increase in SPL where there was less absorbing material.

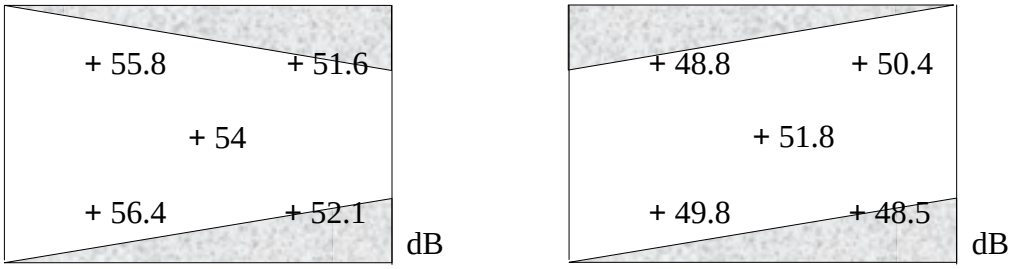

FIGURE 3.14: SPL VARIATION IN DUCT WITH WEDGE ABSORBERS INSTALLED AT 1600 HZ

3.8 TRIANGULAR BAR-SILENCER SIZE

Three equilateral triangles with different volumes of material (27,000 mm^2, 20,250 mm^2 and 13,500 mm^2) were positioned in the centre of the substitution duct and insertion loss measured. The results were recorded with no mean flow.

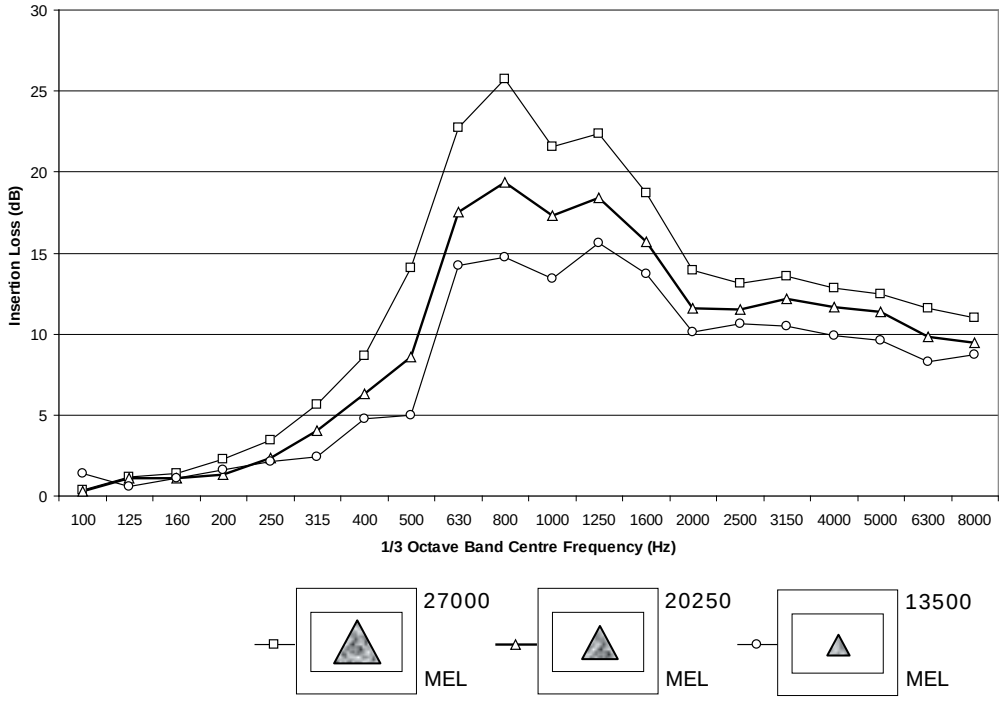

FIGURE 3.15: INSERTION LOSS FOR VARIOUS SIZES OF EQUILATERAL TRIANGULAR BAR-SILENCERS

The results showed the insertion loss increases with increasing volume of material, increase in exposed surface area and a decrease in the ratio between open area and material area. It was expected that, although following the same trend as triangles of smaller volume, that the larger volume triangles would have shifted the peak absorption to lower frequencies as is the case with the thicker duct wall linings as shown in Figure 3.7.

3.9 TRIANGULAR BAR-SILENCER ASPECT RATIO

Three triangles of the same volume of material (27,000 mm^2) were placed in the centre of the substitution duct. The triangles varied in aspect, from an equilateral triangle to a triangle which stretched the width of the duct. It was thought that the longest aspect ratio triangle could be affected by one side of the triangle being in contact with the duct wall.

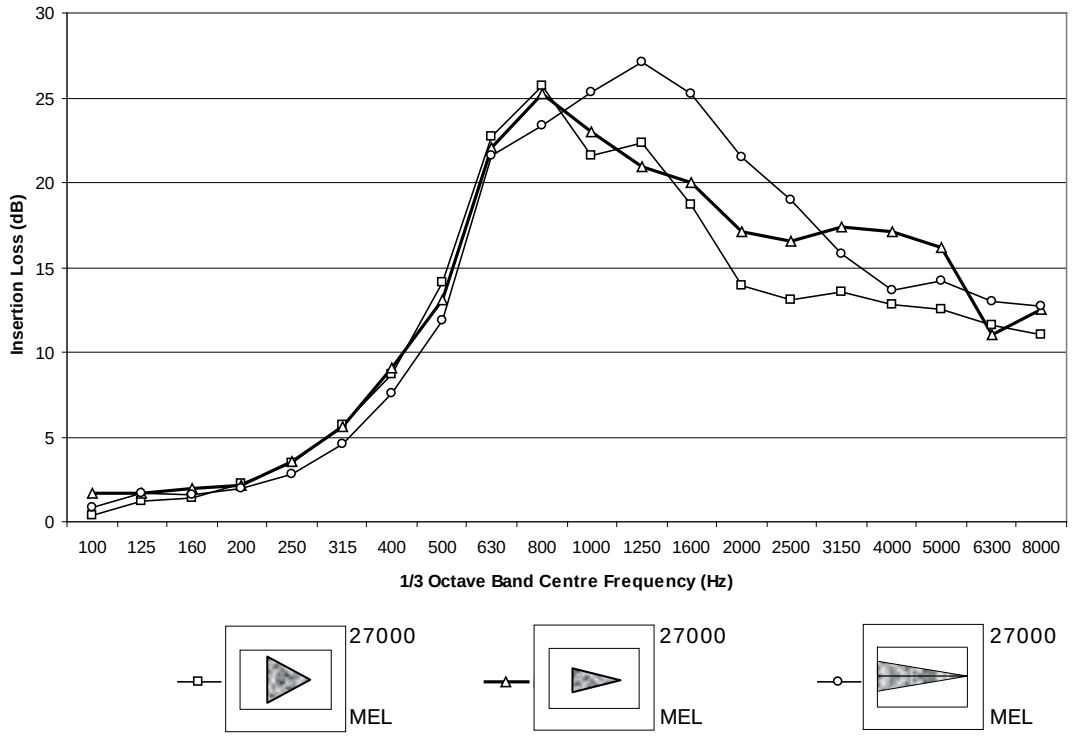

FIGURE 3.16: VARIATION IN TRIANGLE ASPECT RATIO

All three bar-silencers perform similarly at frequencies below 630 Hz. There is some evidence that in the mid to high frequencies, the higher the aspect ratio of the bar-silencer, the greater the insertion loss.

3.10 EFFECT OF BAR-SILENCER LENGTH

A consideration for the practical use of bar-silencers is that there may be limited lengths of straight ducting available in real situations. For such cases shorter length bar-silencers may have to be employed. A constant cross-section equilateral triangle bar-silencer was positioned in the substitution duct and the length increased in increments of 0.6 m.

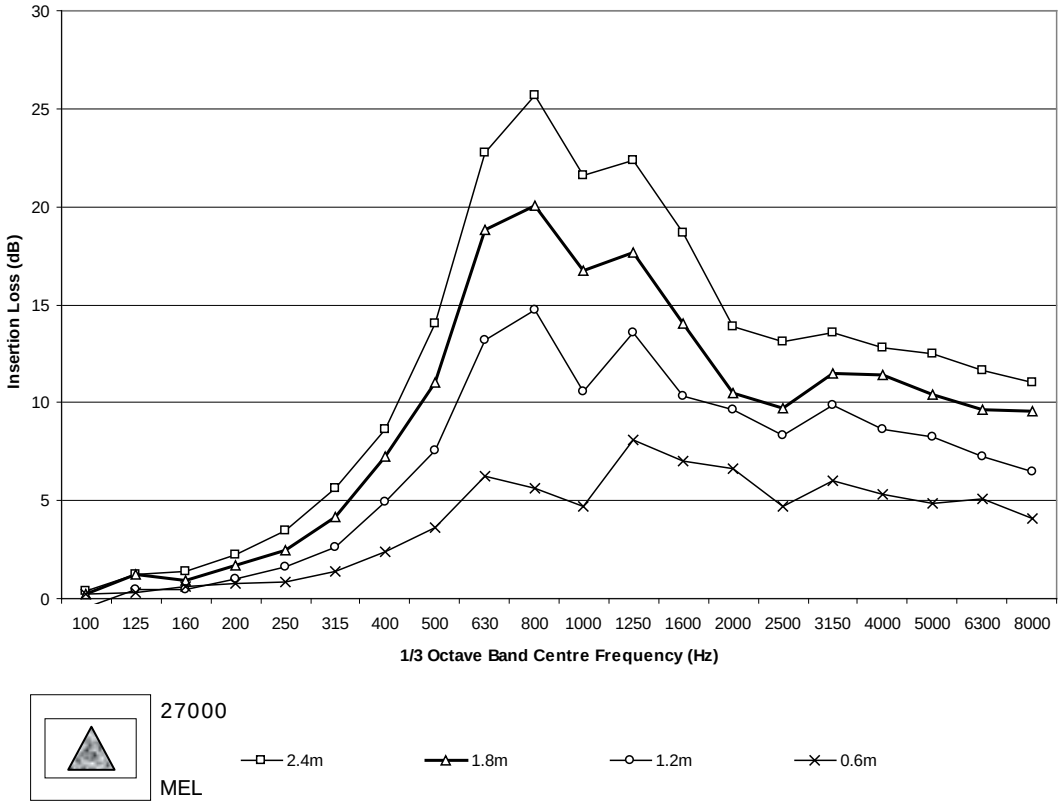

FIGURE 3.17: EFFECT OF BAR-SILENCER LENGTH

All four bar-silencers, have the same end conditions and should have similar end effects. The results show that the returns per extra 0.6 m length slowly diminish.

3.11 MISCELLANEOUS 540 MM x 300 MM DUCT TESTS

3.11.1 Parallel and Wedge Linings

Some miscellaneous tests were carried out in the test facility which did not directly relate to the investigation of bar-silencers. Figures 3.18 and 3.19 show the effect of material lining position, the same linings were positioned on the inside of the substitution duct and then placed in sections of ducting which would allow for the thickness of the material, giving a constant open area along the duct.

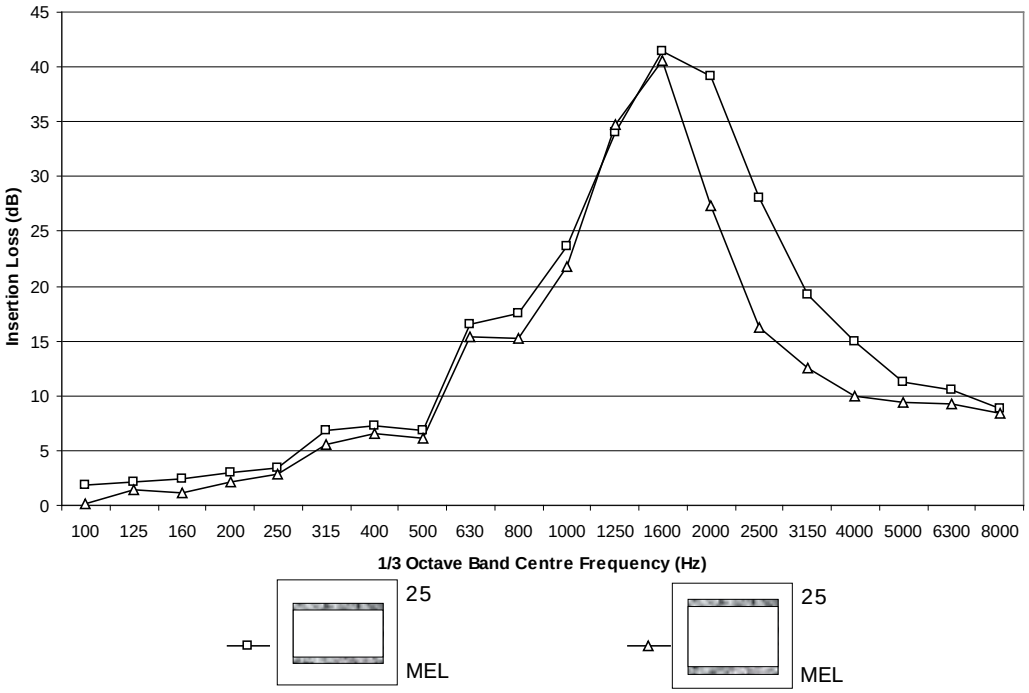

FIGURE 3.18: EFFECT OF 25 MM LINING POSITION

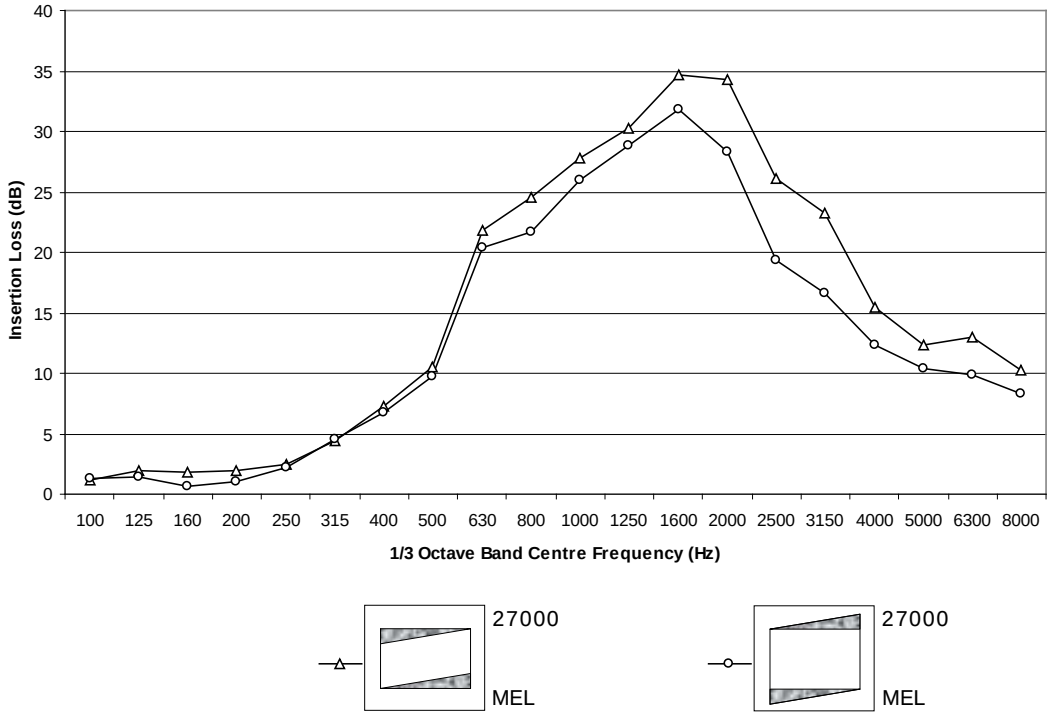

FIGURE 3.19: EFFECT OF WEDGE ABSORBER LINING POSITION

A larger increase in low frequency insertion loss was expected for the cases of the linings on the inside of the ducts. For the linings on the inside of the substitution duct, the increased insertion losses were attributed to the end effects of the linings which were exposed to the noise field, and the decrease in the open area ratio. The open area is reduced when the linings are positioned on the inside of the substitution ducting.

3.11.2 Position of Linings

An investigation into the positions of the lining in the duct (resembling a conventional splitter silencer) was undertaken. The simplified test was performed in the substitution duct

without a mean flow. Two 25 mm melamine foam linings were moved from the outside of the duct towards the centre until they formed a 50 mm splitter in the centre of the duct.

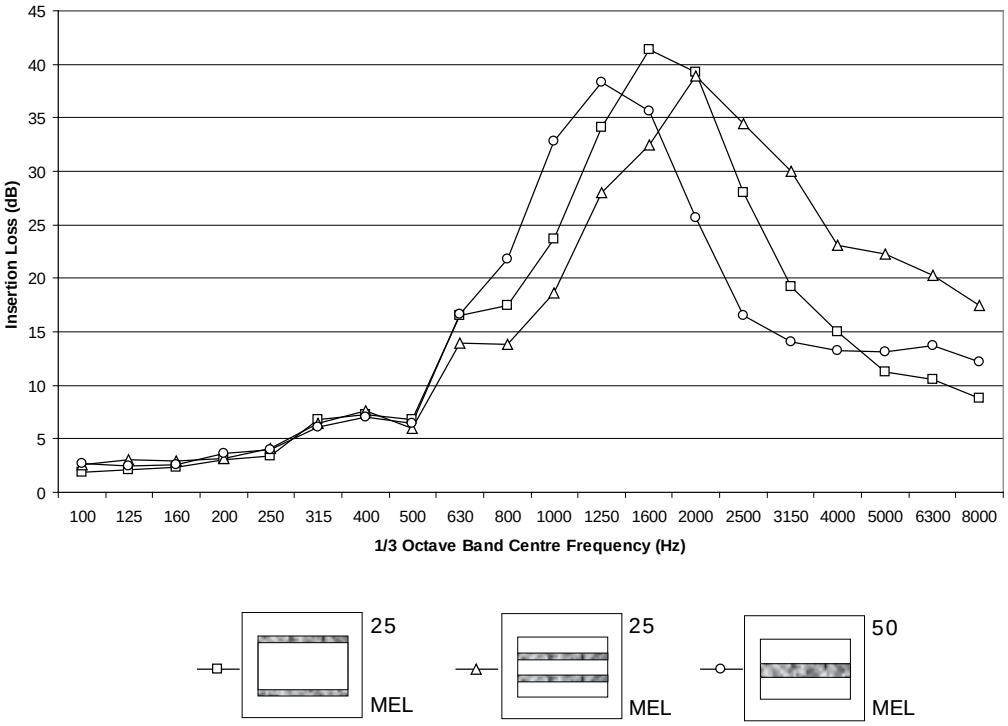

FIGURE 3.20: BASIC SPLITTER SILENCER EXAMPLE

In comparison to the 25 mm linings against the outside of the duct (Figure 3.20), when the linings were positioned with equal spacing between the linings the insertion loss peak moved to the right a single $^{1}/_{3}$ octave band centre frequency, giving substantially larger attenuation at higher frequencies. When the two linings came together in the centre, the peak then moved to lower frequencies, with the material now acting as a 50 mm thick absorber as opposed to two 25 mm individual absorbers. This shift towards low frequencies is consistent with the thicker duct wall lining tested in Figure 3.7.

3.11.3 Combination of Linings

The combination of duct linings with a triangular bar-silencer was tested, and the results are shown in Figure 3.21. The combination gave good insertion loss across the measured spectrum, even increasing attenuation at lower frequencies. In situations where the current sound attenuation method is not providing the required noise attenuation, a bar-silencer could be easily inserted to combine with existing linings and increase the insertion loss at all frequencies.

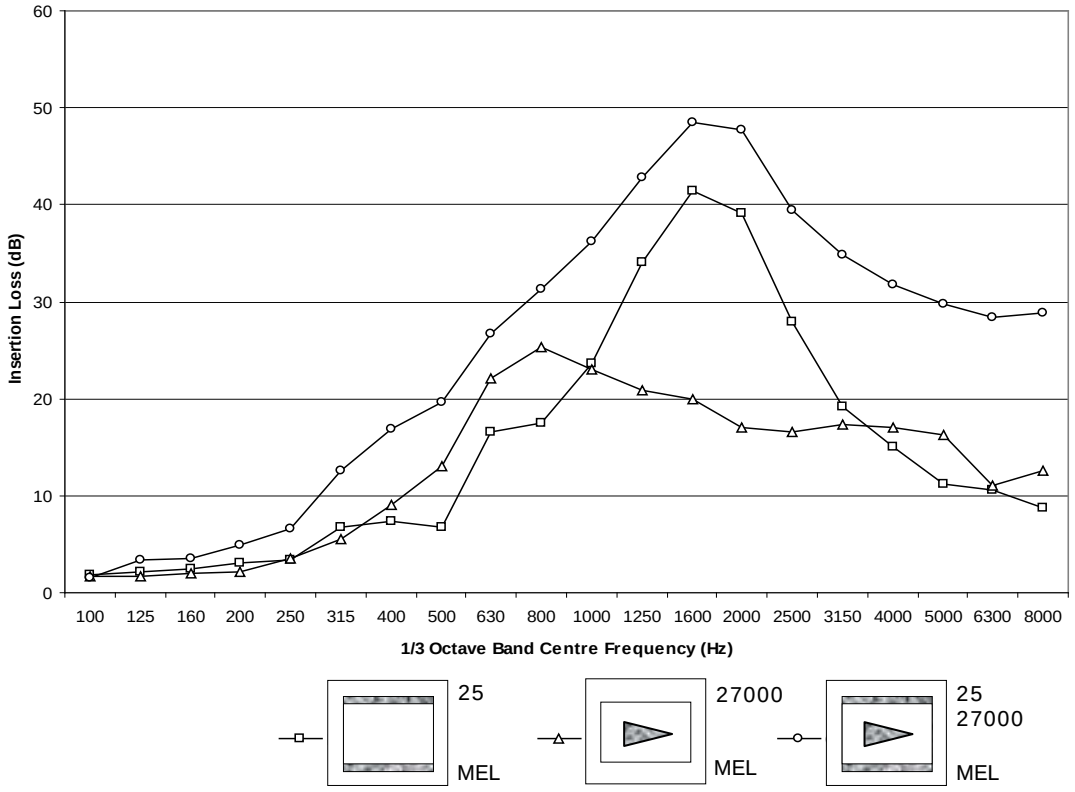

FIGURE 3.21: BAR-SILENCER COMBINED WITH DUCT LINING

The combination of a bar-silencer with two sides lined was compared (Figure 3.22) with a combination of splitter with two sides lined. The 50 mm splitter combination substantially increased the insertion loss at frequencies above the 1600 Hz $^{1}/_{3}$ octave band, which was

unexpected, as a duct lined on two sides and a single splitter (Figure 3.20) performed relatively poorly individually in these frequencies. The triangular bar-silencer had an increased insertion loss in the frequencies below the 1600 Hz $^{1}/_{3}$ octave band centre frequency.

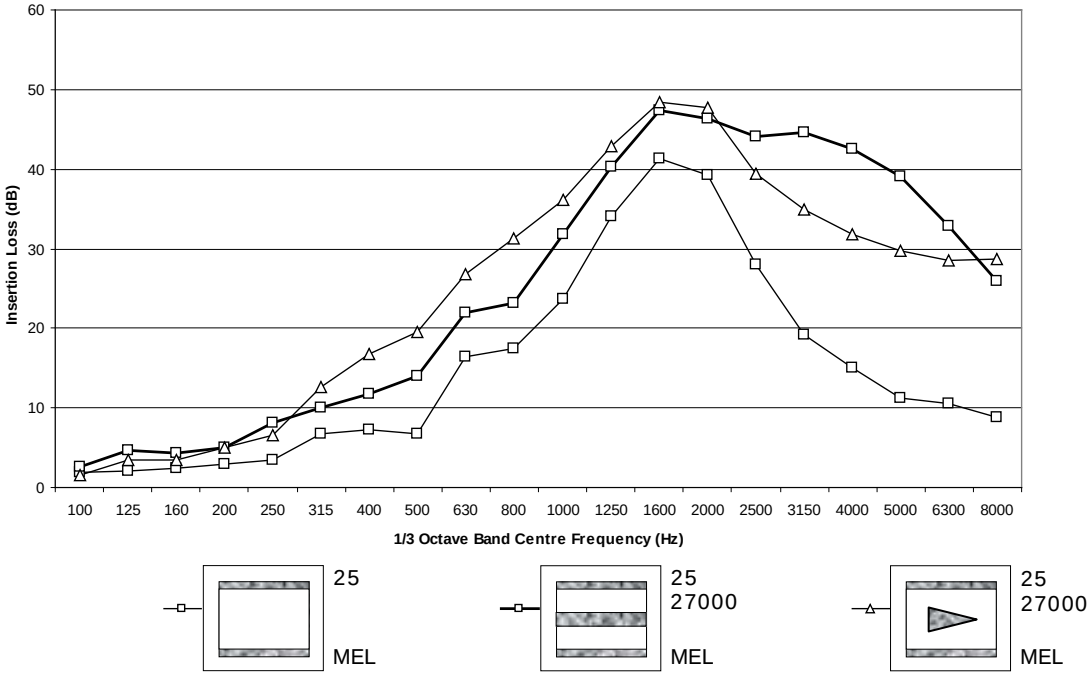

FIGURE 3.22: BAR-SILENCER AND SPLITTER COMPARISON WITH TWO SIDED DUCT LININGS

3.11.4 Four Sided Linings

More traditionally, Australasian duct systems are lined on four sides. As stated, this is due to increased thermal insulation, increases in sound attenuation and general ease of construction. The comparison between two and four sides lined with either melamine or Siliner fibreglass can be seen in Figure 3.23. There is an increase in performance of 5 – 15 dB across most frequencies except below about 400 Hz where there is little or no improvement by increasing the amount or duct lined. The Siliner fibreglass outperforms the melamine foam.

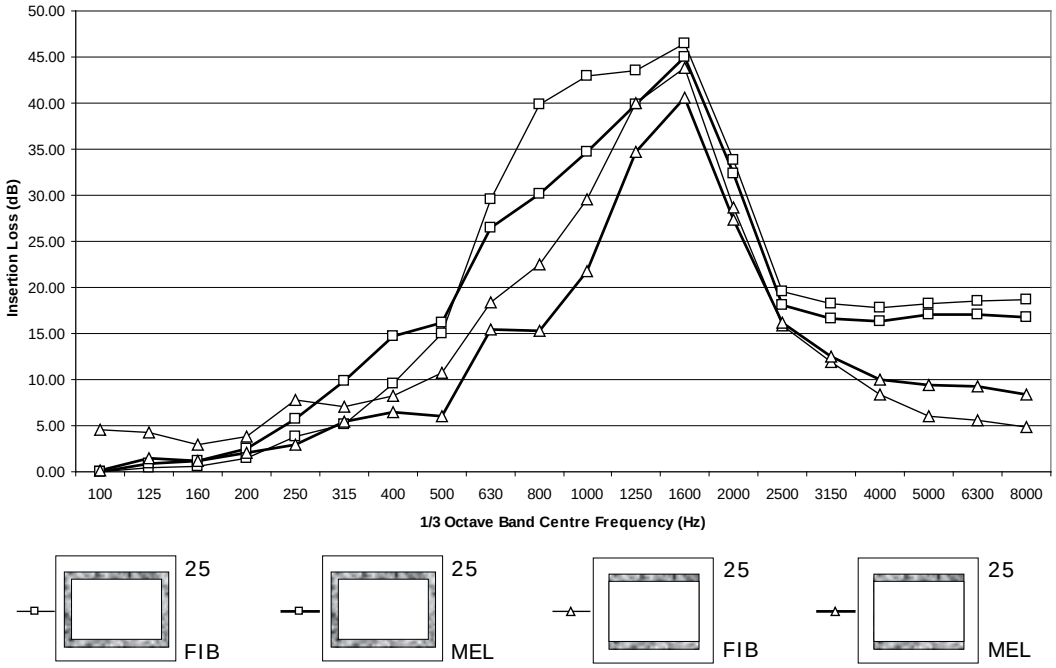

FIGURE 3.23: MELAMINE AND FIBREGLASS COMPARISONS BETWEEN DUCTS LINED ON TWO OR FOUR SIDES

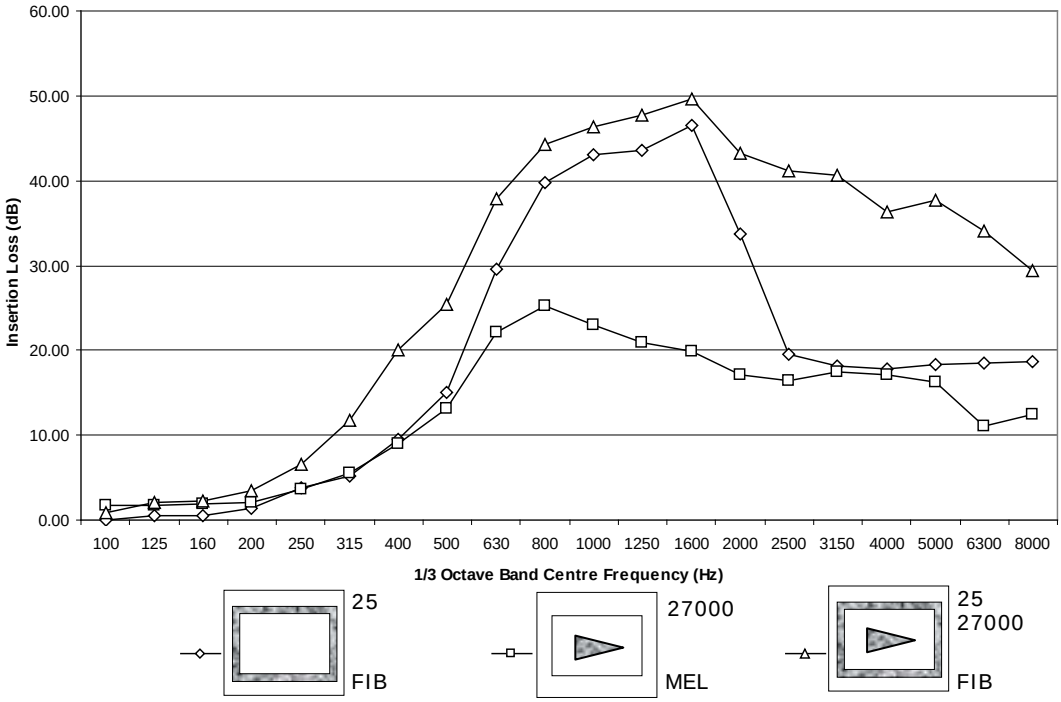

FIGURE 3.24: BAR-SILENCERS IN CONJUNCTION WITH DUCT LINED ON FOUR SIDES

Figure 3.24 indicates the significant improvement in sound attenuation when the two systems are combined. This is a realistic example of a retrofit application, a Siliner fibreglass lined duct with a melamine bar-silencers installed, giving increased noise reductions in both the low and high frequencies. The “retrofit duct”, shows greater attenuation in some frequencies than that of the two individual components combined. There is significantly less improvement (Figure 3.25) in sound attenuation between the “retrofit” applications applied to a four sided over the two sided duct, when compared to the improvements obtained for the two and four side lined ducts alone (Figure 3.23). This appears to show that the bar-silencer negates some of the effects of the duct linings. This could be due to an insertion loss limiting effect or a change in sound field in the duct with the bar-silencer installed.

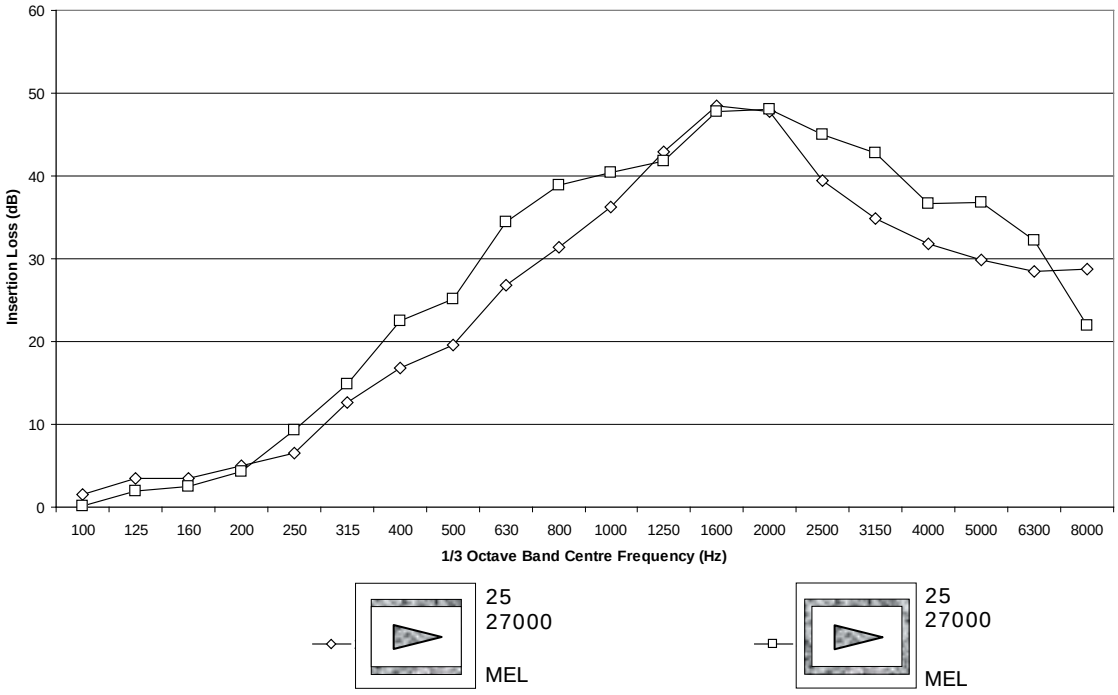

FIGURE 3.25: EXAMPLE RETROFIT APPLICATION OF A BAR-SILENCER IN DUCT LINED WITH TWO OR FOUR SIDES

3.12 270 MM x 300 MM DUCT TESTS

3.12.1 Constant Bar-Silencer Size

Bar-silencers of constant cross-section were tested in both the 540 mm x 300 mm and 270 mm x 300 mm ducts. Figure 3.26 and Figure 3.27 show bar-silencers of 20,250 mm^2 and 13,500 mm^2 respectively and indicate that the insertion loss increases with decreasing duct size. Figure 3.26 shows an almost doubling of insertion loss across all frequencies as the duct size is halved. This trend is also seen at frequencies above 1250 Hz in Figure 3.27. Below this frequency, there is an increase, but it is obscured by the peak in and around the 630 Hz $^1/_3$ octave band centre frequency observed in the 540 mm x 300 mm duct.

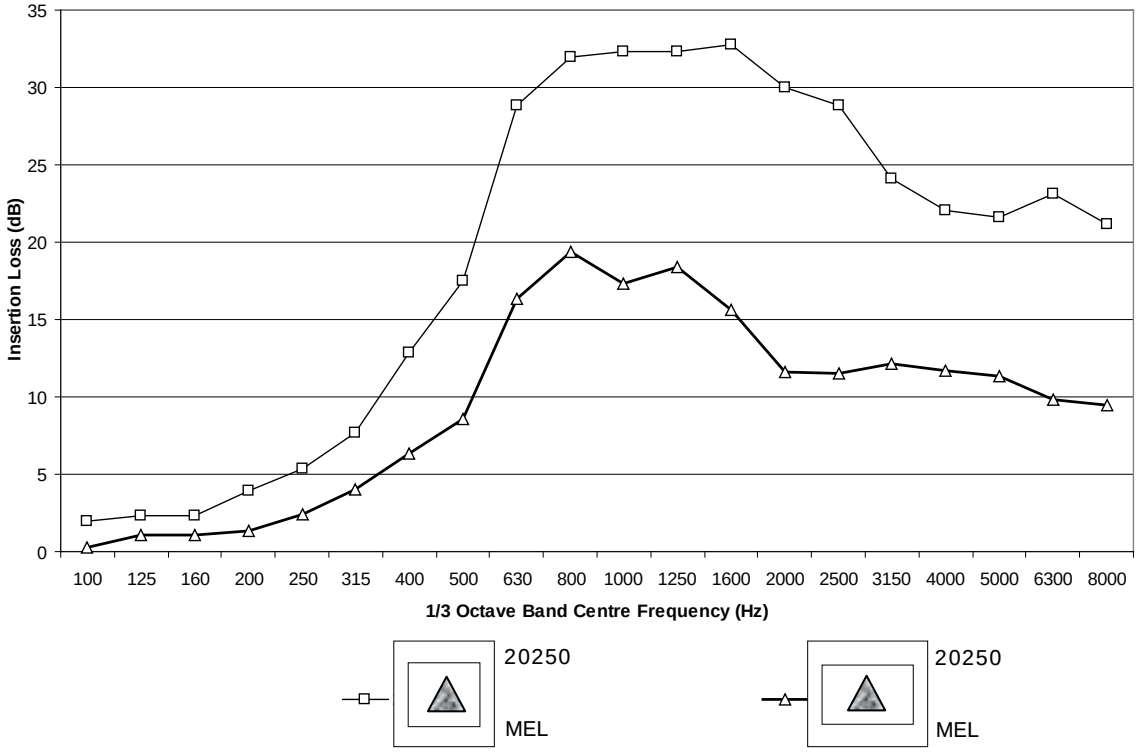

FIGURE 3.26: EFFECT OF DUCT SIZE ON 20,250 MM^2 EQUILATERAL TRIANGLE BAR-SILENCER

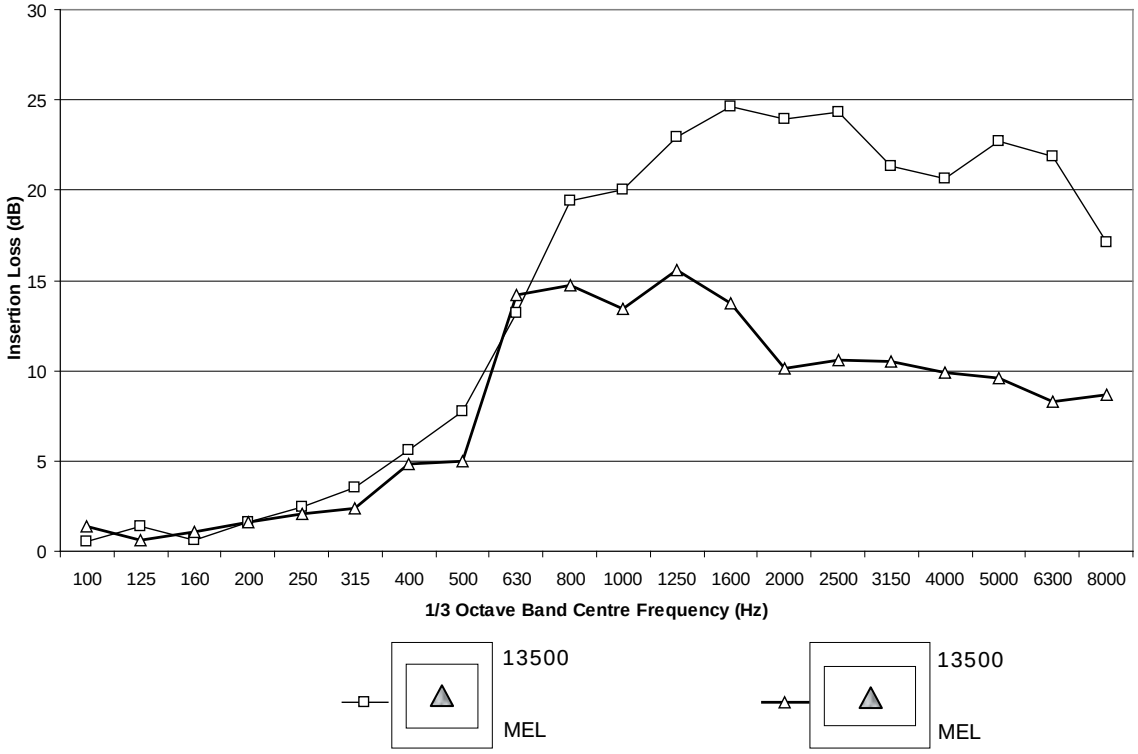

FIGURE 3.27: EFFECT OF DUCT SIZE ON 13,500 MM^2 EQUILATERAL TRIANGLE BAR-SILENCER

3.12.2 Bar-Silencer Open Area Ratio

Some traditional duct lining prediction schemes such as Beranek (1988) utilize the open area ratio (OAR) as a variable in determining the insertion loss.

$$OAR = \frac{(\text{Total duct cross section} - \text{Cross section of absorbing material})}{\text{Total duct cross section}} \qquad (3.4)$$

Using the two duct systems available, systems of constant OAR were tested. The objective was to illustrate if the OAR could be extended to bar-silencers as an indication of performance. However, there was no obvious correlation between the OAR and the insertion loss (Figure 3.28 and Figure 3.29).

The results indicate the duct size ratio has a significant effect on insertion loss. The 540 mm x 300 mm duct system has a more prominent peak, while the squarer 270 mm x 300 mm duct system moves the absorption towards higher frequencies and flattens out absorption at higher frequencies. This aligns it more with the melamine random incidence absorption characteristics.

OAR may still be able to be applied to bar-silencers, but with constant duct ratios of height to width. This would require verification by experimental testing of ducts of similar ratio.

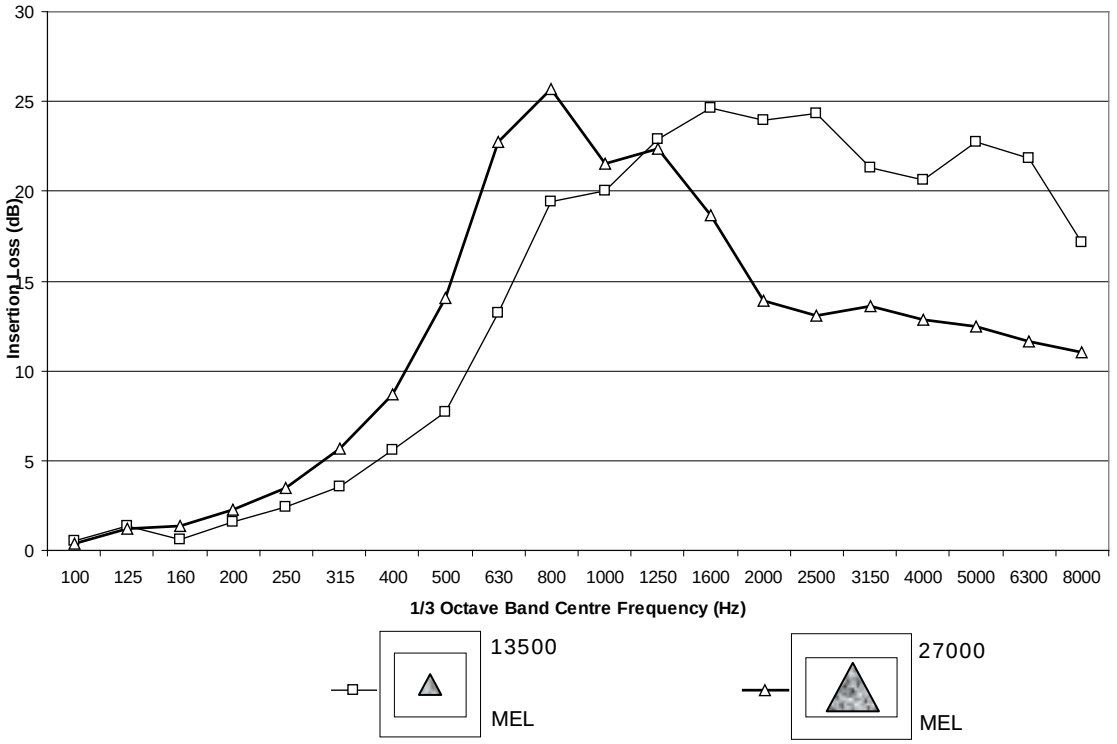

FIGURE 3.28: EQUILATERAL TRIANGLES OF CONSTANT OPEN AREA RATIO: 0.833

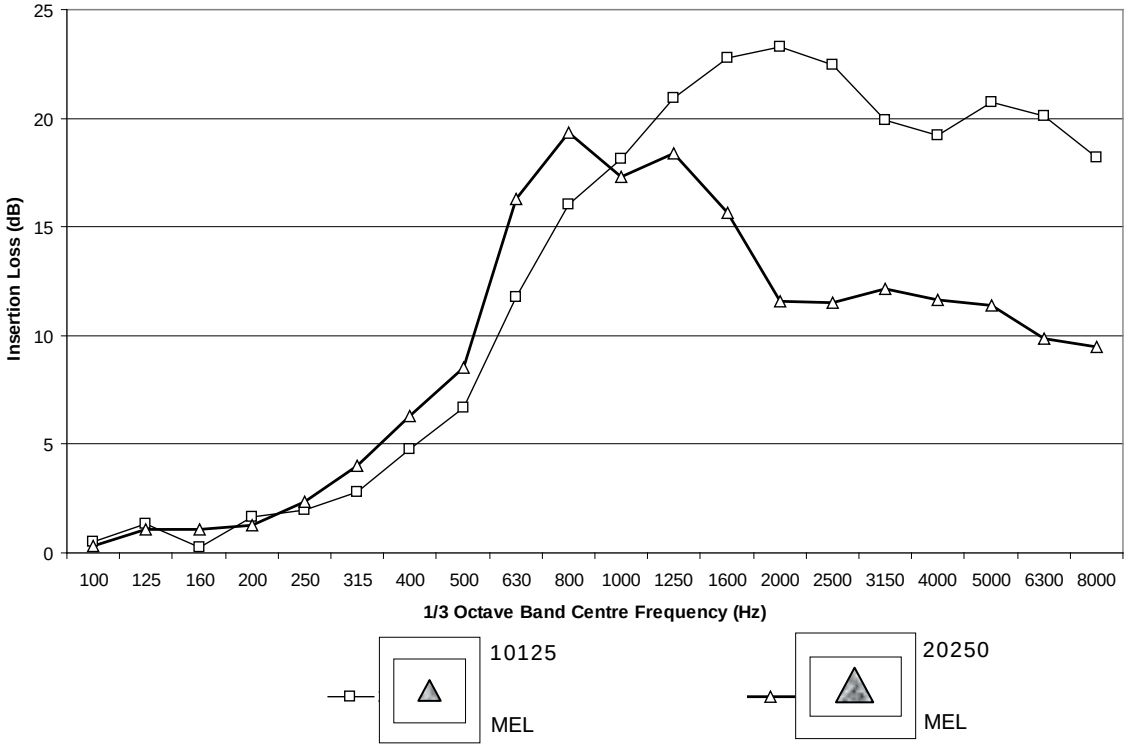

FIGURE 3.29: EQUILATERAL TRIANGLES OF CONSTANT OPEN AREA RATIO: 0.875

3.12.3 Duct Linings for Different Sized Ducts

Figure 3.30 and Figure 3.31 show the effect of duct size and proportion of lined duct for both melamine and fibreglass linings. Differences in material type become more pronounced when the duct is lined on four sides. The step in insertion loss performance from two sides to four sides lined is similar between the 540 mm x 300 mm and 270 mm x 300 mm ducts. The most significant deviation is in the smaller duct when lined on four sides, gaining additional attenuation directly after the peak absorption at 1600 Hz.

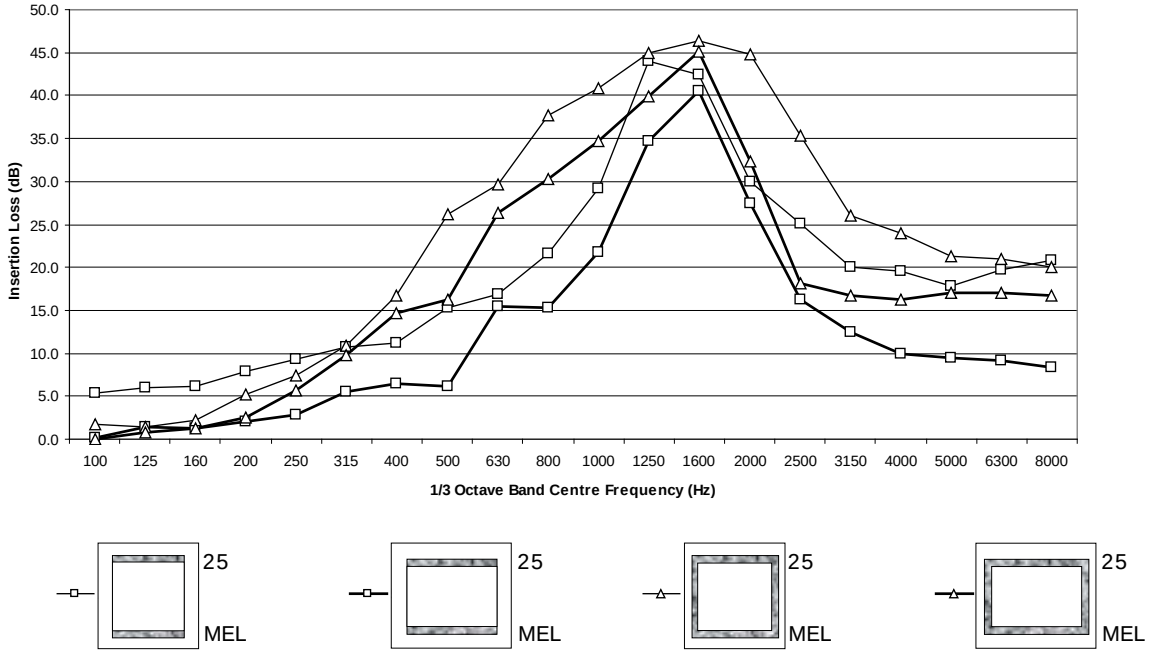

FIGURE 3.30: EFFECT OF DUCT SIZE ON SOUND ABSORPTION DUE TO MELAMINE DUCT LININGS

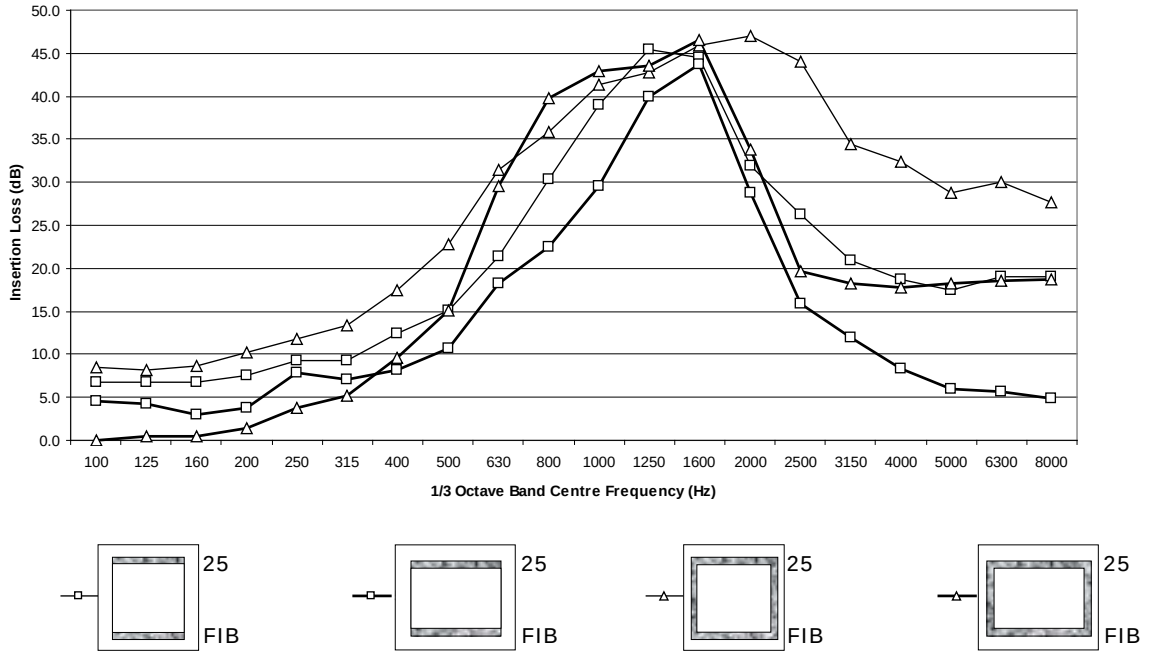

FIGURE 3.31: EFFECT OF DUCT SIZE ON SOUND ABSORPTION DUE TO FIBREGLASS DUCT LININGS

3.12.4 Effect of Retrofit and Duct Size

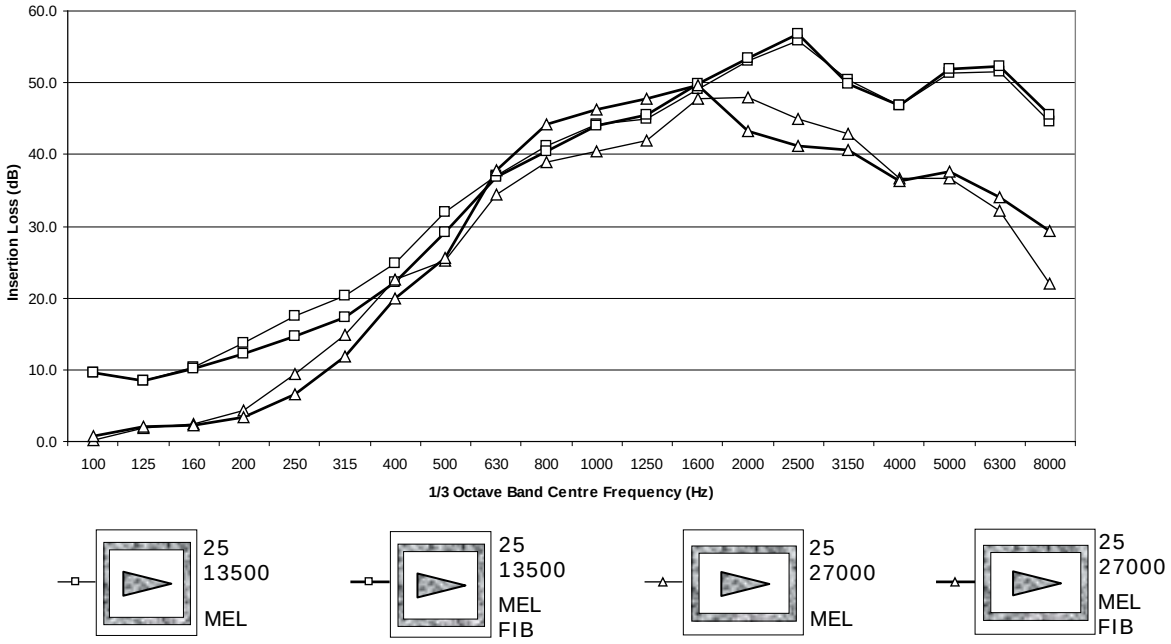

FIGURE 3.32: EFFECT OF DUCT SIZE ON RETRO FIT SILENCERS WITH DUCT LININGS

In contrast, the material lining is seen to have little effect when a bar-silencer is introduced. The two duct systems no longer have a constant open area ratio. The smaller ducts are again seen to improve the lower frequencies below 400 Hz. A plateau in insertion loss at high frequencies above 1600 Hz is also seen in the smaller 270 mm x 300 mm ducts.

3.13 PRESSURE LOSSES

Due to the nature of the bar-silencers causing a blockage in the ducting, there is an associated pressure loss. If the pressure drop across the bar-silencer is too great, they may not be feasible, as larger fan units would be required to accommodate the loss in pressure. Two methods of investigating the pressure losses in the ducting were used:

(i) Experimentally measured static pressures, at both the up and downstream reference planes by use of two water manometers.

(ii) Computational fluid dynamics (CFD) package was used to predict the pressure drops in the ducting system due to blockages.

The tested bar-silencers had square ends, with no aerodynamically designed noses or tailings. This would give worst case pressure losses in the system as any additions of aerodynamic noses or tailings would reduce the pressure losses across the bar-silencers. For each bar-silencer the pressure losses were measured at 5 different average flow velocities of 5, 10, 15, 20 and 25 ms^{-1} (corresponding volume flow rates: 0.81, 1.62, 2.43, 3.24 and 4.05 m^3s^{-1}). Figure 3.33 shows the pressure measurement plane locations in relationship to the test section.

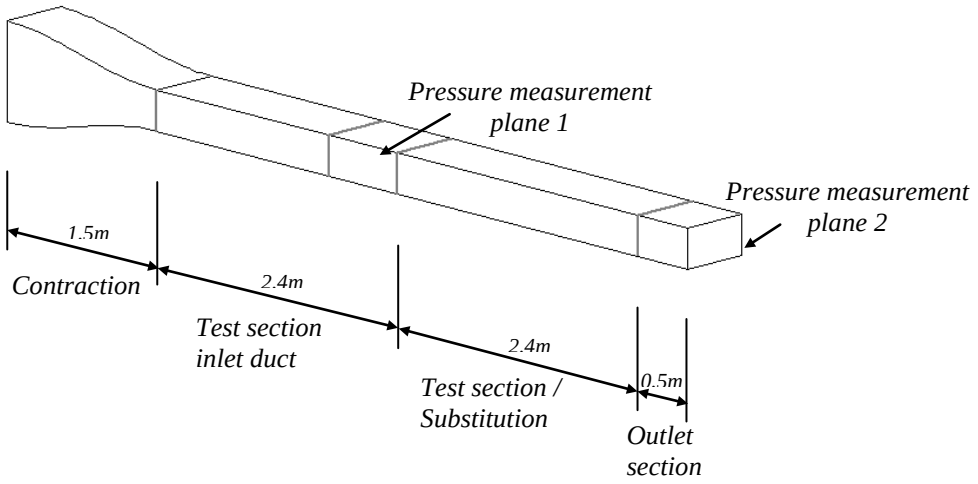

FIGURE 3.33: PRESSURE MEASUREMENT PLANES

Conventional duct linings

Figure 3.34 shows the measured relationship between volume flow rate and pressure loss in the duct with no obstruction. There is a power-law relationship between the flow rate and pressure loss. The pressure losses due to the duct being lined with melamine foam are also shown, the increase in surface roughness of the foam over the galvanised sheet metal can be seen by the increase in pressure loss. Specification and data sheets often present pressure loss data in a log-log form to obtain a straight line for extending the data range past the experimental.

The data in Figure 3.34 presented in log-log form (Figure 3.35) with the lines of best fit is extended past their respective range of data points.

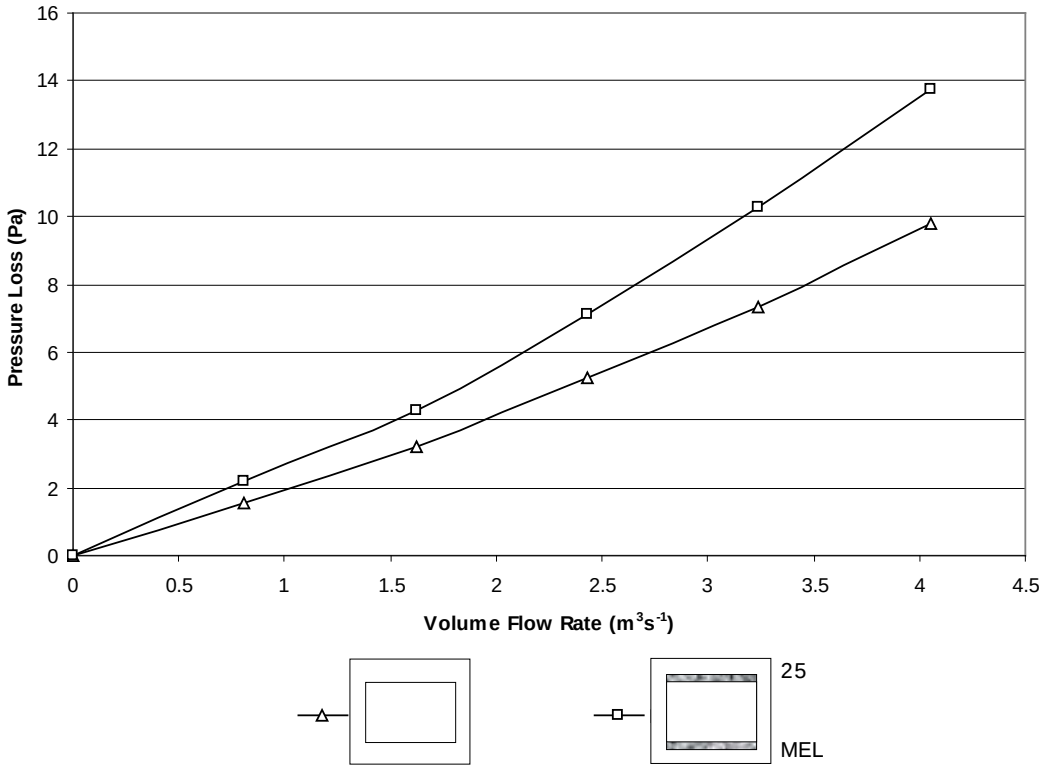

FIGURE 3.34: MEASURED PRESSURE LOSSES DUE TO AN UNLINED AND LINED DUCT SECTION

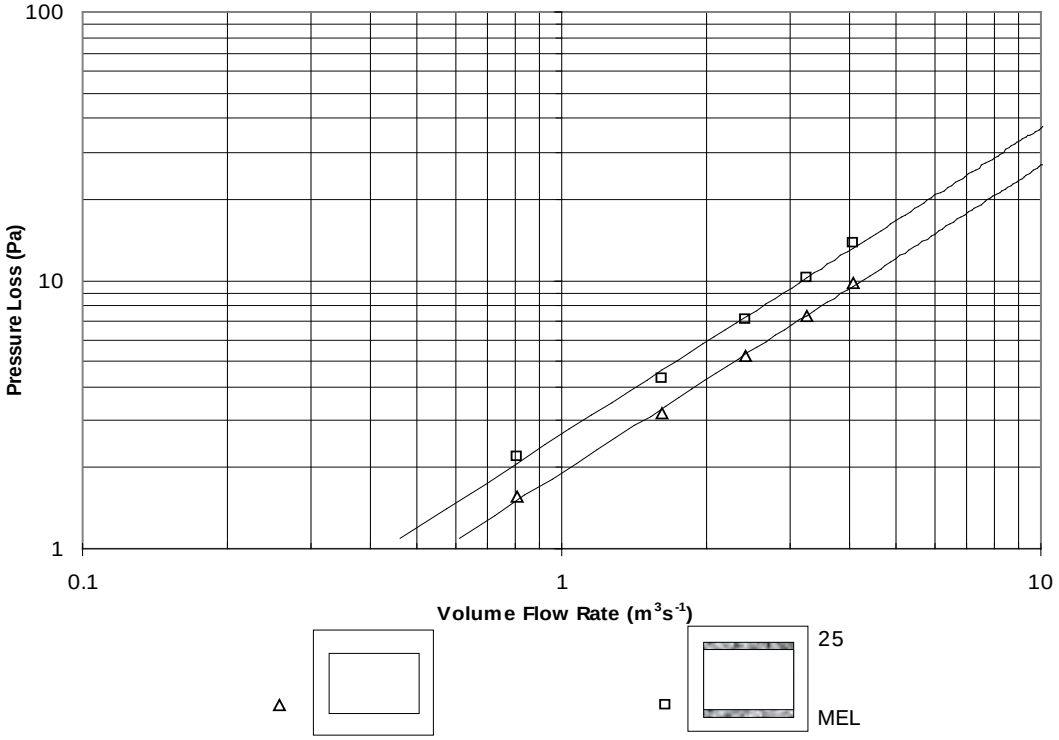

FIGURE 3.35: MEASURED PRESSURE LOSSES DUE TO AN UNLINED AND LINED DUCT SECTION, LOG-LOG FORMAT

Bar-Silencer position

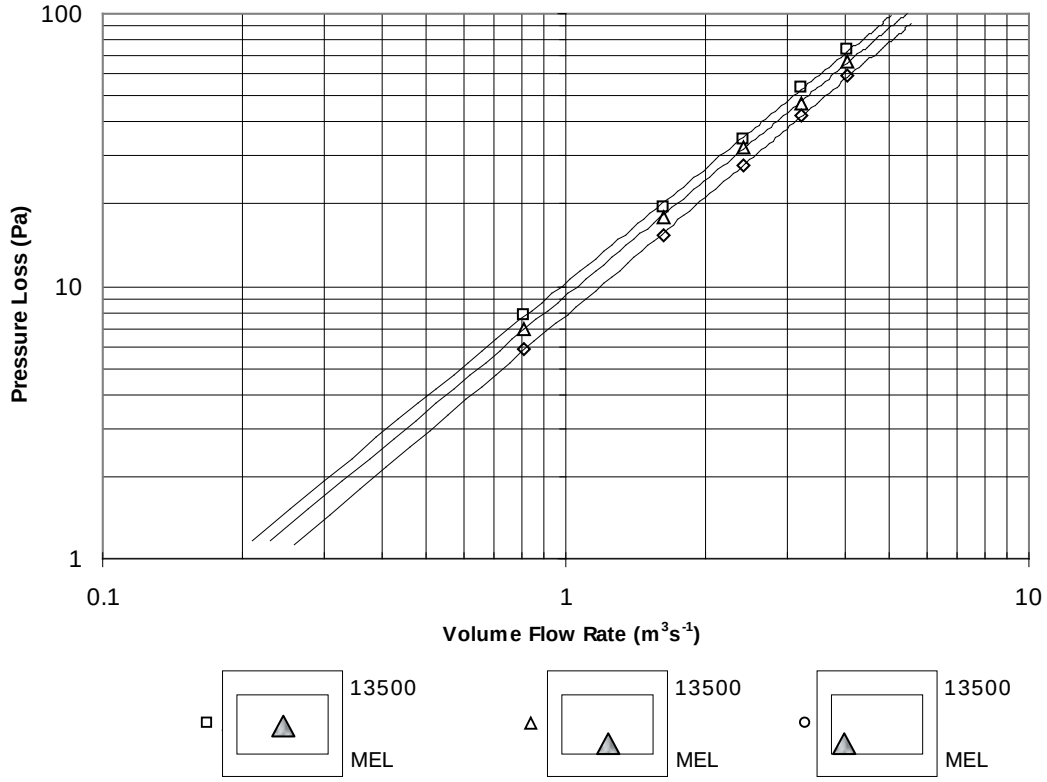

FIGURE 3.36: EFFECT OF BAR-SILENCER POSITION ON PRESSURE LOSS

There were limited increases in pressure loss due to the position of the bar-silencer (Figure 3.36). These relatively small increases in pressure loss may be acceptable given the large percentage increase in insertion loss for the bar-silencer at mid to high frequencies, if positioned in the centre of the duct (Figure 3.12).

Bar-Silencer Size

In comparison to the position, the effect of bar-silencer size, (or volume of material) effects the pressure loss significantly. Increasing the size of the silencer, dramatically increases the

pressure losses (Figure 3.26). However there is also a significant increase in the acoustic insertion loss shown by the larger bar-silencer (Figure 3.15). Whether the pressure loss was acceptable for the increase in insertion loss would be situation dependant.

Both Figures 3.36 and 3.37 show the expected power-law relationship between the volume flow rate and pressure loss.

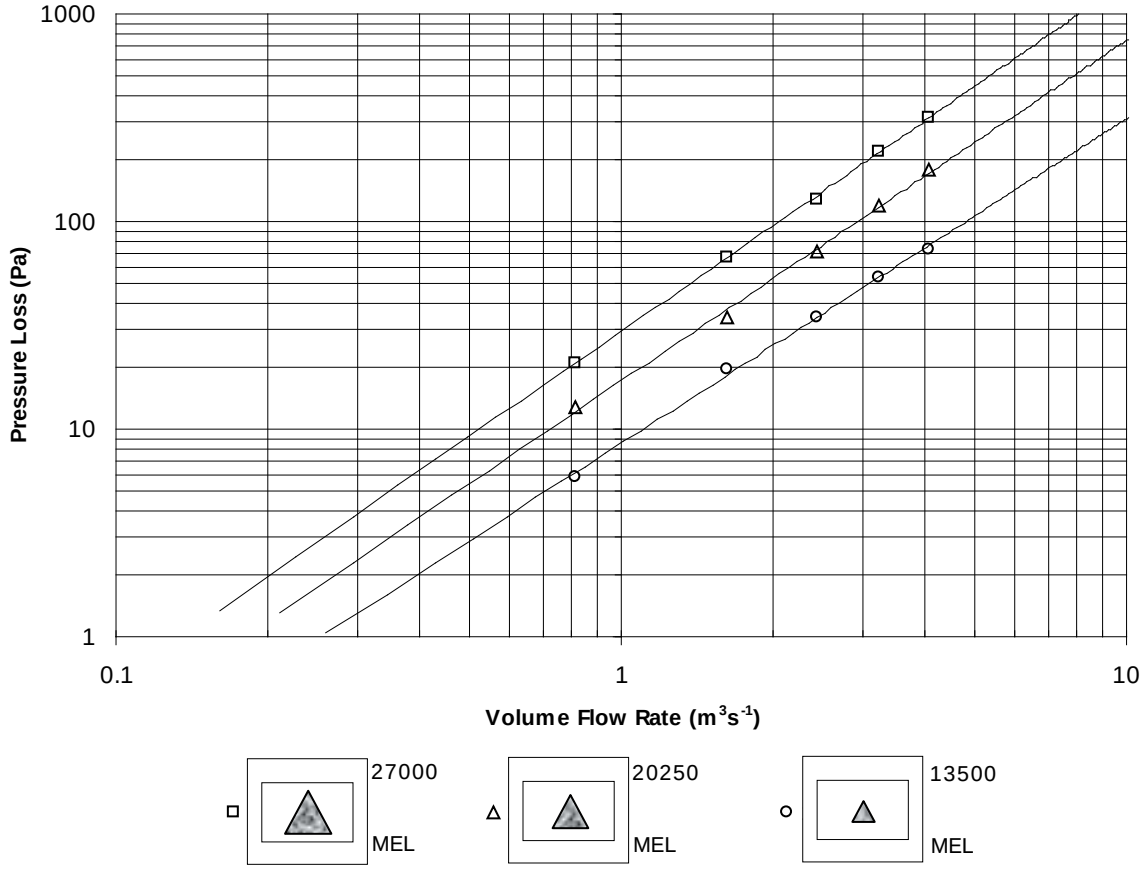

FIGURE 3.37: EFFECT OF BAR-SILENCER SIZE ON PRESSURE LOSS

Predicted Pressure Losses

The CFD predicted pressure losses, tended to over predict the pressure losses measured from the test facilities. Figure 3.38 shows the pressure losses due to an isosceles shaped bar-silencer. The CFD package values can be seen to tend away from actual values with increasing volume flow rate. Some of the boundary conditions for the computational method such as inlet conditions not matching that of the centrifugal fan, the bar-silencers being modelled as solid no-slip walls instead of a porous medium, and the possibility of incorrect turbulence model parameter settings, may have caused the deviation from the true values.

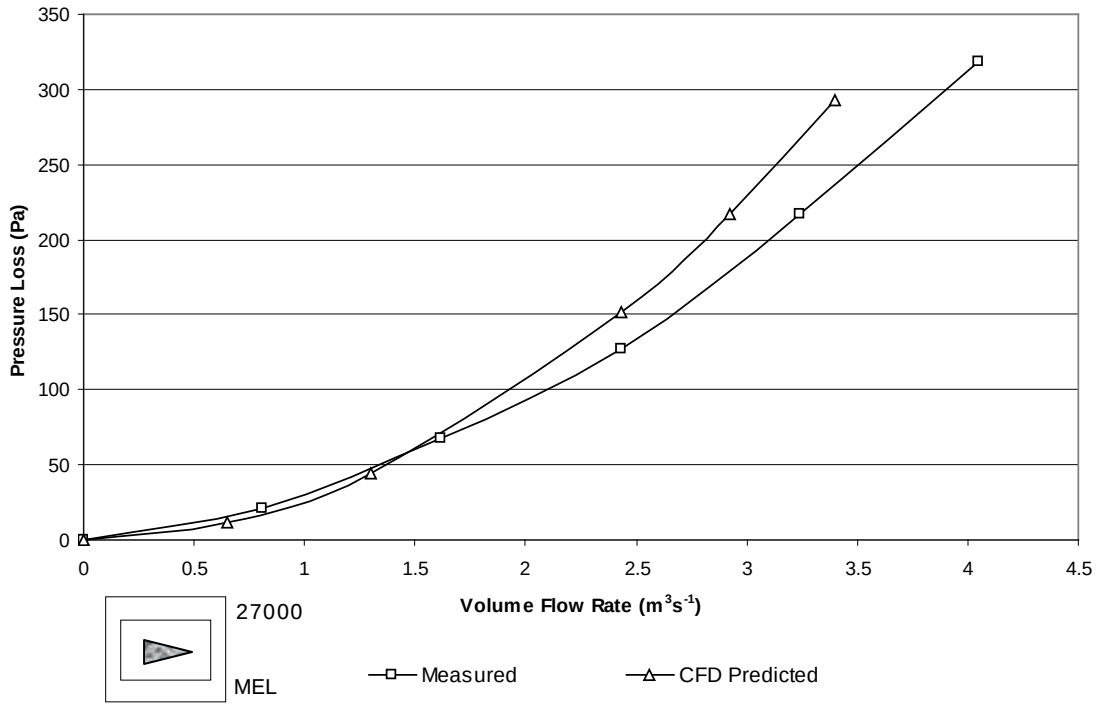

FIGURE 3.38: EXAMPLE COMPARISON BETWEEN CFD PREDICTED AND EXPERIMENTALLY MEASURED PRESSURE LOSSES

Both measured and CFD predicted pressure loss data can be seen in Appendix 9.

3.14 REFERENCES

Beranek, L,L. 1988. *Noise and Vibration control*, Washington DC, Institute of noise control engineering.

Cummings, A., and Astley, R.J. 1996. "Finite element computation of attenuation in bar-silencers and comparisons with measured data." *Journal of Sound and Vibration* 196: 351-369.

ISO 7235 1991 "Measurement procedures for ducted silencers - Insertion loss, flow noise and total pressure loss."

Nilsson, N-A., and Soderquist, S. 1983. "The bar silencer-improving attenuation by constricted two-dimensional wave propagation." *Proceedings of Internoise 83*: 1-4.

Parkinson, J.P. 1999. *Acoustic absorber design*, a thesis submitted in partial fulfilment of the requirement for a Masters of Engineering degree in the Department of Mechanical Engineering, University of Canterbury.

Pettersson, M.J. 2002. *Duct absorber design*, a thesis submitted in partial fulfilment of the requirement for a Masters of Engineering degree in the Department of Mechanical Engineering, University of Canterbury.

Sabine, H.J. 1940. “The absorption of noise in ventilating ducts.” *Journal of Sound and Vibration* 12: 53-57.

Vér, I.L. 1978. “A review of the attenuation of sound in straight lined and unlined ductwork of rectangular cross section.” ASHRAE Transactions 84: 122-149

Wassilieff, C. 1985. “Performance of duct acoustic linings available in New Zealand.” *Transactions of The Institution of Professional Engineers New Zealand (IPENZ)* vol 12.

Wassilieff, C. 1987. “Experimental verification of duct attenuation models with bulk reacting linings.” *Journal of Sound and Vibration* 114(2): 239-251.

4

DESIGN GUIDELINES

4.1 SUMMARY

This chapter outlines the project findings and provides guidelines for the development of bar-silencers. The guidelines were developed from the results shown in Chapter 3, and were assessed according to their potential as an alternative to traditional methods of sound attenuation in ducts.

Although based on a limited number of tests, the results both confirmed and extended some important concepts regarding the application of bar-silencers. These included the magnitude of the pressure losses, the spectrum of insertion loss of various shapes, how the bar-silencers compared to duct linings and how they work in conjunction with duct linings. The guidelines are specific to the Australian and New Zealand markets, with reference to locally available materials, standards and costs.

4.2 DESIGN

In any given application there is usually more than one criterion for selecting a sound absorbing system for ducts. Generally, in order of importance, price, safety (fire issues), pressure losses and finally acoustic performance are considered. However, the order of these issues varies depending on the application. The decibel losses given in these design guides apply to this work and are an indication of performance for the specified variable.

Material

There are a limited number of materials which will absorb sound adequately while remaining rigid enough to hold the form of the tested bar-silencers. A less rigid material would require fixed framing or rigid facings to hold the material in shape, increasing the cost of the system.

The melamine foam used throughout the testing is a material which meets almost all of the requirements of an induct absorber or bar-silencer. It has relatively high sound absorption characteristics (similar to fibreglass), it has a low smoke development index, and self extinguishes. The bulk material is rigid enough to form and maintain shapes. The advantage of melamine over fibreglass is the absence of fibres and particles which can separate from the bulk material. This extends the allowable applications to those which require no foreign substances, such as hospitals, scientific clean room and class rooms. In some states of Australia workplace practices will not allow the handling of mineral fibre, so alternative materials are required for lining ducting.

Shape

The cross-sectional profile was found to have a significant effect on the insertion loss characteristics of bar-silencers. Building on previous research (Nilsson and Söderquist 1983, Cummings and Astley 1996, Pettersson 2002), triangular silencers were confirmed to have increased attenuation at mid to high frequencies. Figure 4.1 below illustrates the significant increase in attenuation for the triangular silencer of an increased aspect ratio (2:1) over other shapes.

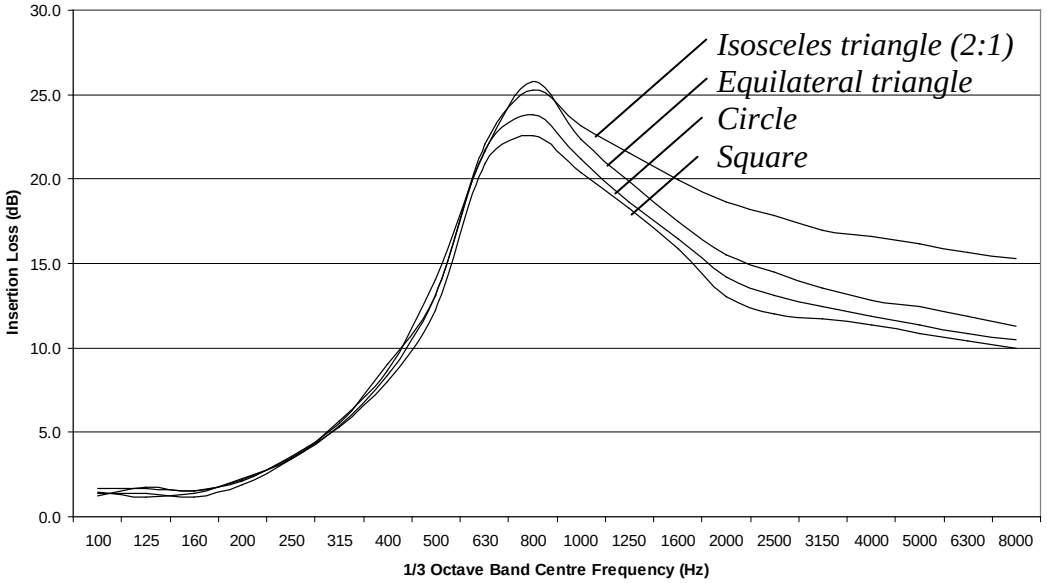

FIGURE 4.1: DESIGN CURVE FOR BAR-SILENCER SHAPE

The effect of this aspect ratio in the triangular bar-silencers can be seen in Figure 4.2. The trend observed was that as the aspect ratio increased, so did the insertion loss. However the higher (5:1) aspect triangle falls away at frequencies above 3150 Hz. A disadvantage of the 5:1 ratio triangular bar-silencer was that it became thin and consequently fragile towards the point.

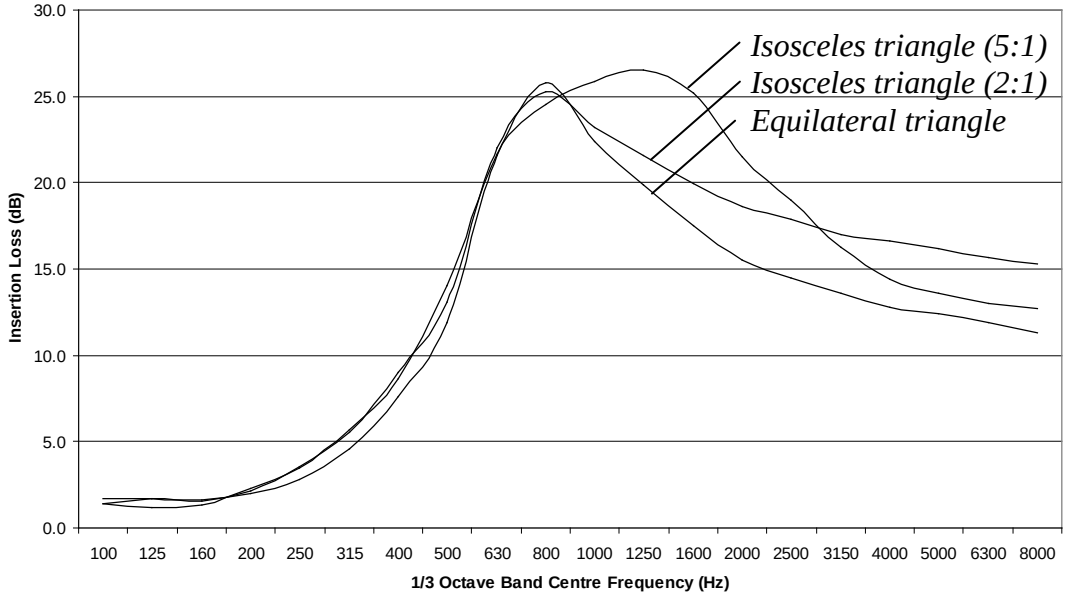

FIGURE 4.2: DESIGN CURVE FOR TRIANGULAR BAR-SILENCER ASPECT RATIO

A triangular silencer of ratio in the region between 2:1 and 3:1 is recommended. This would provide a relatively high insertion loss, with a plateau at higher frequencies, while remaining rigid enough to avoid damage when being handled.

Position

Position within the duct was seen to have a large influence on insertion loss. As the bar-silencers moved away from the centre of the duct, both the peak and higher frequency insertion loss diminished. This can be seen in Figure 4.3. It is advisable to install bar-silencers as centrally as possible.

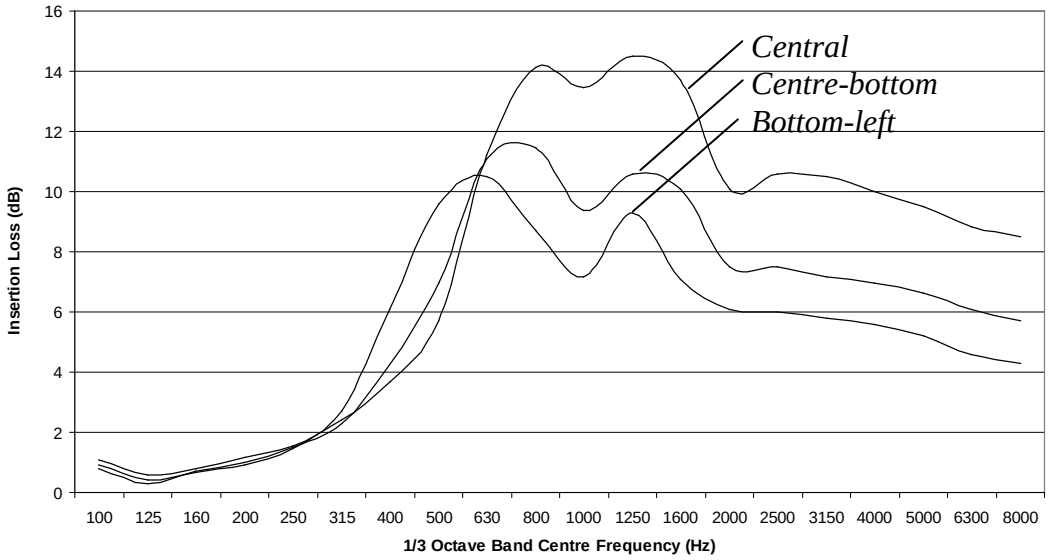

FIGURE 4.3: DESIGN CURVE FOR BAR-SILENCER POSITION

Duct Size

Smaller ducts sizes were seen to yield large increases in insertion loss. Figure 4.4 shows the same bar-silencer positioned centrally in two ducts, one duct being half the volume of the other. The result was a doubling of insertion loss across all frequencies.

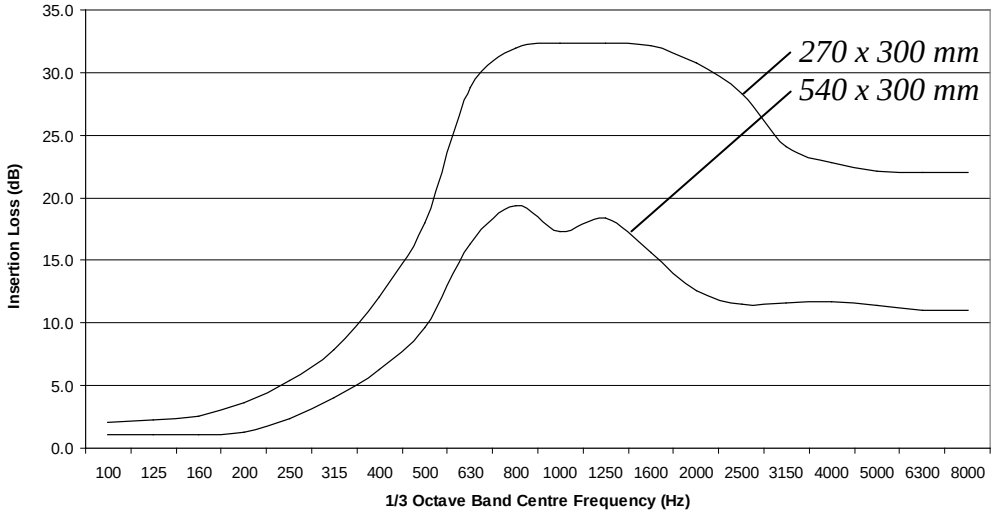

FIGURE 4.4: DESIGN CURVE FOR THE SAME BAR-SILENCER POSITIONED CENTRALLY IN TWO DIFFERENT DUCT SIZES

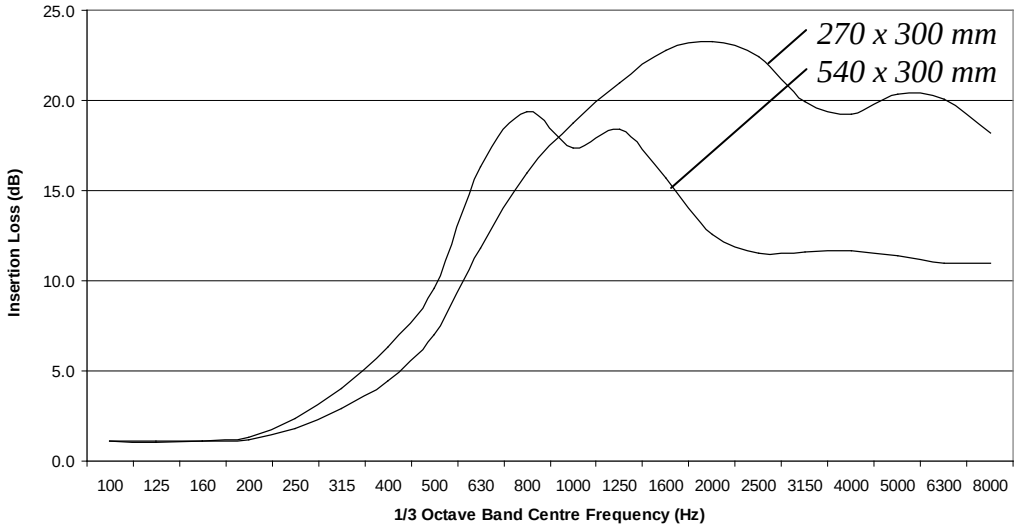

FIGURE 4.5: DESIGN CURVE FOR BAR-SILENCERS OF CONSTANT OPEN AREA RATIO (0.875)

This result was extended by holding the proportion of absorbing material to duct size constant. With the open area ratio constant, the smaller duct was seen to gain large improvements above 1000 Hz (Figure 4.5). The effect of the shape of the ducting was not investigated, and could have influenced these results.

If feasible, a smaller duct should be installed because for a given proportion of absorbing material, a higher insertion loss is achieved inside smaller ducting.

Linings

The combination of a bar-silencer and duct linings returned high insertion losses across the measured frequency range. This increase in performance is particularly applicable to systems requiring modifications where the required attenuation is not being meet.

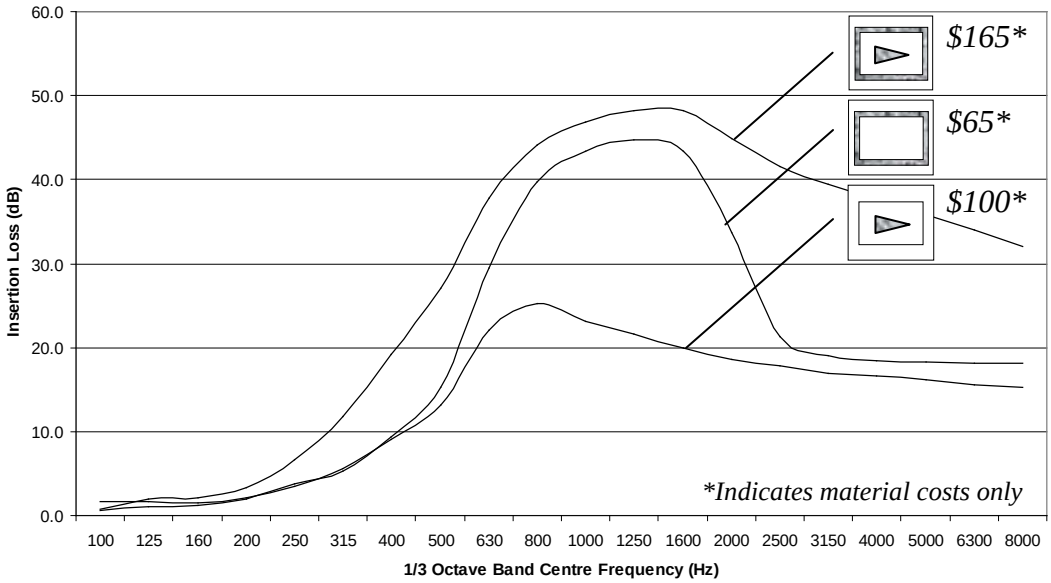

FIGURE 4.6: DESIGN CURVE FOR RETRO-FIT BAR-SILENCER APPLICATIONS

Figure 4.6 illustrates the improvement in attenuation when a bar-silencer is employed in parallel with traditional duct linings. Improvements between 5 – 20 dB can be expected across most frequencies.

Costs

Melamine foam is an expensive product, ($1540 per m^3). Comparatively, a much lower insertion loss is received per dollar when compared against Siliner (fibreglass) linings (Figure 4.6). This may result in the need for other materials to be developed for use as bar-silencers.

Applications

Pressure losses are an important criteria for engineers commissioning HVAC systems and consequently the pressure losses across the bar-silencers were measured. At higher flow rates, the pressure losses can become quite substantial. It is believed that these pressure losses could be reduced considerably if nose and tail aerodynamics were introduced. However, these pressure losses could restrict bar-silencers to smaller systems where the pressure losses are not so important.

Other applications of bar-silencers are where it is impracticable to use prefabricated splitters, linings and pod-silencers, as in boats, domestic ventilation, hospital isolation rooms, and recording studios.

4.3 REFERENCES

Cummings, A., and R.J. Astley. 1996. "Finite element computation of attenuation in bar-silencers and comparisons with measured data." *Journal of Sound and Vibration* 196: 351-369.

Nilsson, N-A., and S. Soderquist. 1983. "The bar silencer-improving attenuation by constricted two-dimensional wave propagation." *Proceedings of Internoise 83*: 1-4.

Pettersson, M.J. 2002. *Duct absorber design*. A thesis submitted in partial fulfilment of the requirements for a Masters of Engineering degree in the Department of Mechanical Engineering, University of Canterbury.

5

CONCLUSION AND RECOMMENDATIONS

5.1 CONCLUSION

A review of the relevant literature outlined the current duct attenuation technology; that of passive duct linings, splitter/baffle absorbers, active and reactive attenuators. A discussion of previous research into porous absorbing mediums, effects of fluid flow on attenuation, and the performance of attenuators was presented, as well as a review of bar-silencers. This highlighted the gap in bar-silencer knowledge which was explored throughout this thesis.

The test room and facilities were successfully re-established and calibrated in accordance with ISO 7235, before being used for the test program. This included acoustically treating the test room to reduce the sound field around the facility, refurbishment of the existing 540 mm x 300 mm duct rig, and the design, construction and commissioning of a 270 mm x 300 mm duct rig.

A number of bar-silencers were tested, with both the insertion loss and pressure loss data measured. The tests were performed in two ducts sizes (540 mm x 300 mm and 270 mm x 300 mm) and the results presented and discussed in this thesis. The bar-silencers were compared with traditional duct lining methods for sound attenuation. A combination of varied cross-sectional area bar-silencers (i.e. triangular) with traditional duct linings proved to be particularly effective for sound absorption.

Design guides and recommendations were established based on the data collected. It was concluded that the bar-silencers would not be a cost effective method of sound attenuation on their own, due to less effective noise absorption and higher pressure losses than traditionally lined sections of ducting. However, there is promising application for the bar-silencers in combination with duct linings. These applications include, low velocity terminations, boats, recording studios and hospitals.

5.2 FURTHER WORK

The research has raised many questions. Outlined below are some thoughts on further research and study in the bar-silencer / duct attenuation field.

Bar-silencers in circular ducting

All the testing to date on bar-silencers has been confined to rectangular ducts. Some experimental testing should be performed in both lined and unlined circular ducting as these types of ducts are occassionally employed.

Effect of aerodynamics on bar-silencer acoustic insertion loss

Pressure losses across the bar-silencers at higher flow velocities were quite substantial. It is believed that these pressure losses could be reduced considerably if streamlined nose and tail fittings were introduced. However, the effects of these fittings on the acoustic insertion loss characteristics of the bar-silencers are largely unknown.

Bar-silencer materials

The bar-silencers have been restricted to melamine foam. The mechanism which causes the bar-silencers to perform so well in combination with lined ducts may be due to other phenomenon such as, the disruption of modes inside the duct as opposed to pure absorption via the bar-silencer. This may indicate that the material for the bar-silencer is less important and a cheaper equally rigid material may have advantages.

Duct bends

An investigation into the attenuation and reflection of sound by lined and unlined duct bends would be useful. This would be done with and without a mean flow. Other extensions could include bends with solid turning vanes and sound absorbing turning vanes.

Facility Upgrading

In order to better improve the productivity of the test facility, a number of upgrades could be made. These include an array of microphones, rather than a single microphone for measurements, and a system of quick release duct sections which do not require numerous bolts to be released and tightened for each test.

Duct grill exits

It has been shown that, smaller ducts attenuate more sound for the same volume of material. One of the costs of using smaller ventilation exits is higher exit flow velocities and therefore higher self-induced noise. An investigation into whether the attenuation benefits of a smaller duct outweigh those of the exit flow noise could be carried out.

Research into flanking

The research found little work done on flanking paths and the effect flanking paths have on the limiting of insertion loss. Modifications could be made to the existing test facility to investigate these phenomena. A proportion of this flanking is associated with structure-borne sound travelling in the walls of the ducts. A study or investigation could go into easily installed, cheap and feasibly methods of decoupling sections of ducting to stop the structure-borne noise.

Sound transmission through duct walls

An experimental and theoretical evaluation could be undertaken on sound transmission through duct walls. This evaluation could include unlined, internally and externally lined ducts. The investigation could also be further expanded to look at different constructions of duct wall, including different weights of sheet-metal and, possibly glass fibre walls.

A1

APPENDIX 1 – MOTOR ENCLOSURE

A.1.1 SUMMARY

Modifications were required to the existing motor enclosure to meet the new size constraints of the test room. An air intake duct for the motor was redesigned and lined with 50 mm acoustic foam.

A.1.2 MOTOR ENCLOSURE DESIGN

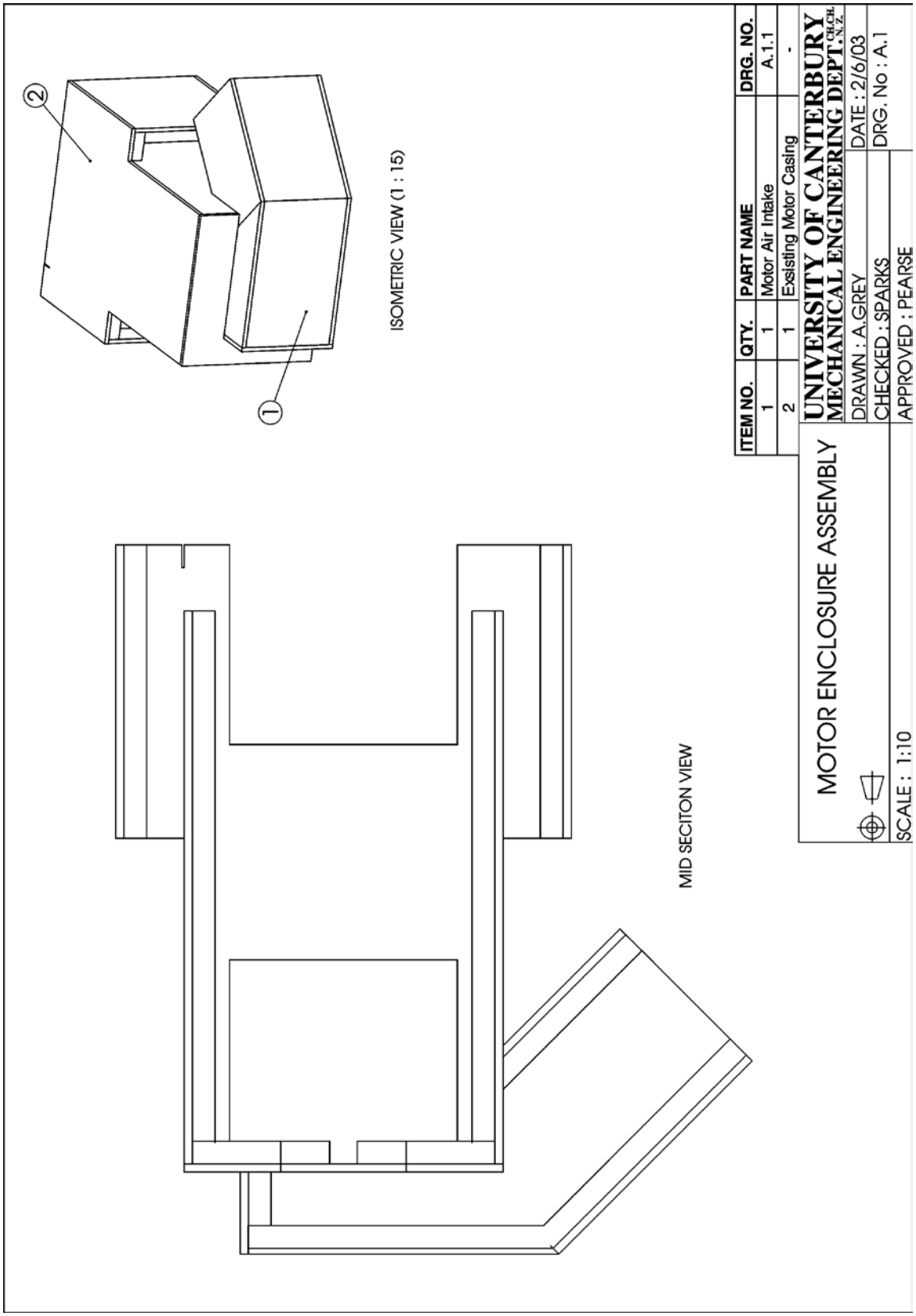

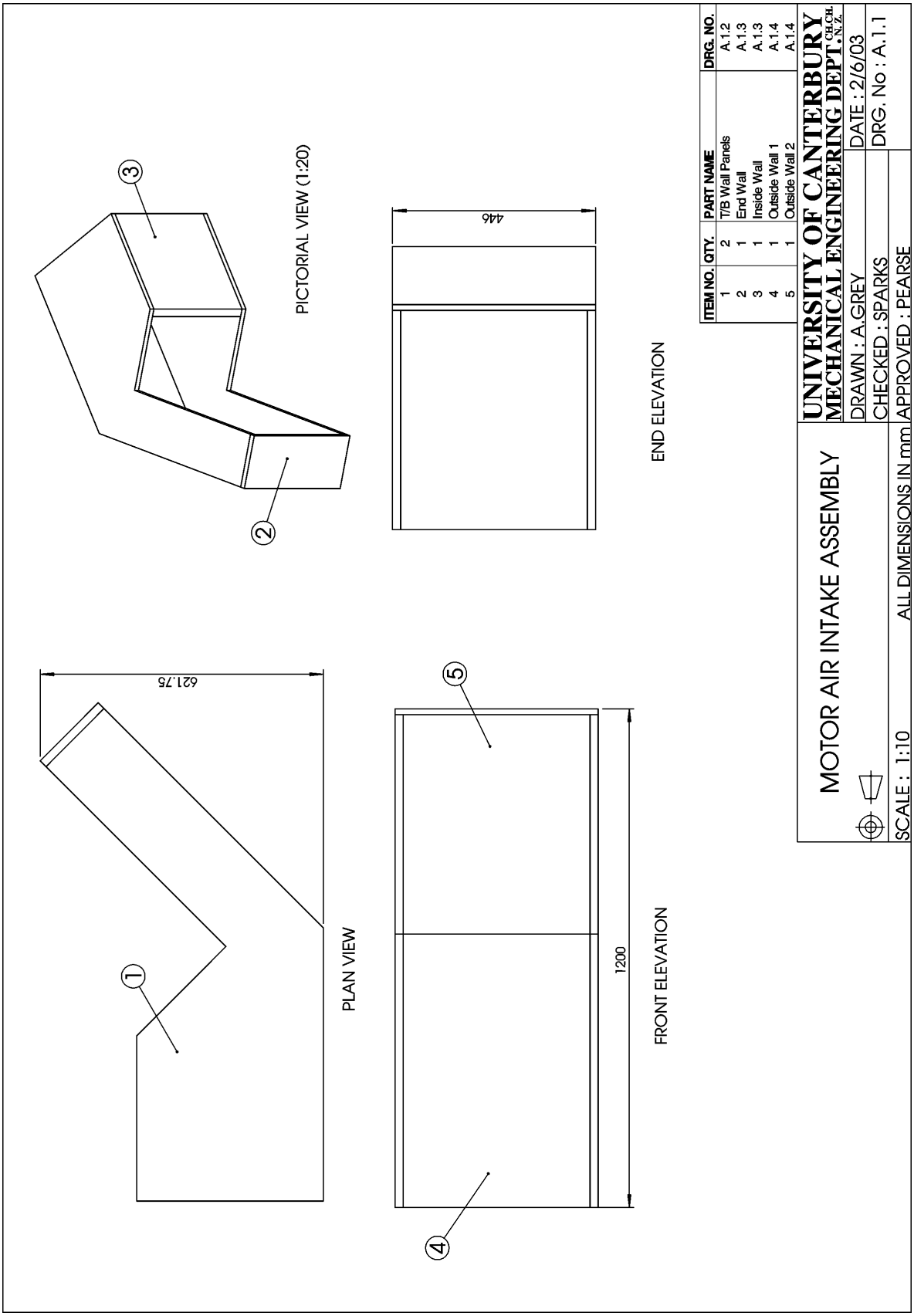
PICTORIAL VIEW (1:20)
END ELEVATION
446
PLAN VIEW
621.75
FRONT ELEVATION
1200
ITEM NO. QTY. PART NAME DRG. NO.
1 2 T/B Wall Panels A.1.2
2 1 End Wall A.1.3
3 1 Inside Wall A.1.3
4 1 Outside Wall 1 A.1.4
5 1 Outside Wall 2 A.1.4
UNIVERSITY OF CANTERBURY
MECHANICAL ENGINEERING DEPT. CH.CH. N.Z.
MOTOR AIR INTAKE ASSEMBLY
DRAWN : A.GREY
DATE : 2/6/03
CHECKED : SPARKS
DRG. No : A.1.1
SCALE : 1:10
ALL DIMENSIONS IN mm
APPROVED : PEARSE

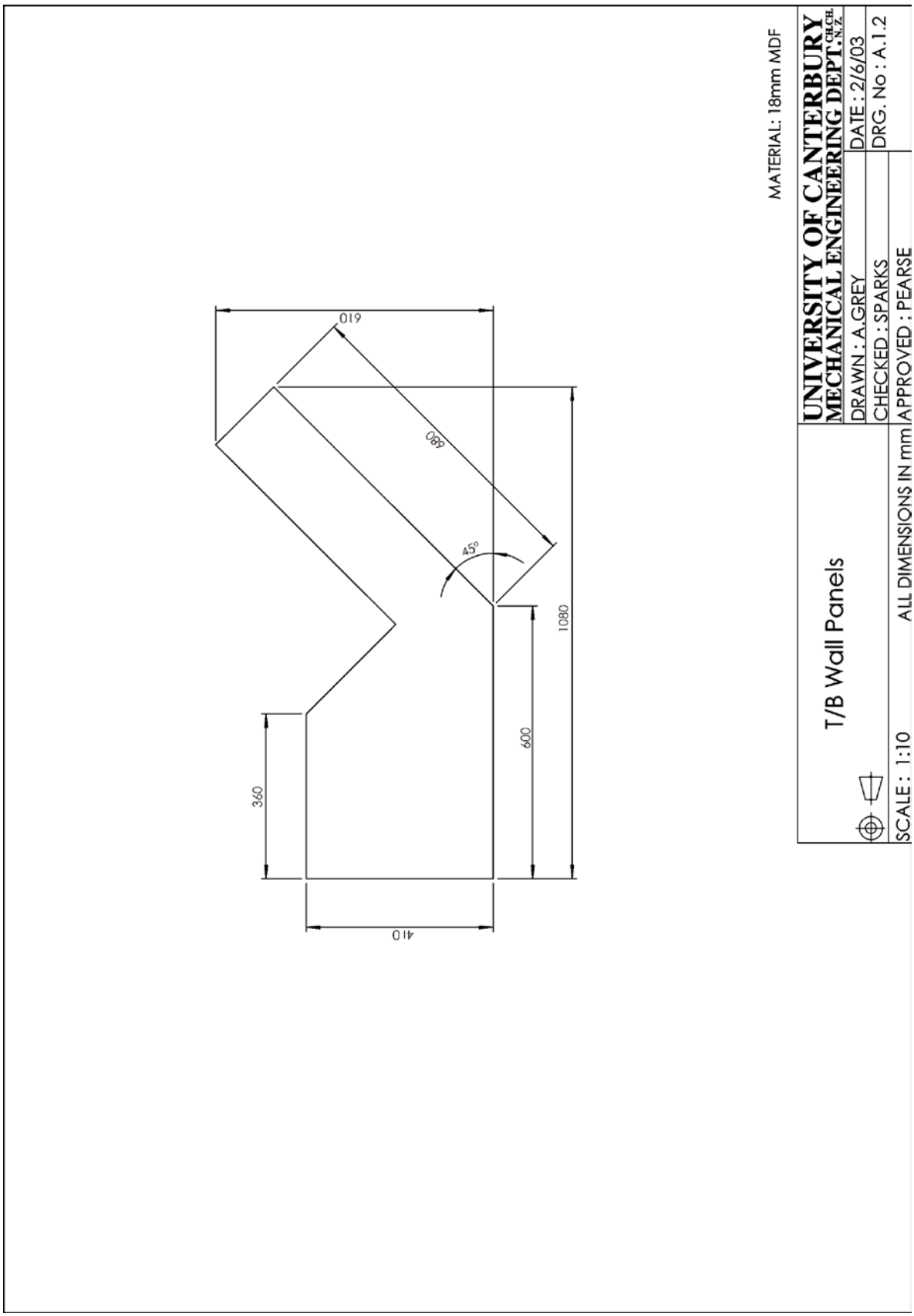
610
680
45°
1080
600
360
410
MATERIAL: 18mm MDF
UNIVERSITY OF CANTERBURY
MECHANICAL ENGINEERING DEPT. CHCH. N.Z.
DRAWN : A.GREY
DATE : 2/6/03
CHECKED : SPARKS
DRG. No : A.1.2
APPROVED : PEARSE
T/B Wall Panels
SCALE : 1:10
ALL DIMENSIONS IN mm

INSIDE WALL
PLAN VIEW
Mitre 45°
FRONT ELEVATION
410
381.50
MATERIAL: 18mm MDF
END WALL
FRONT ELEVATION
446
180
MATERIAL: 18mm MDF
END WALL / INSIDE WALL
UNIVERSITY OF CANTERBURY
MECHANICAL ENGINEERING DEPT. CHCH. N.Z.
DRAWN : A.GREY
DATE : 2/6/03
CHECKED : SPARKS
DRG. No : A.1.3
SCALE : 1:10
ALL DIMENSIONS IN mm
APPROVED : PEARSE

OUTSIDE WALL 1

PLAN VIEW

FRONT ELEVATION

ATERIAL: 18mm MDF

OUTSIDE WALL 2

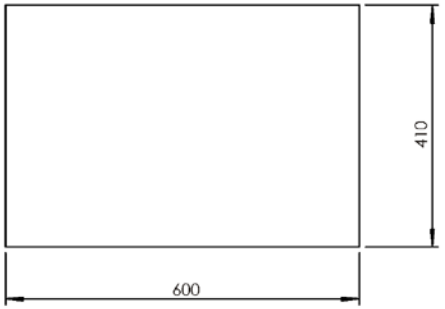

FRONT ELEVATION

MATERIAL: 18mm MDF

OUTSIDE WALL 1 + 2

SCALE : 1:10

ALL DIMENSIONS IN mm

UNIVERSITY OF CANTERBURY
MECHANICAL ENGINEERING DEPT. CH.CH. N.Z.

DRAWN : A.GREY	DATE : 2/6/03
CHECKED : SPARKS	DRG. No : A.1.4
APPROVED : PEARSE	

A2

APPENDIX 2 – 540 MM X 300 MM DUCT DESIGN

A.2.1 SUMMARY

Various components were constructed to expand the available testing options for the existing duct rig. An angled duct test section was designed and manufactured. This provided the same cross-sectional area inside the duct when lined with absorbing material. This duct section was used to investigate the effect of the shape of absorbent on insertion loss.

A test duct section which allowed 25 mm lining on all four sides was also constructed. This traditionally lined duct allowed comparisons with bar-silencers to be made.

A new transition section was designed and constructed to meet the requirements of ISO 7235:1991. The contraction section was required due to a change in area between the centrifugal fan unit and the test duct.

A.2.2 CONTRACTION DESIGN

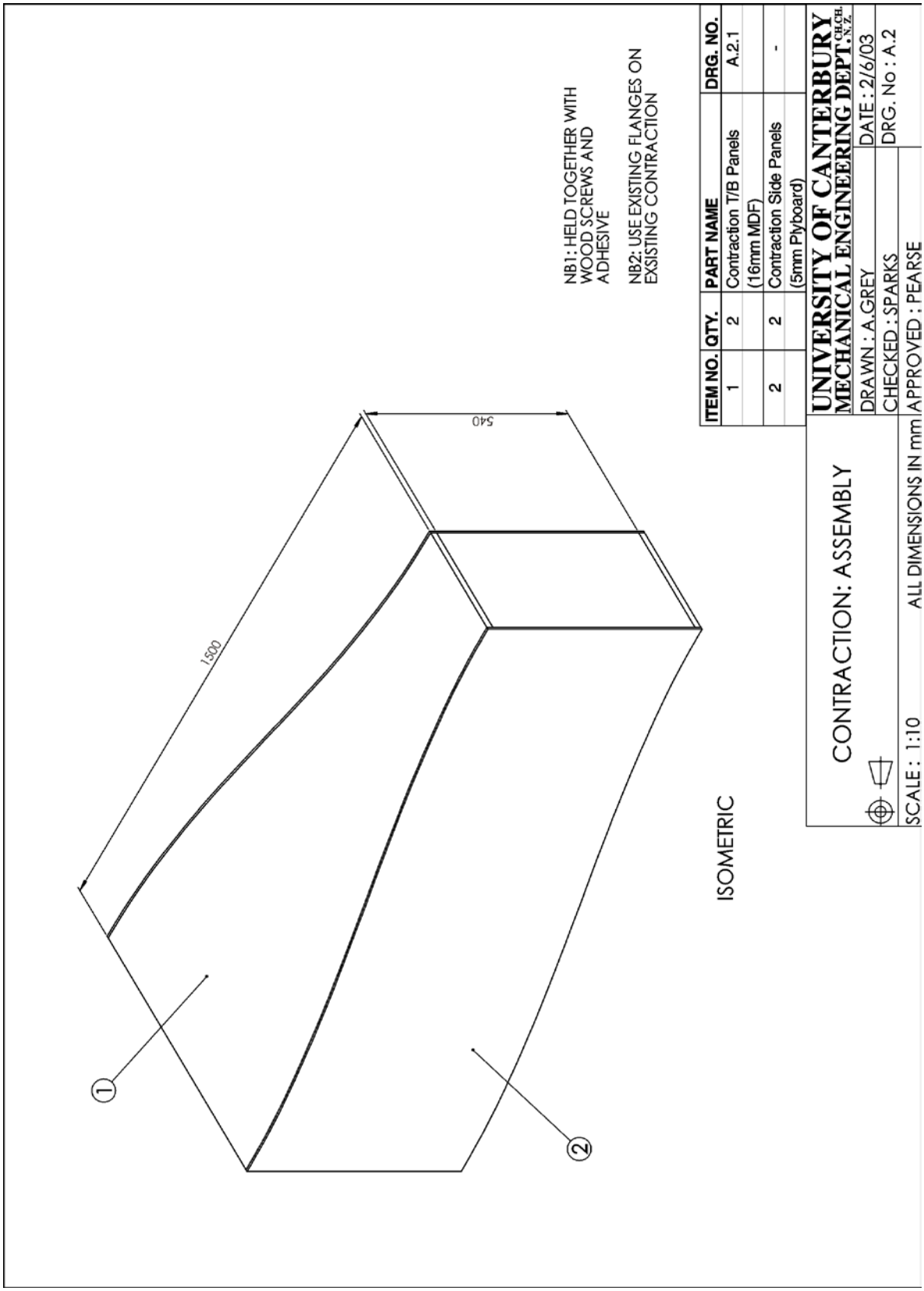

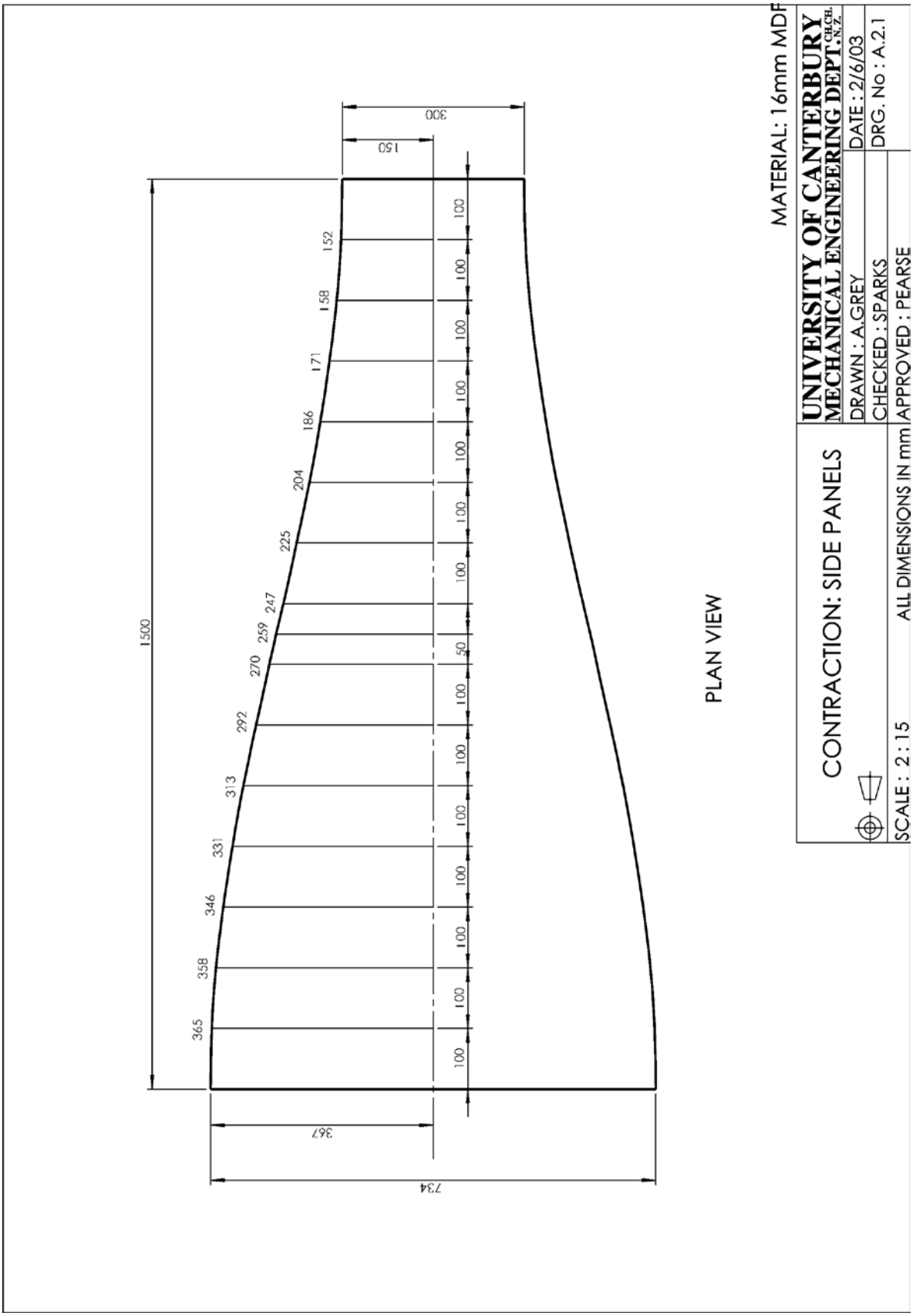
MATERIAL: 16mm MDF
UNIVERSITY OF CANTERBURY
MECHANICAL ENGINEERING DEPT. CH.CH. N.Z.
DRAWN : A.GREY
DATE : 2/6/03
CHECKED : SPARKS
DRG. No : A.2.1
APPROVED : PEARSE
CONTRACTION: SIDE PANELS
SCALE : 2 : 15
ALL DIMENSIONS IN mm
PLAN VIEW
300
150
1500
152
158
171
186
204
225
247
259
270
292
313
331
346
358
365
100
50
367
734

A.2.3 ANGLED DUCT DESIGN

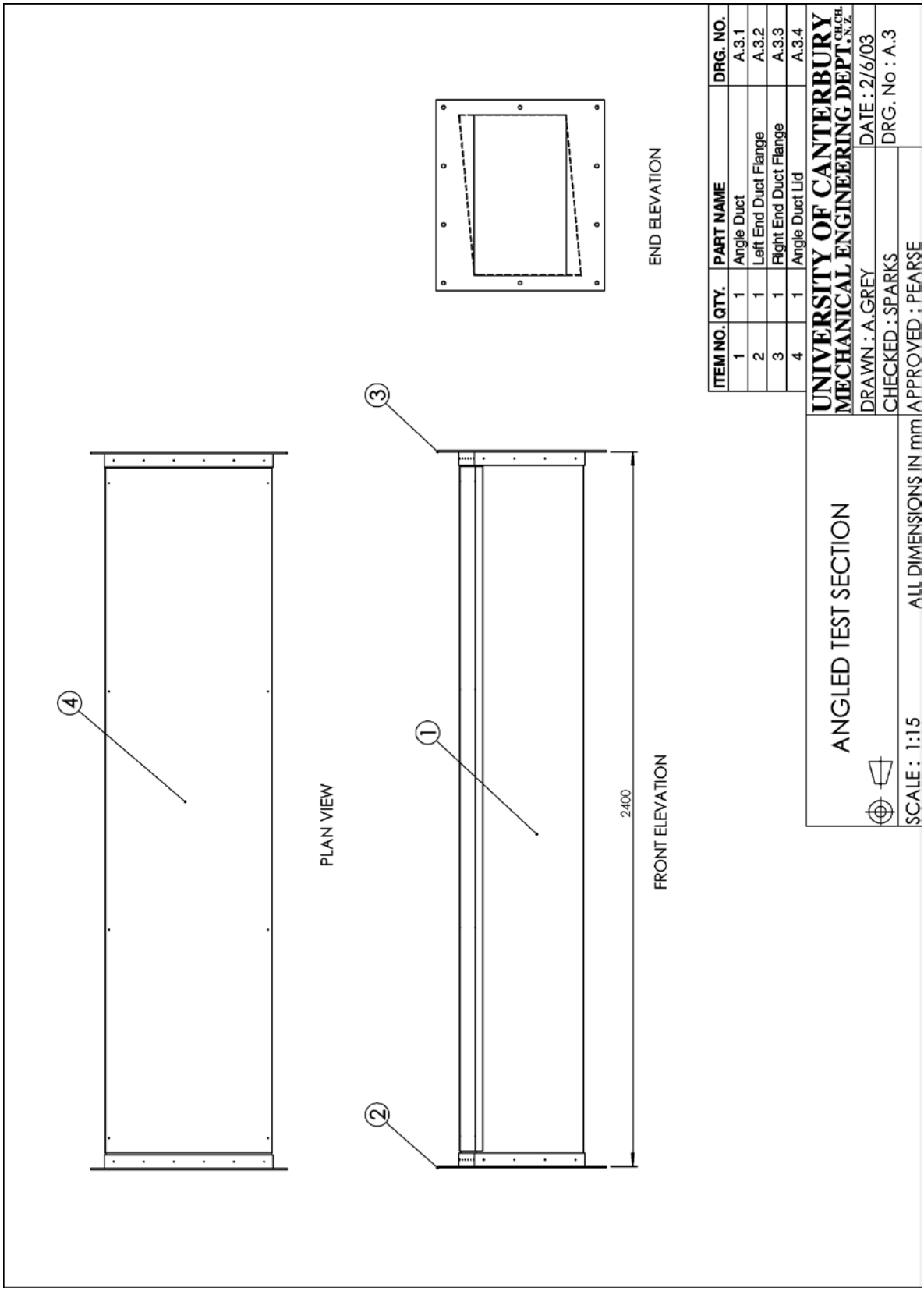

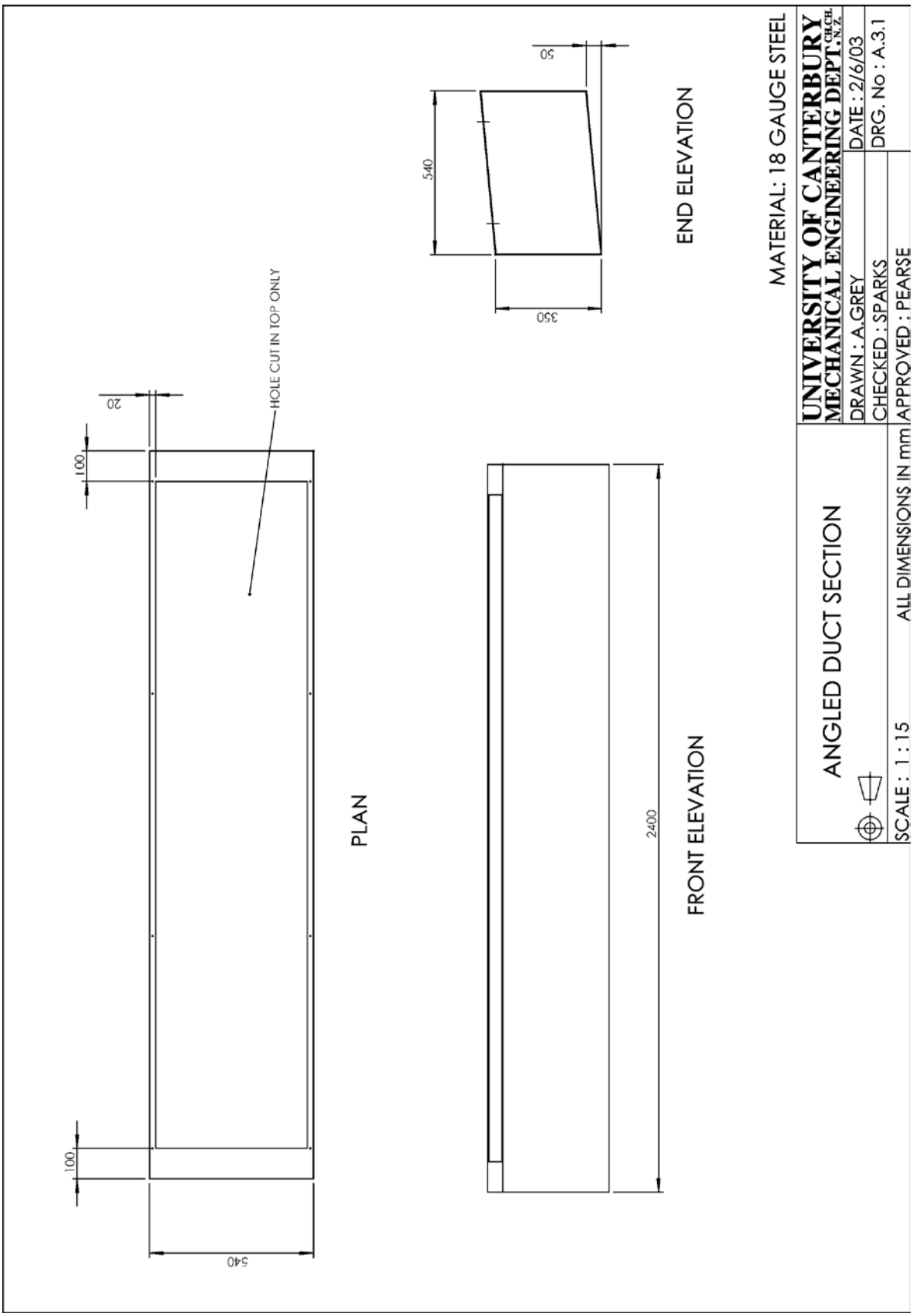
END ELEVATION
50
540
350
MATERIAL: 18 GAUGE STEEL
UNIVERSITY OF CANTERBURY
MECHANICAL ENGINEERING DEPT. CHCH. N.Z.
DRAWN : A.GREY
DATE : 2/6/03
CHECKED : SPARKS
DRG. No : A.3.1
ANGLED DUCT SECTION
SCALE : 1 : 15
ALL DIMENSIONS IN mm
APPROVED : PEARSE
HOLE CUT IN TOP ONLY
20
100
100
540
PLAN
FRONT ELEVATION
2400

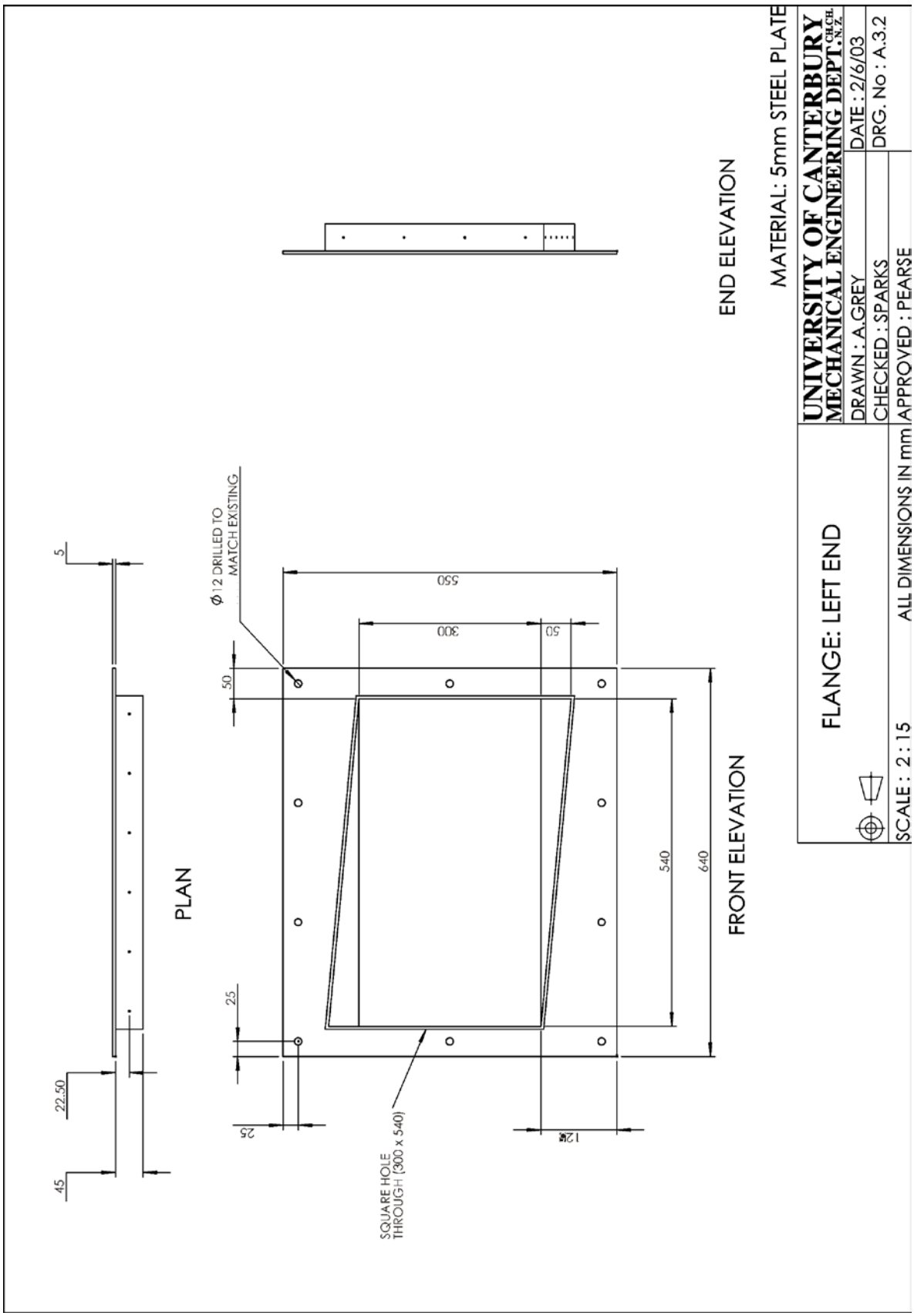
END ELEVATION
MATERIAL: 5mm STEEL PLATE
UNIVERSITY OF CANTERBURY
MECHANICAL ENGINEERING DEPT. CHCH. N.Z.
DRAWN : A.GREY
DATE : 2/6/03
CHECKED : SPARKS
DRG. No : A.3.2
APPROVED : PEARSE
FLANGE: LEFT END
SCALE : 2 : 15
ALL DIMENSIONS IN mm
PLAN
FRONT ELEVATION
Ø 12 DRILLED TO MATCH EXISTING
SQUARE HOLE THROUGH (300 x 540)
5
22.50
45
550
300
50
50
25
25
540
640
12ø

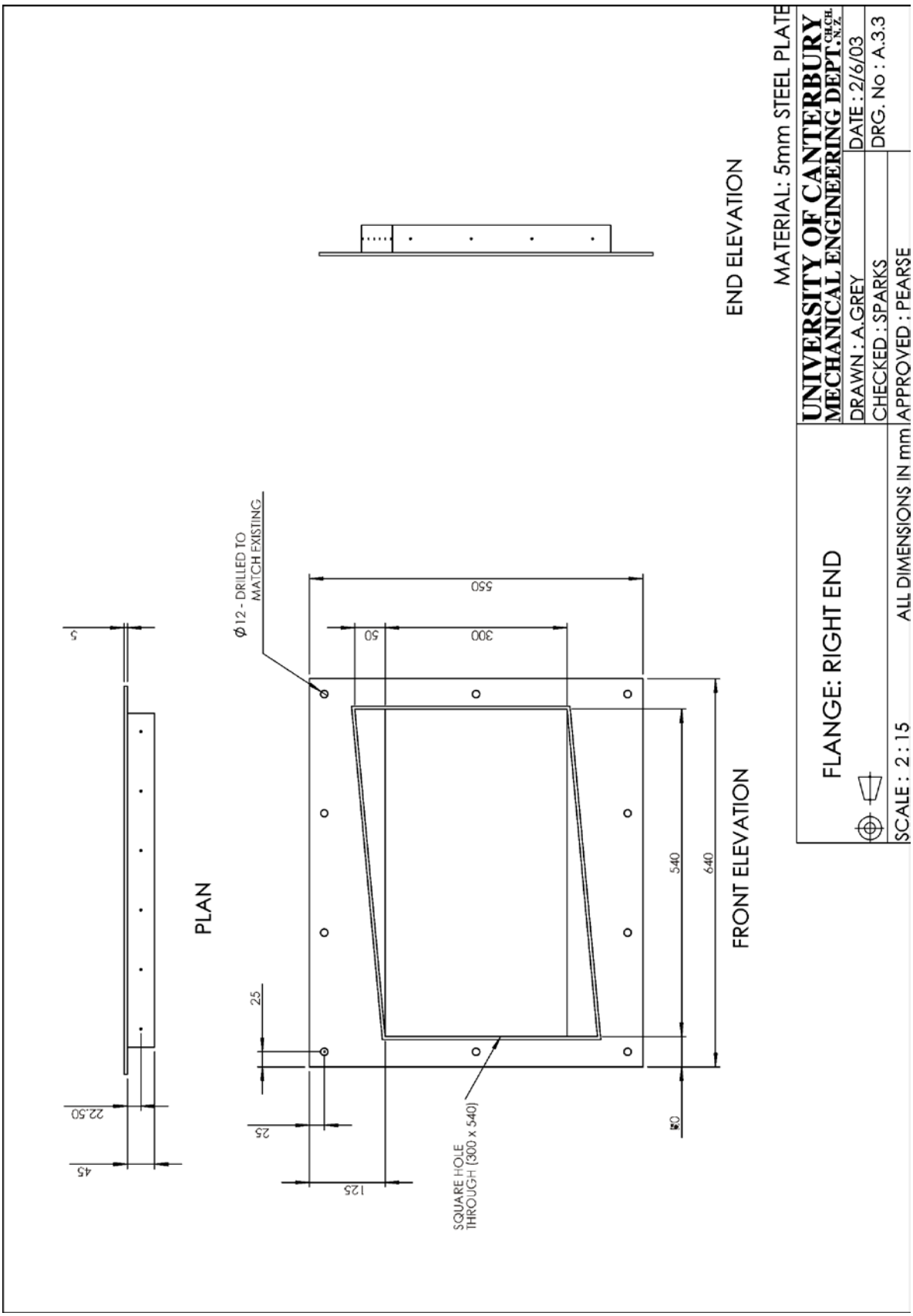
END ELEVATION
MATERIAL: 5mm STEEL PLATE
UNIVERSITY OF CANTERBURY
MECHANICAL ENGINEERING DEPT. CH.CH. N.Z.
DRAWN : A.GREY
DATE : 2/6/03
CHECKED : SPARKS
DRG. No : A.3.3
FLANGE: RIGHT END
SCALE : 2 : 15
ALL DIMENSIONS IN mm
APPROVED : PEARSE
PLAN
FRONT ELEVATION
Ø12 - DRILLED TO MATCH EXISTING
SQUARE HOLE THROUGH (300 x 540)
550
300
50
540
640
25
125
5
22.50
45

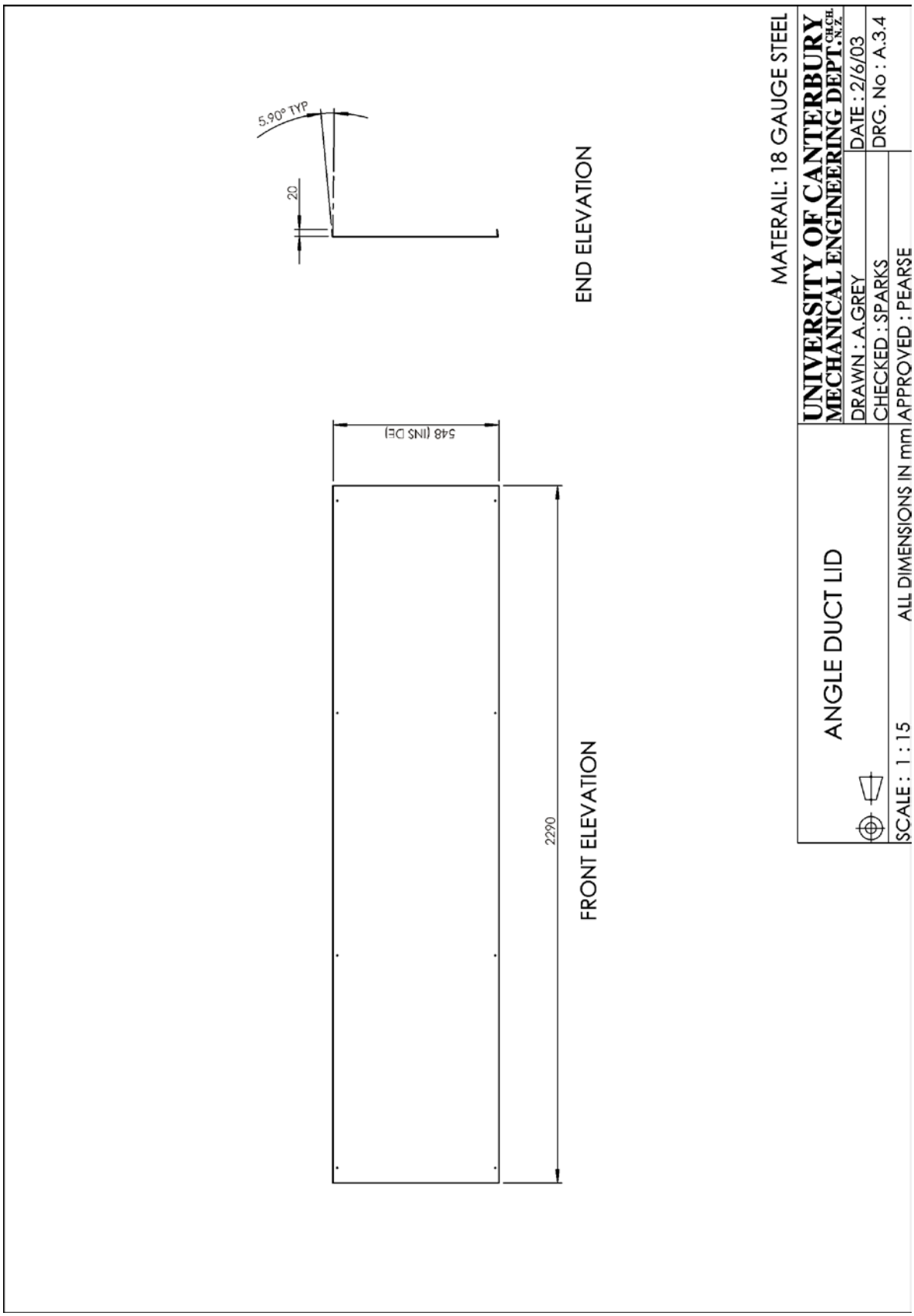
5.90° TYP
20
END ELEVATION
548 (INS DE)
2290
FRONT ELEVATION
MATERAIL: 18 GAUGE STEEL
UNIVERSITY OF CANTERBURY
MECHANICAL ENGINEERING DEPT. CH.CH. N.Z.
DRAWN : A.GREY
DATE : 2/6/03
CHECKED : SPARKS
DRG. No : A.3.4
ANGLE DUCT LID
SCALE : 1 : 15
ALL DIMENSIONS IN mm
APPROVED : PEARSE

A.2.4 4-SIDED DUCT DESIGN

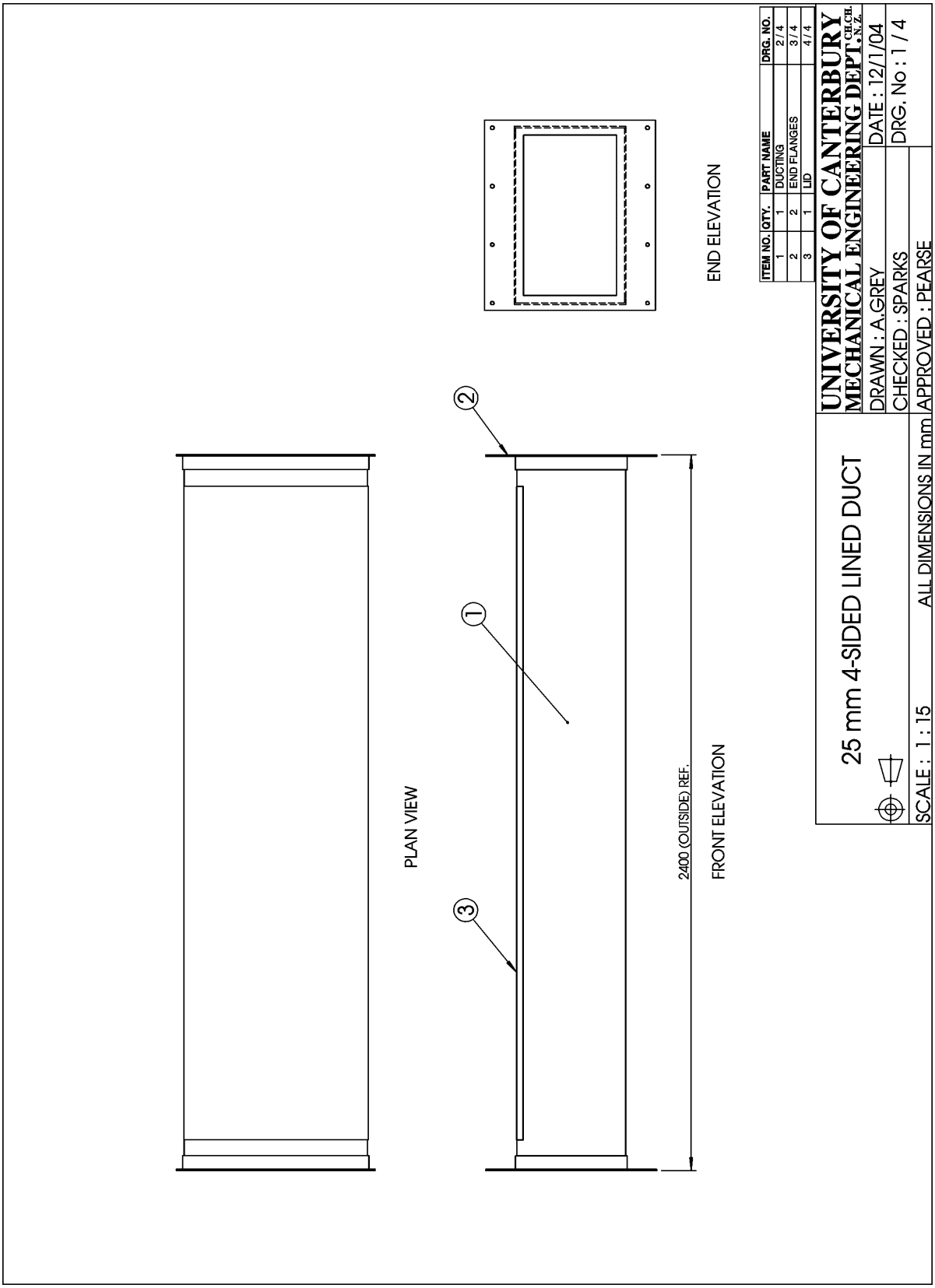

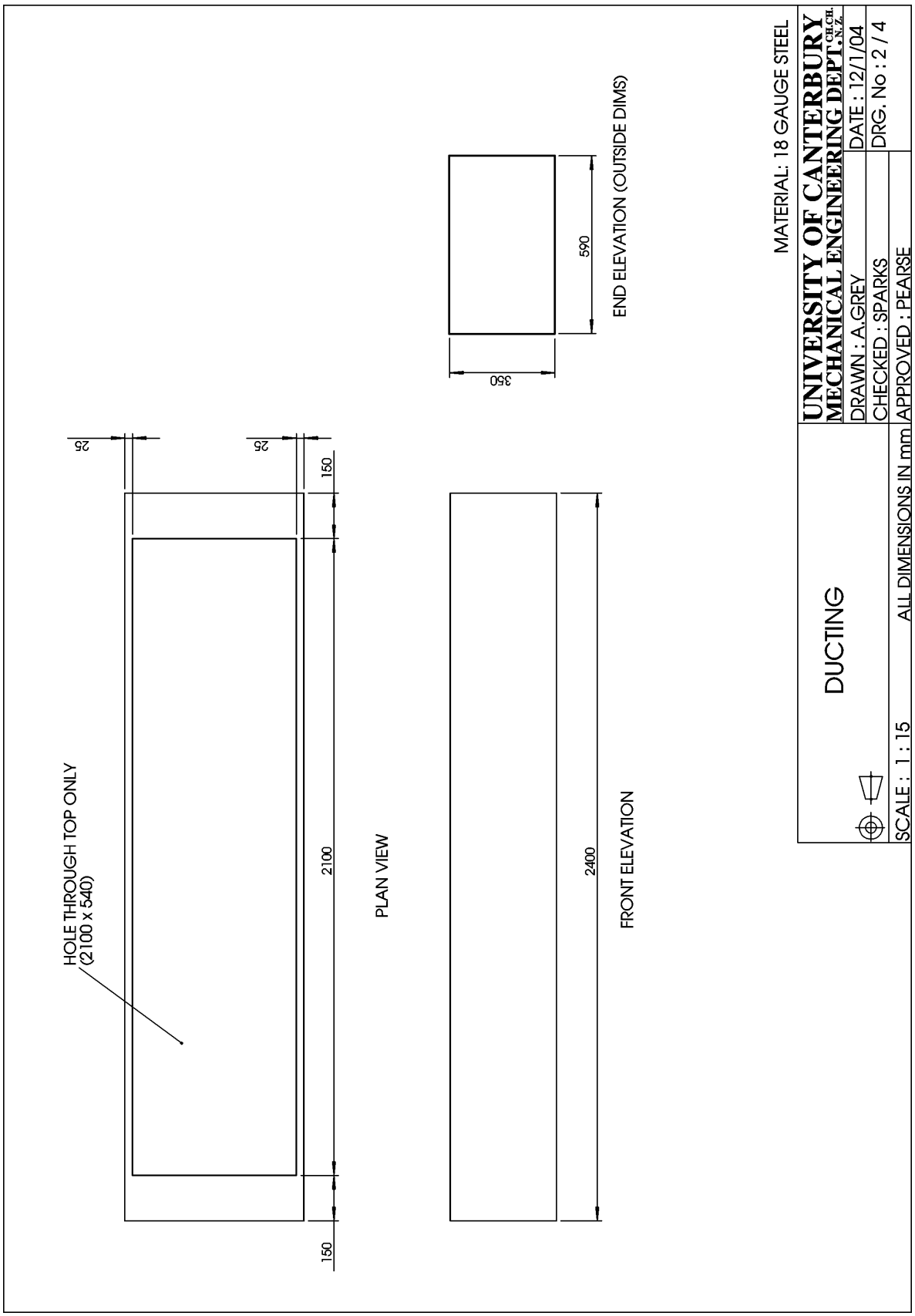
MATERIAL: 18 GAUGE STEEL
UNIVERSITY OF CANTERBURY
MECHANICAL ENGINEERING DEPT. CHCH. N.Z.
DUCTING
DRAWN : A.GREY
DATE : 12/1/04
CHECKED : SPARKS
DRG. No : 2 / 4
SCALE : 1 : 15
ALL DIMENSIONS IN mm
APPROVED : PEARSE
END ELEVATION (OUTSIDE DIMS)
590
350
FRONT ELEVATION
2400
PLAN VIEW
2100
150
150
25
25
HOLE THROUGH TOP ONLY
(2100 x 540)

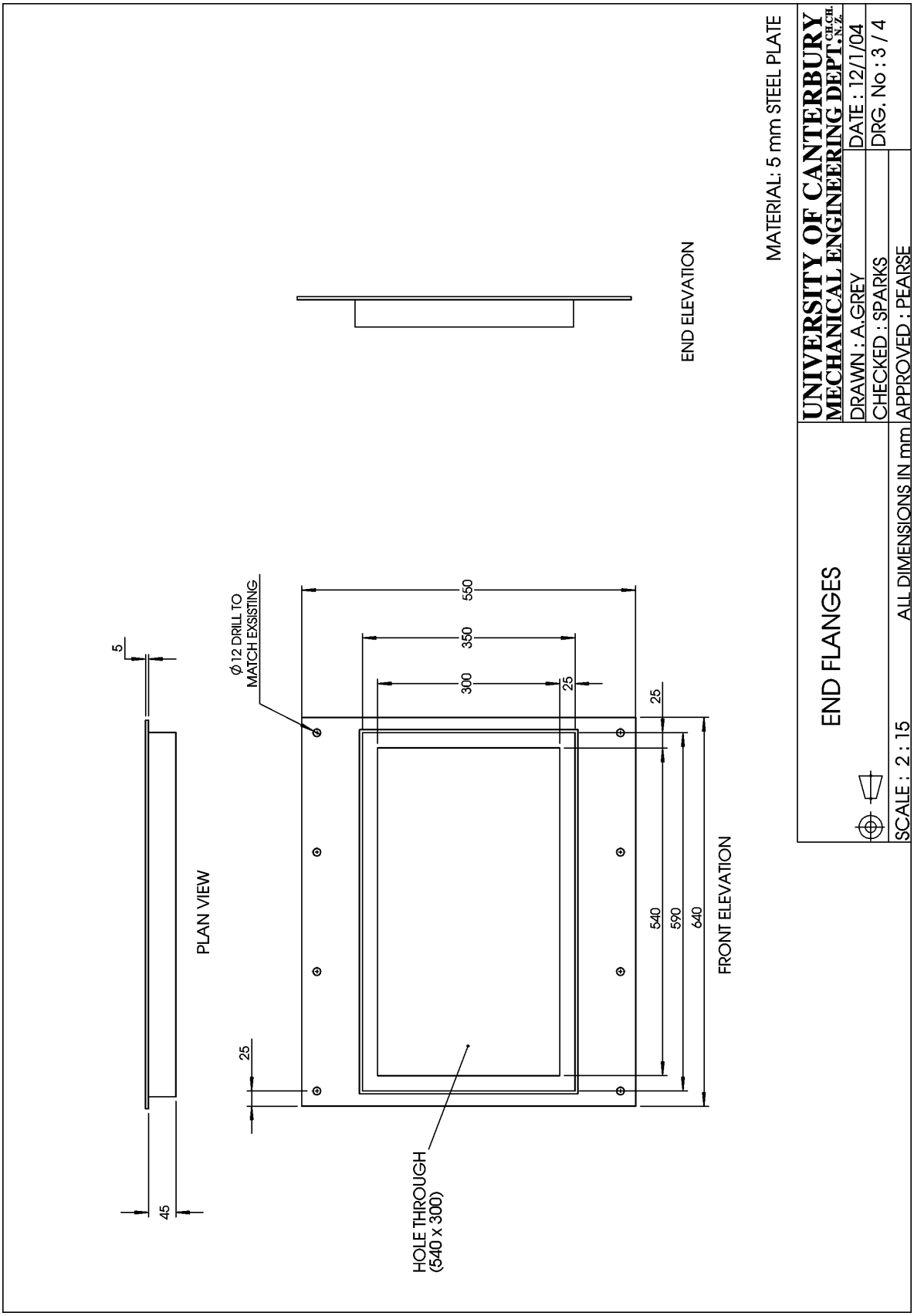
MATERIAL: 5 mm STEEL PLATE
END ELEVATION
PLAN VIEW
FRONT ELEVATION
Ø 12 DRILL TO MATCH EXSISTING
HOLE THROUGH (540 x 300)
5
45
550
350
300
25
540
590
640
END FLANGES
UNIVERSITY OF CANTERBURY
MECHANICAL ENGINEERING DEPT. CHCH. N.Z.
DRAWN : A.GREY
DATE : 12/1/04
CHECKED : SPARKS
DRG. No : 3 / 4
SCALE : 2 : 15
ALL DIMENSIONS IN mm
APPROVED : PEARSE

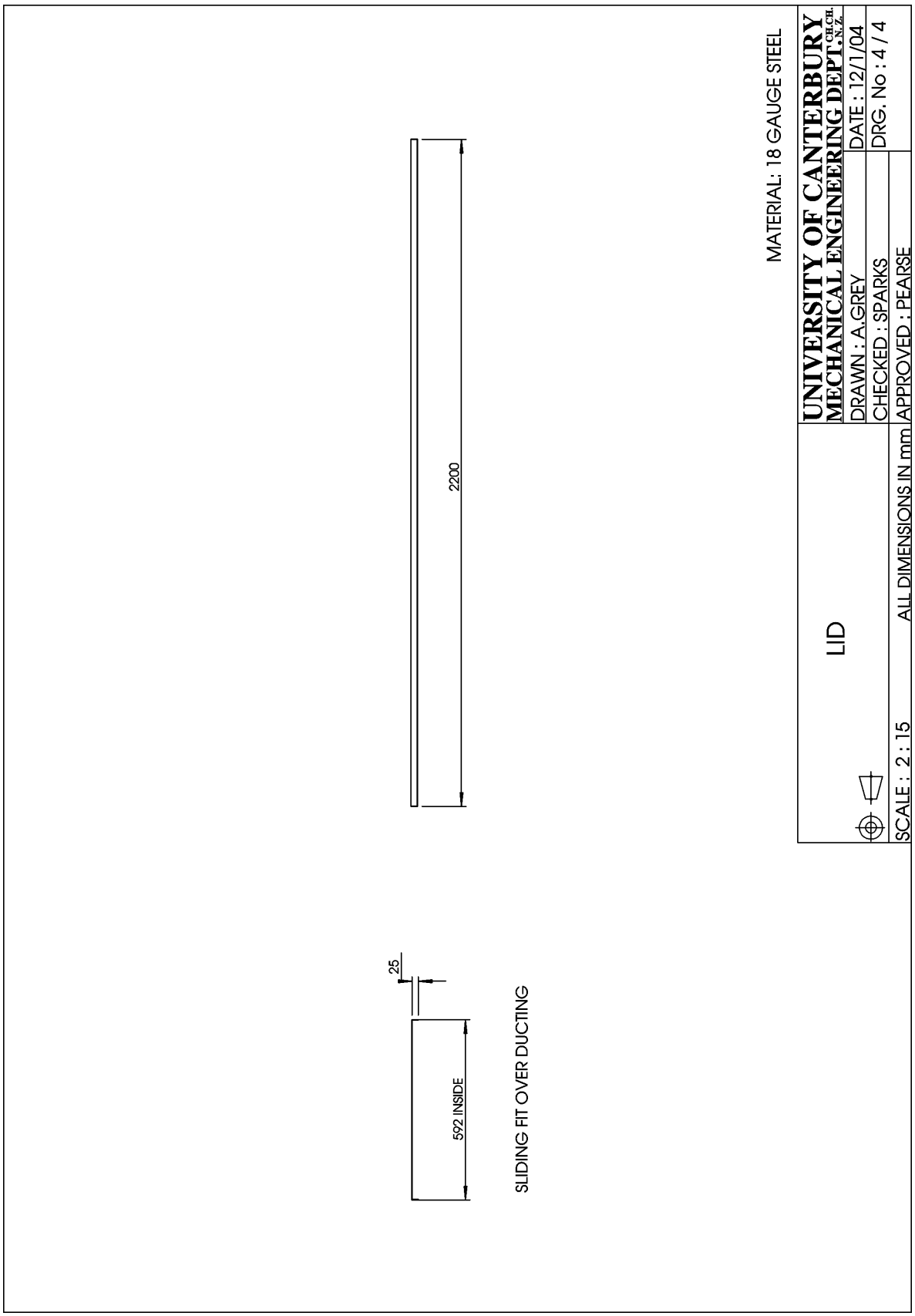
2200
25
592 INSIDE
SLIDING FIT OVER DUCTING
MATERIAL: 18 GAUGE STEEL
LID
UNIVERSITY OF CANTERBURY
MECHANICAL ENGINEERING DEPT. CHCH. N.Z.
DRAWN : A.GREY
DATE : 12/1/04
CHECKED : SPARKS
DRG. No : 4 / 4
SCALE : 2 : 15
ALL DIMENSIONS IN mm
APPROVED : PEARSE

A3

APPENDIX 3 – 270 MM X 300 MM DUCT DESIGN

A.3.1 SUMMARY

A set of ducts with 270 mm x 300 mm cross-section were design and constructed. The ducts included a settling section, inlet duct, substitution duct, outlet section, and two ducts which allowed lining on two and four sides with 25 mm lining, while maintaining a constant open area.

A.3.2 270 mm x 300 mm DUCT DRAWINGS

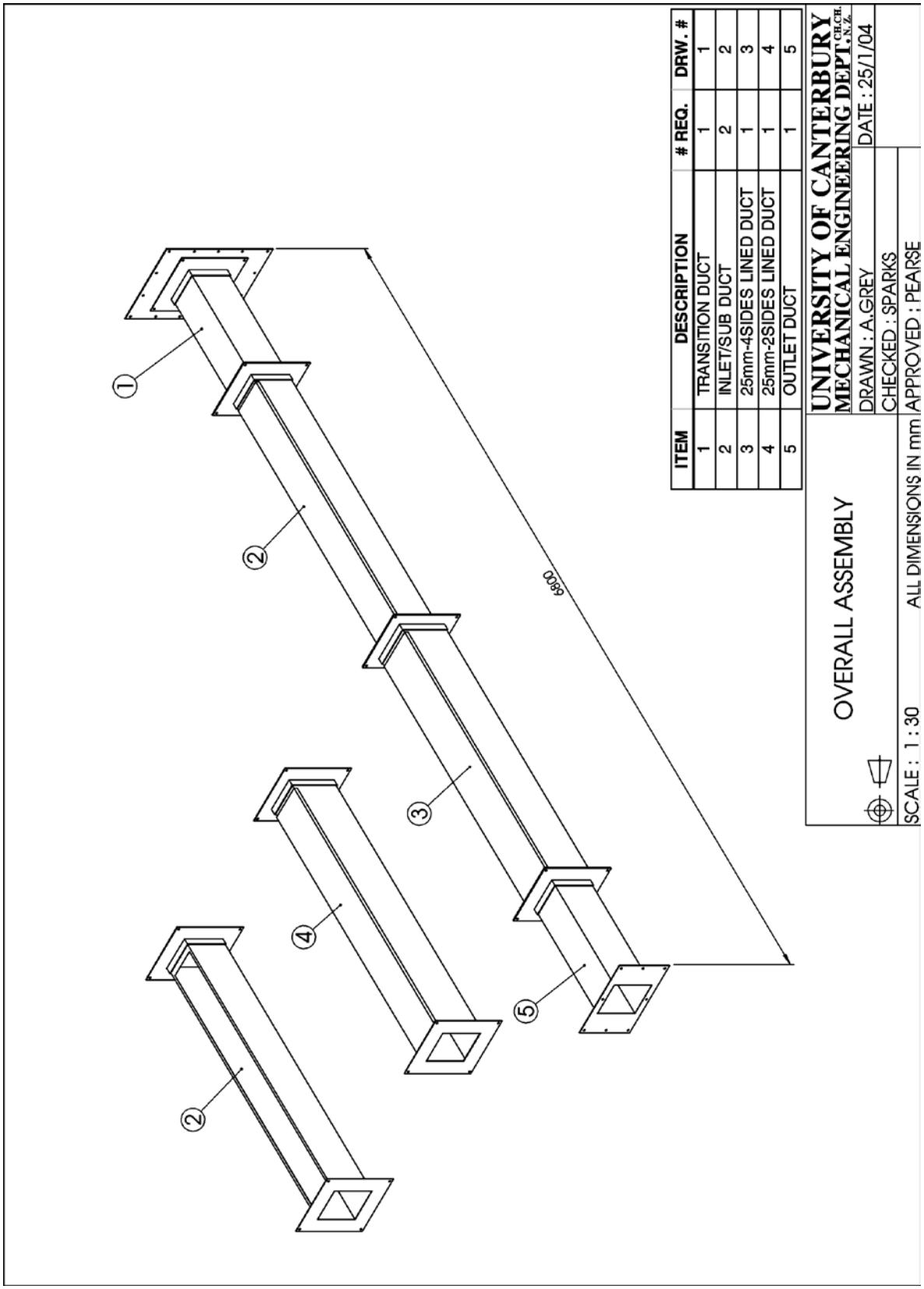

ITEM
DESCRIPTION
REQ.
DRW. #
1
END COVER PLATE
1
1a
2
NORMAL FLANGE
2
1b
3
TRANSITION/OUTLET WALL
1
1c
UNIVERSITY OF CANTERBURY
MECHANICAL ENGINEERING DEPT. CHCH. N.Z.
TRANSITION DUCT
DRAWN : A.GREY
DATE : 25/1/04
CHECKED : SPARKS
DRG. No : 1
SCALE : 1 : 10
ALL DIMENSIONS IN mm
APPROVED : PEARSE
1000 (OUTSIDE) REF.
ISOMETRIC
1
2
3

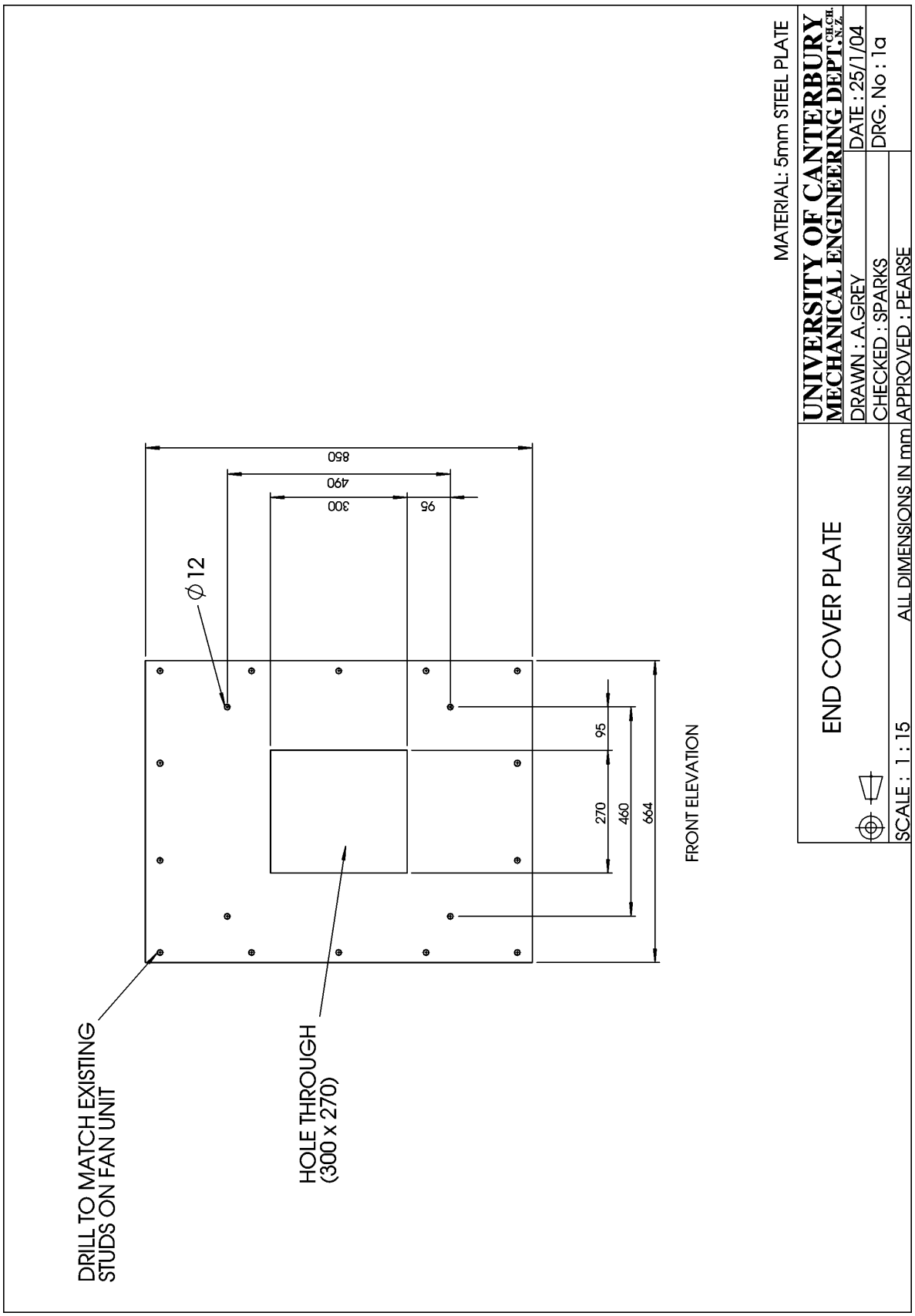
MATERIAL: 5mm STEEL PLATE
UNIVERSITY OF CANTERBURY
MECHANICAL ENGINEERING DEPT. CHRISTCHURCH, N.Z.
END COVER PLATE
DRAWN : A.GREY
DATE : 25/1/04
CHECKED : SPARKS
DRG. No : 1a
SCALE : 1 : 15
ALL DIMENSIONS IN mm
APPROVED : PEARSE
FRONT ELEVATION
850
490
300
95
ϕ12
95
270
460
664
DRILL TO MATCH EXISTING STUDS ON FAN UNIT
HOLE THROUGH (300 x 270)

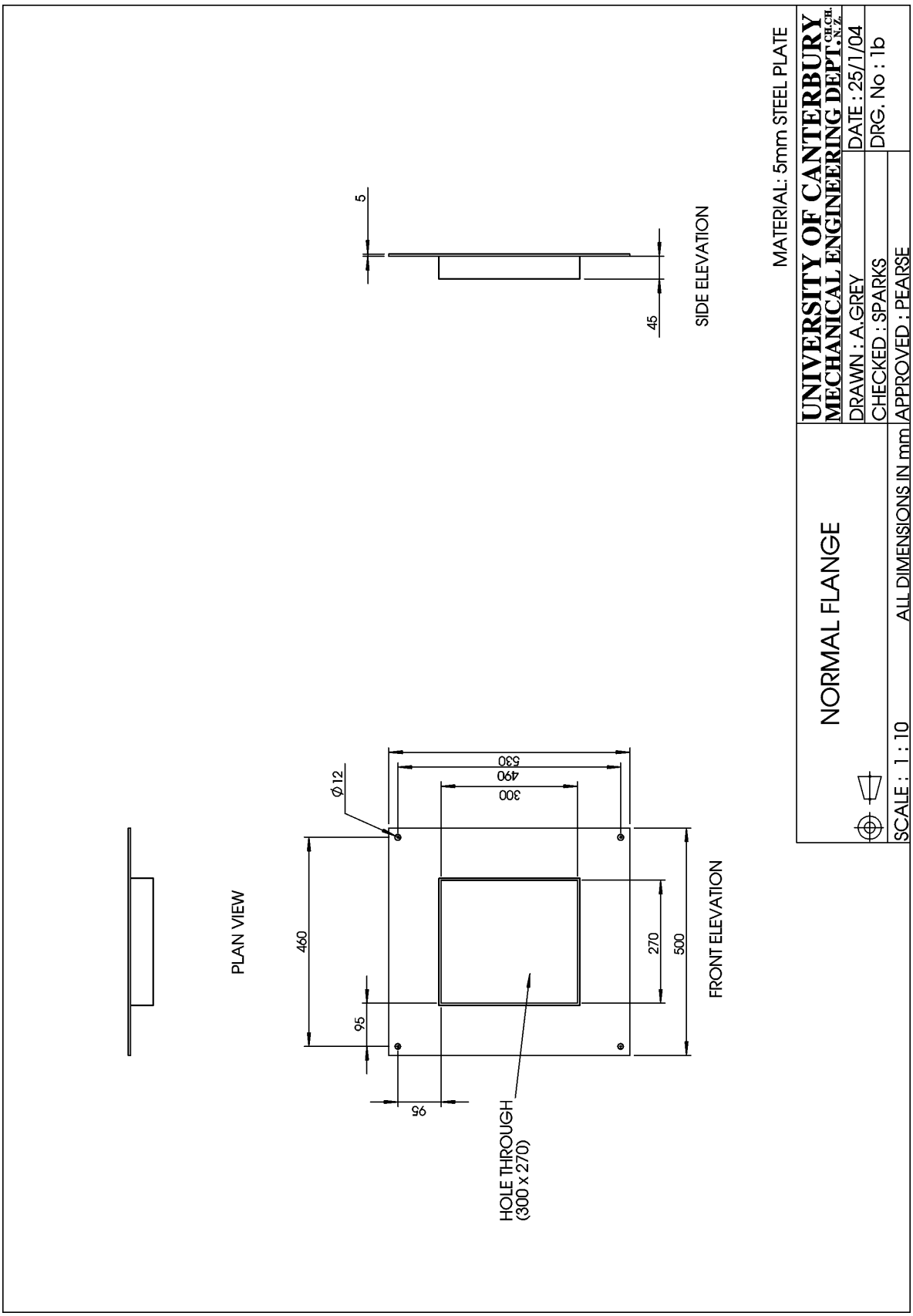
MATERIAL: 5mm STEEL PLATE
UNIVERSITY OF CANTERBURY
MECHANICAL ENGINEERING DEPT. CHCH. N.Z.
NORMAL FLANGE
DRAWN : A.GREY
DATE : 25/1/04
CHECKED : SPARKS
DRG. No : 1b
SCALE : 1 : 10
ALL DIMENSIONS IN mm
APPROVED : PEARSE
SIDE ELEVATION
5
45
PLAN VIEW
FRONT ELEVATION
Ø 12
530
490
300
460
270
500
95
95
HOLE THROUGH
(300 x 270)

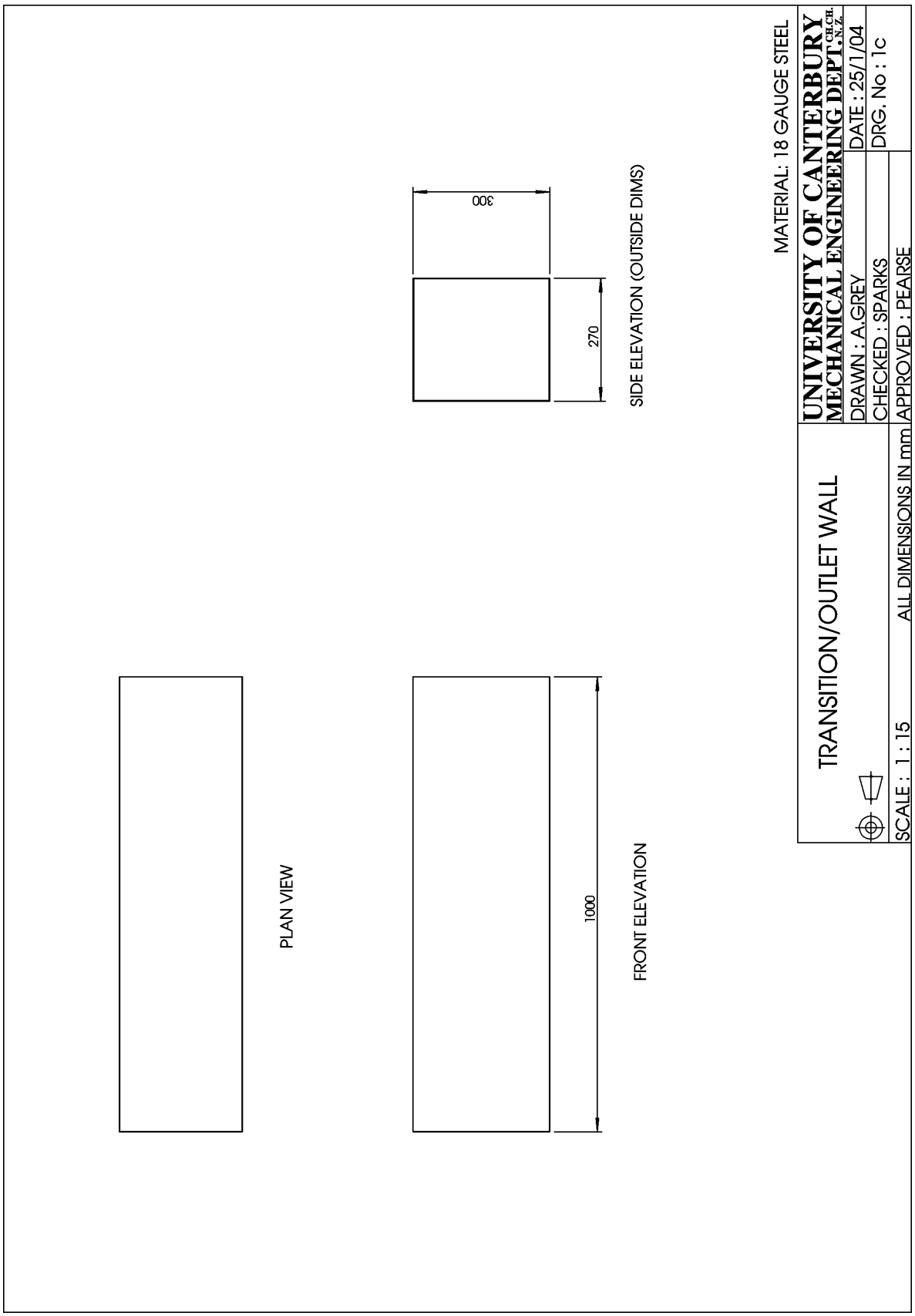
MATERIAL: 18 GAUGE STEEL
UNIVERSITY OF CANTERBURY
MECHANICAL ENGINEERING DEPT. CHCH. N.Z.
TRANSITION/OUTLET WALL
DRAWN : A.GREY
DATE : 25/1/04
CHECKED : SPARKS
DRG. No : 1c
SCALE : 1 : 15
ALL DIMENSIONS IN mm
APPROVED : PEARSE
SIDE ELEVATION (OUTSIDE DIMS)
300
270
PLAN VIEW
FRONT ELEVATION
1000

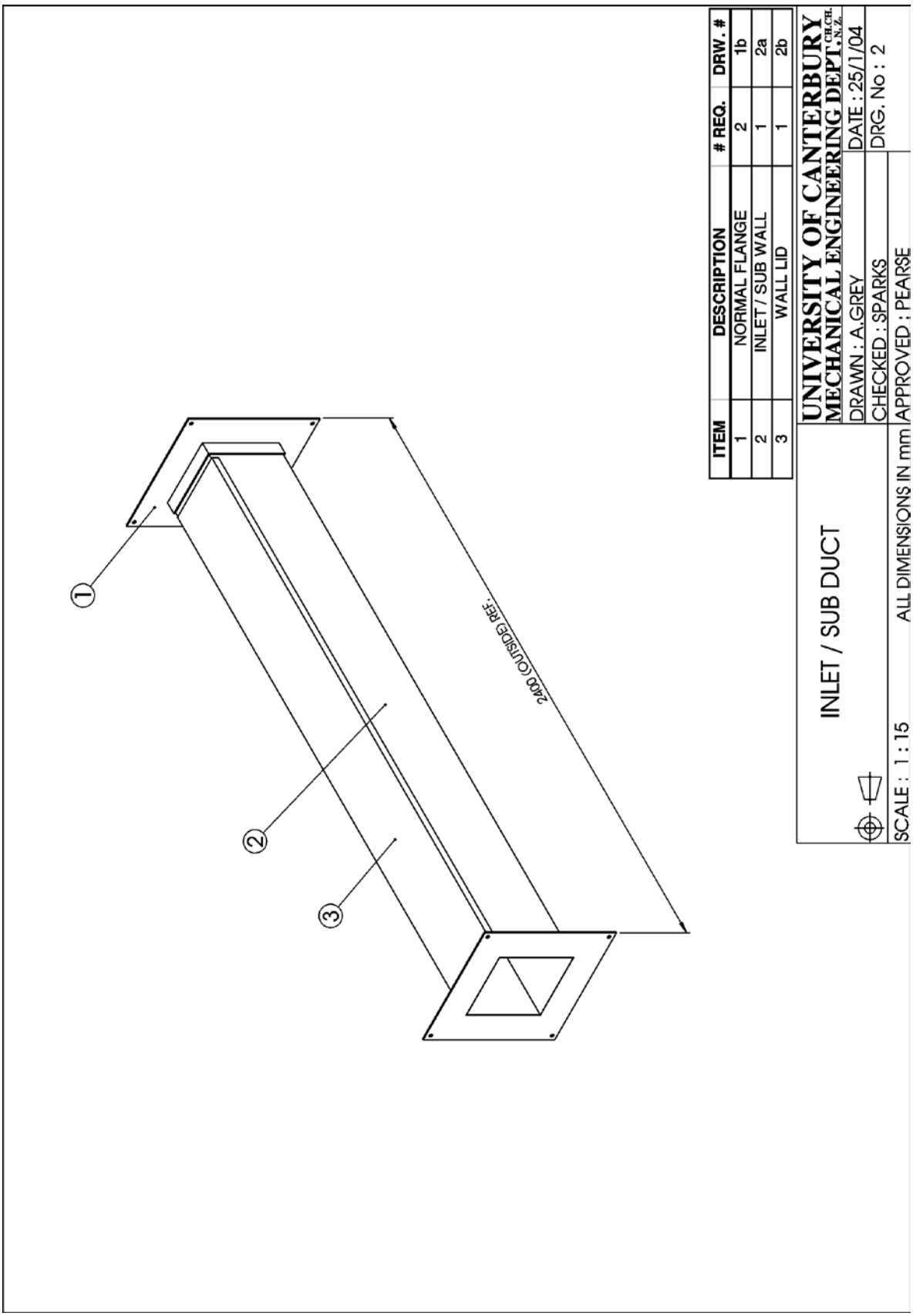
ITEM
DESCRIPTION
REQ.
DRW. #
1
NORMAL FLANGE
2
1b
2
INLET / SUB WALL
1
2a
3
WALL LID
1
2b
UNIVERSITY OF CANTERBURY
MECHANICAL ENGINEERING DEPT. CHCH. N.Z.
INLET / SUB DUCT
DRAWN : A.GREY
DATE : 25/1/04
CHECKED : SPARKS
DRG. No : 2
SCALE : 1 : 15
ALL DIMENSIONS IN mm
APPROVED : PEARSE
2400 (OUTSIDE) REF.
1
2
3

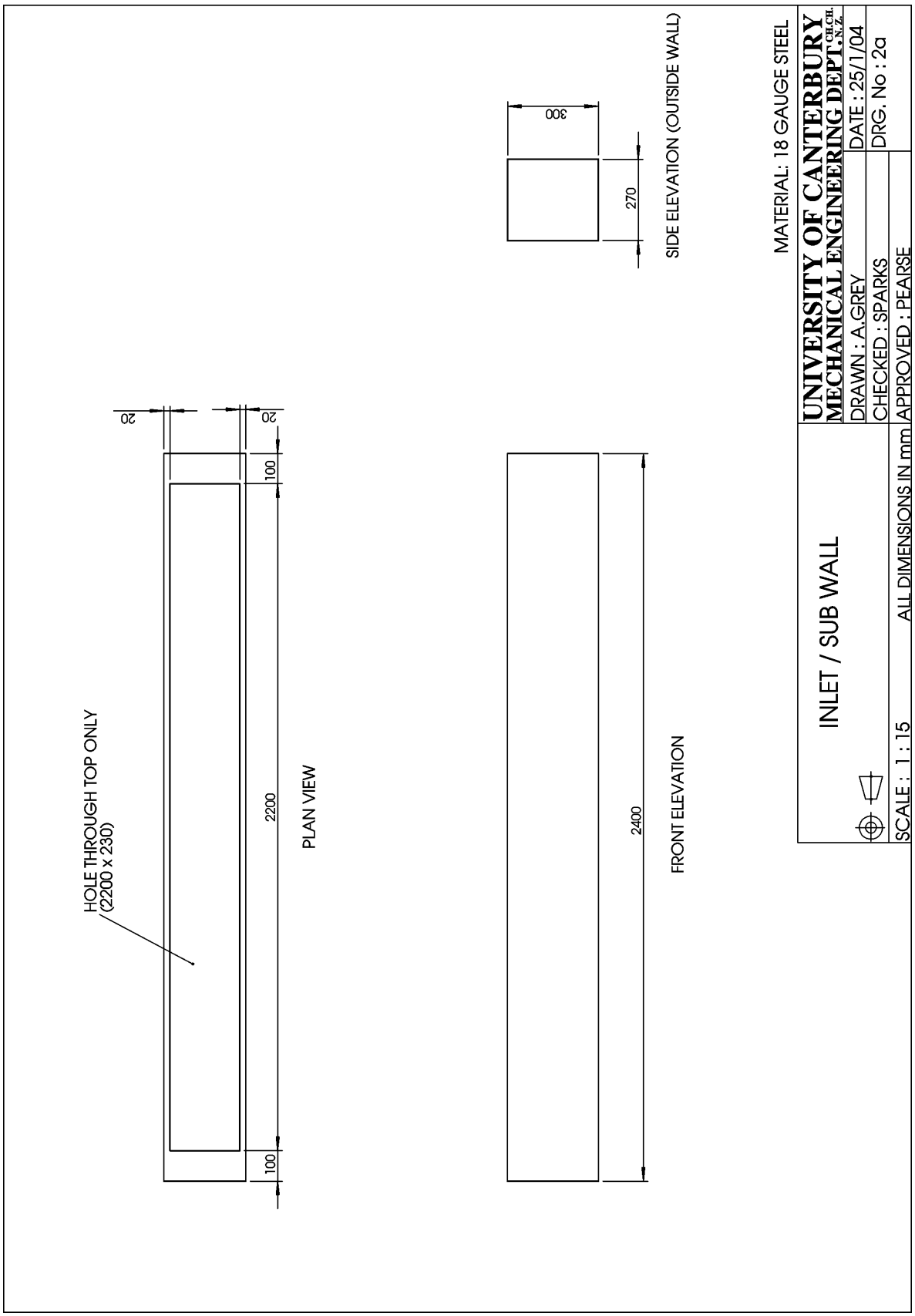
HOLE THROUGH TOP ONLY
(2200 x 230)
20
20
100
2200
100
PLAN VIEW
300
270
SIDE ELEVATION (OUTSIDE WALL)
2400
FRONT ELEVATION
MATERIAL: 18 GAUGE STEEL
INLET / SUB WALL
UNIVERSITY OF CANTERBURY
MECHANICAL ENGINEERING DEPT. CHCH. N.Z.
DRAWN : A.GREY
DATE : 25/1/04
CHECKED : SPARKS
DRG. No : 2a
SCALE : 1 : 15
ALL DIMENSIONS IN mm
APPROVED : PEARSE

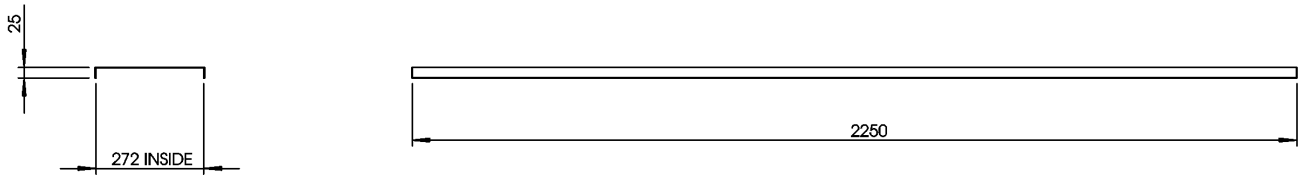

SLIDING FIT OVER
- INLET/SUB WALL
- 2 SIDES LINED DUCT WALL

MATERIAL: 18 GAUGE STEEL

WALL LID	**UNIVERSITY OF CANTERBURY** MECHANICAL ENGINEERING DEPT. CH.CH. N.Z.	
	DRAWN : A.GREY	DATE : 25/1/04
	CHECKED : SPARKS	DRG. No : 2b
SCALE : 1 : 15 ALL DIMENSIONS IN mm	APPROVED : PEARSE	

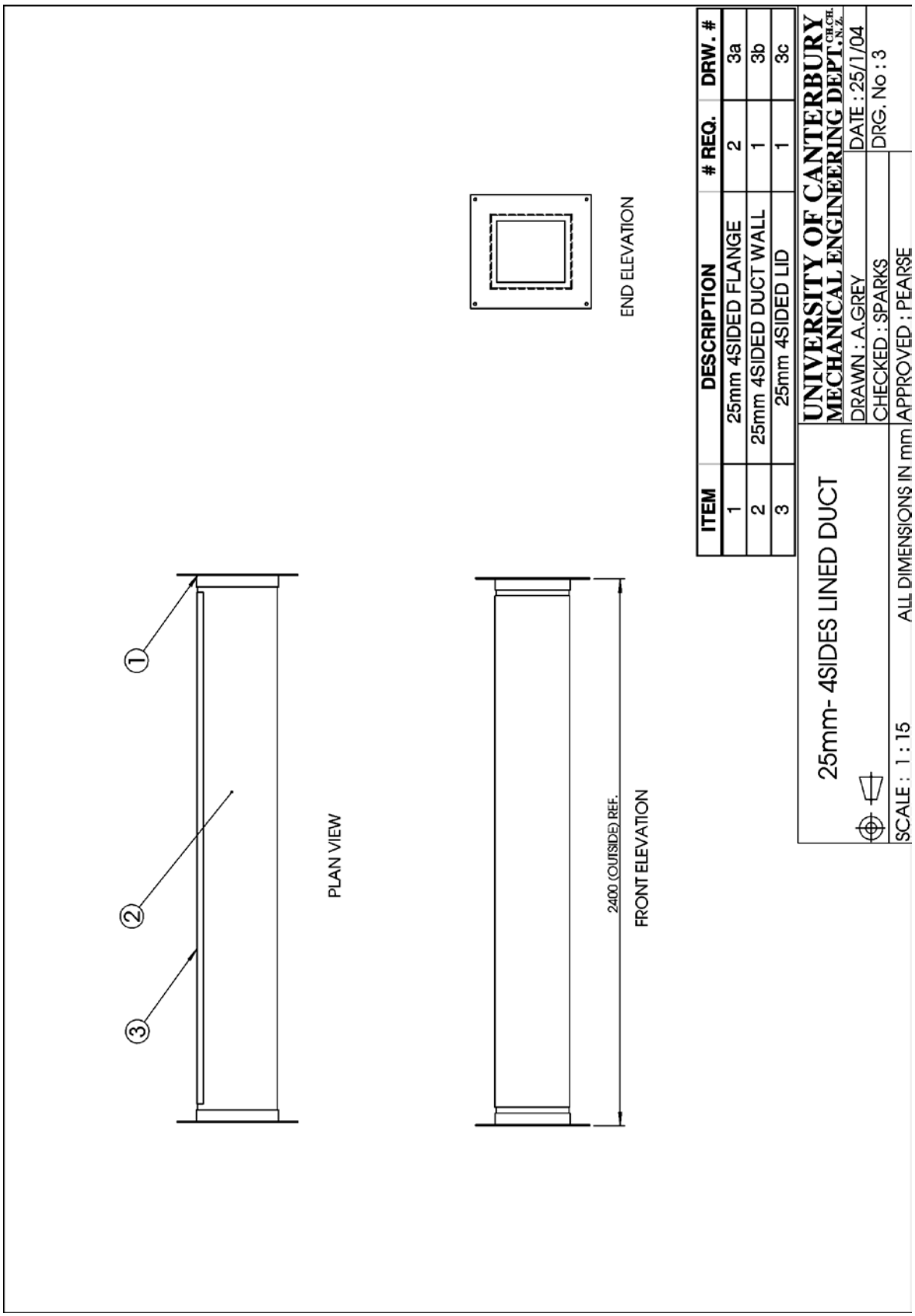
ITEM
DESCRIPTION
REQ.
DRW. #
1
25mm 4SIDED FLANGE
2
3a
2
25mm 4SIDED DUCT WALL
1
3b
3
25mm 4SIDED LID
1
3c
UNIVERSITY OF CANTERBURY
MECHANICAL ENGINEERING DEPT. CHRISTCHURCH, N.Z.
25mm- 4SIDES LINED DUCT
DRAWN : A.GREY
DATE : 25/1/04
CHECKED : SPARKS
DRG. No : 3
SCALE : 1 : 15
ALL DIMENSIONS IN mm
APPROVED : PEARSE
END ELEVATION
PLAN VIEW
FRONT ELEVATION
2400 (OUTSIDE) REF.
1
2
3

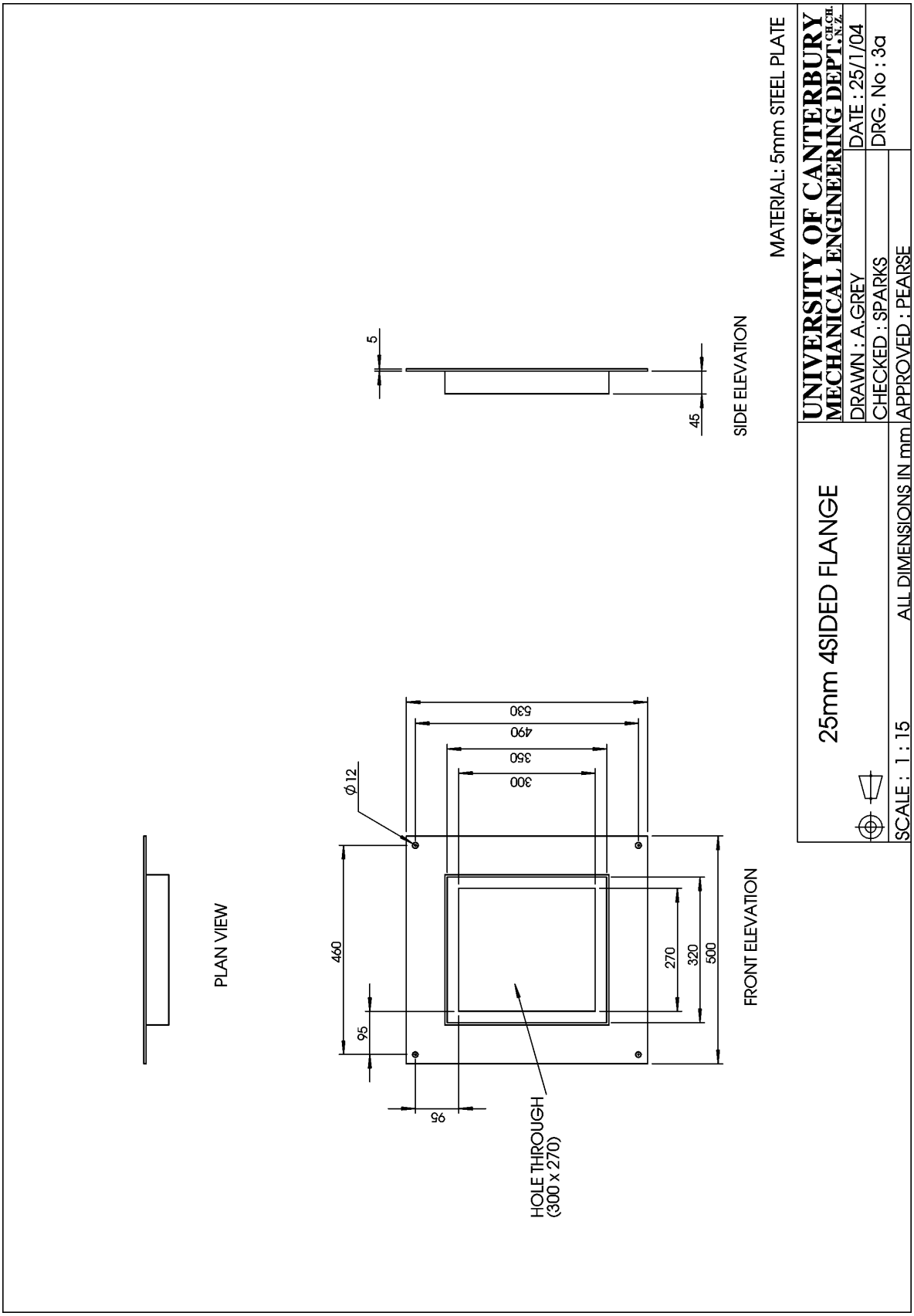
MATERIAL: 5mm STEEL PLATE
SIDE ELEVATION
5
45
PLAN VIEW
FRONT ELEVATION
Ø12
530
490
350
300
460
95
95
270
320
500
HOLE THROUGH
(300 x 270)
25mm 4SIDED FLANGE
UNIVERSITY OF CANTERBURY
MECHANICAL ENGINEERING DEPT. CHCH. N.Z.
DRAWN : A.GREY
DATE : 25/1/04
CHECKED : SPARKS
DRG. No : 3a
SCALE : 1 : 15
ALL DIMENSIONS IN mm
APPROVED : PEARSE

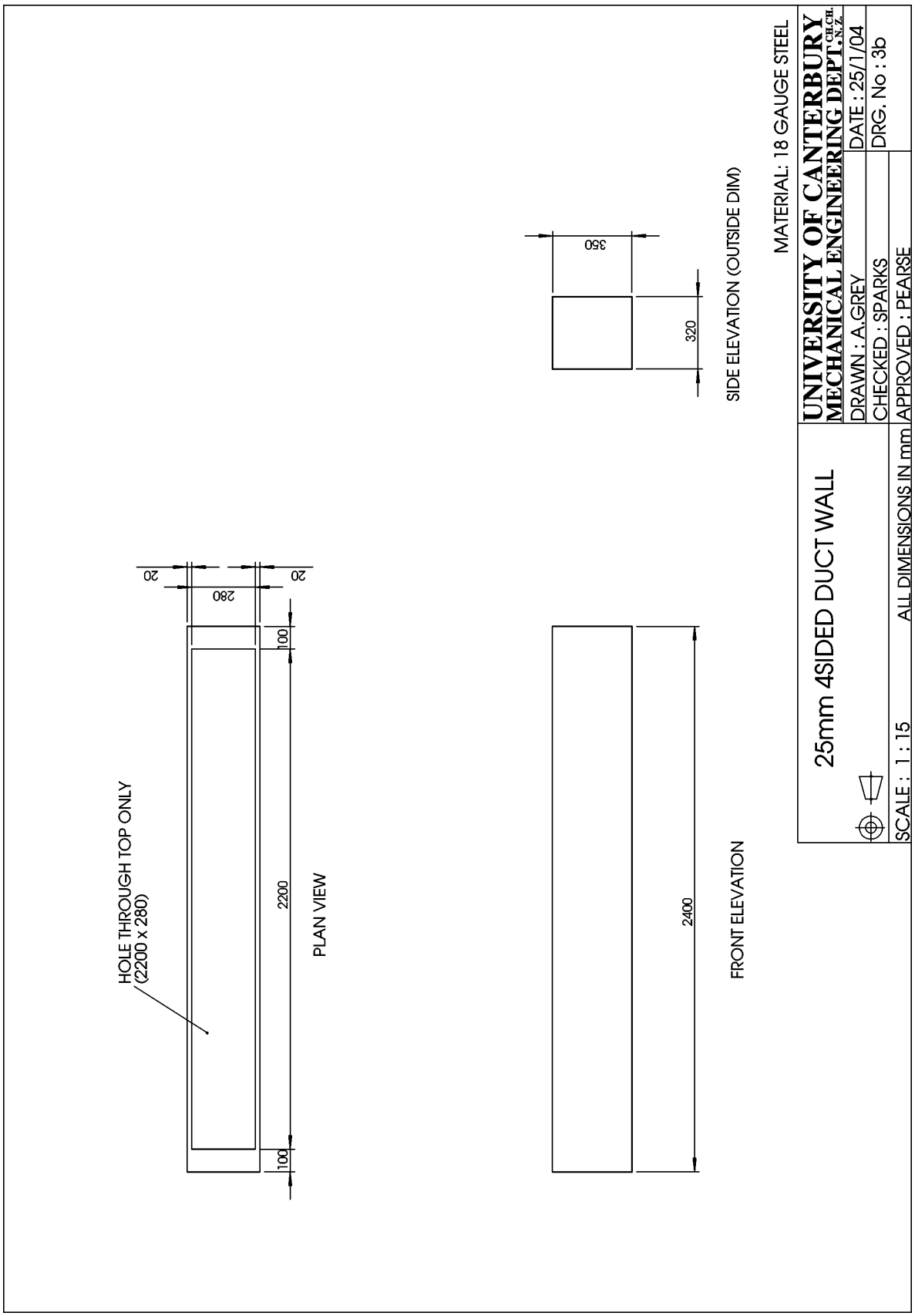
HOLE THROUGH TOP ONLY
(2200 x 280)
20
280
20
100
2200
100
PLAN VIEW
350
320
SIDE ELEVATION (OUTSIDE DIM)
2400
FRONT ELEVATION
MATERIAL: 18 GAUGE STEEL
25mm 4SIDED DUCT WALL
UNIVERSITY OF CANTERBURY
MECHANICAL ENGINEERING DEPT. CHCH. N.Z.
DRAWN : A.GREY
DATE : 25/1/04
CHECKED : SPARKS
DRG. No : 3b
SCALE : 1 : 15
ALL DIMENSIONS IN mm
APPROVED : PEARSE

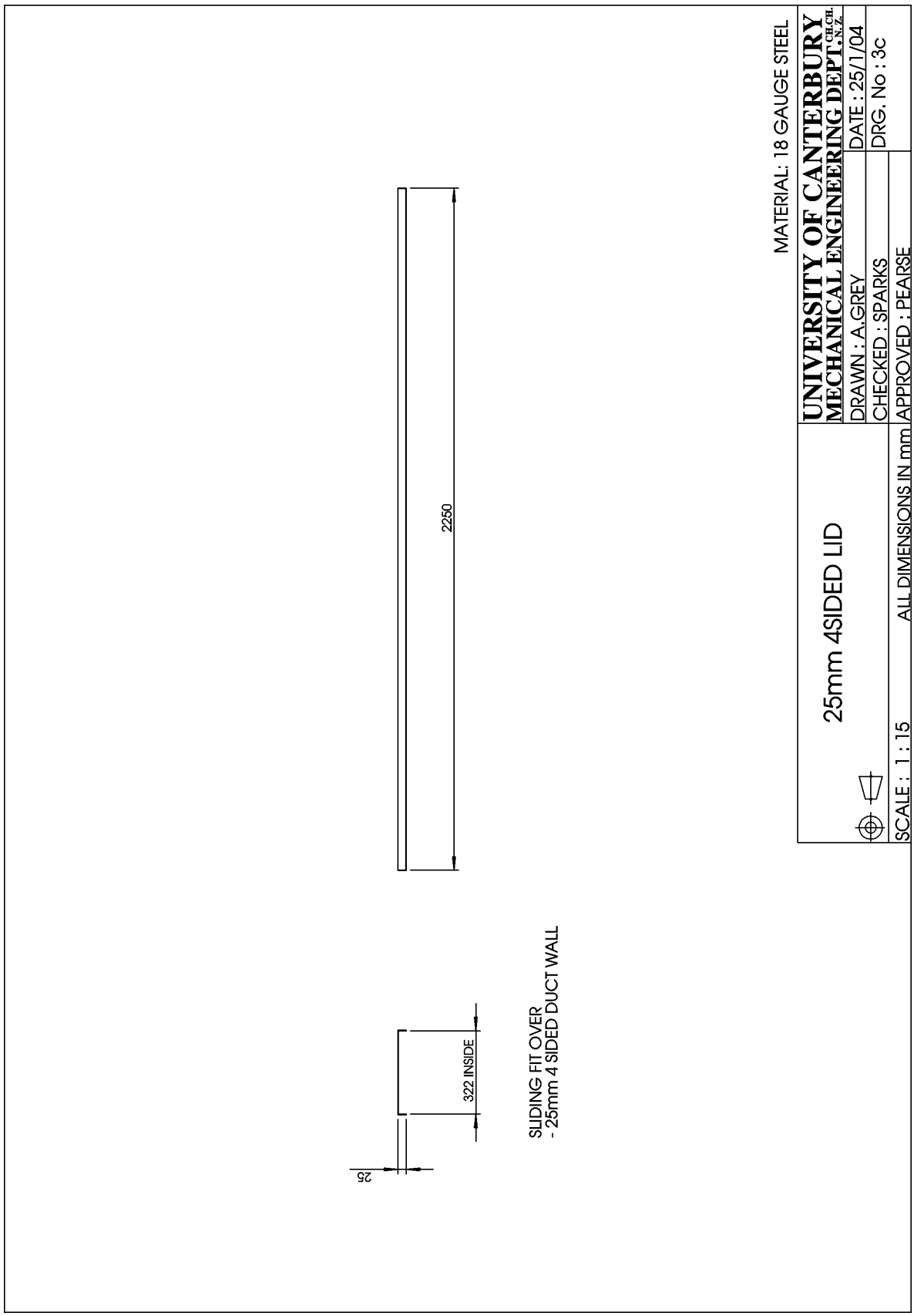
MATERIAL: 18 GAUGE STEEL
UNIVERSITY OF CANTERBURY
MECHANICAL ENGINEERING DEPT. CHCH. N.Z.
25mm 4SIDED LID
DRAWN : A.GREY
DATE : 25/1/04
CHECKED : SPARKS
DRG. No : 3c
SCALE : 1 : 15
ALL DIMENSIONS IN mm
APPROVED : PEARSE
2250
322 INSIDE
25
SLIDING FIT OVER
- 25mm 4 SIDED DUCT WALL

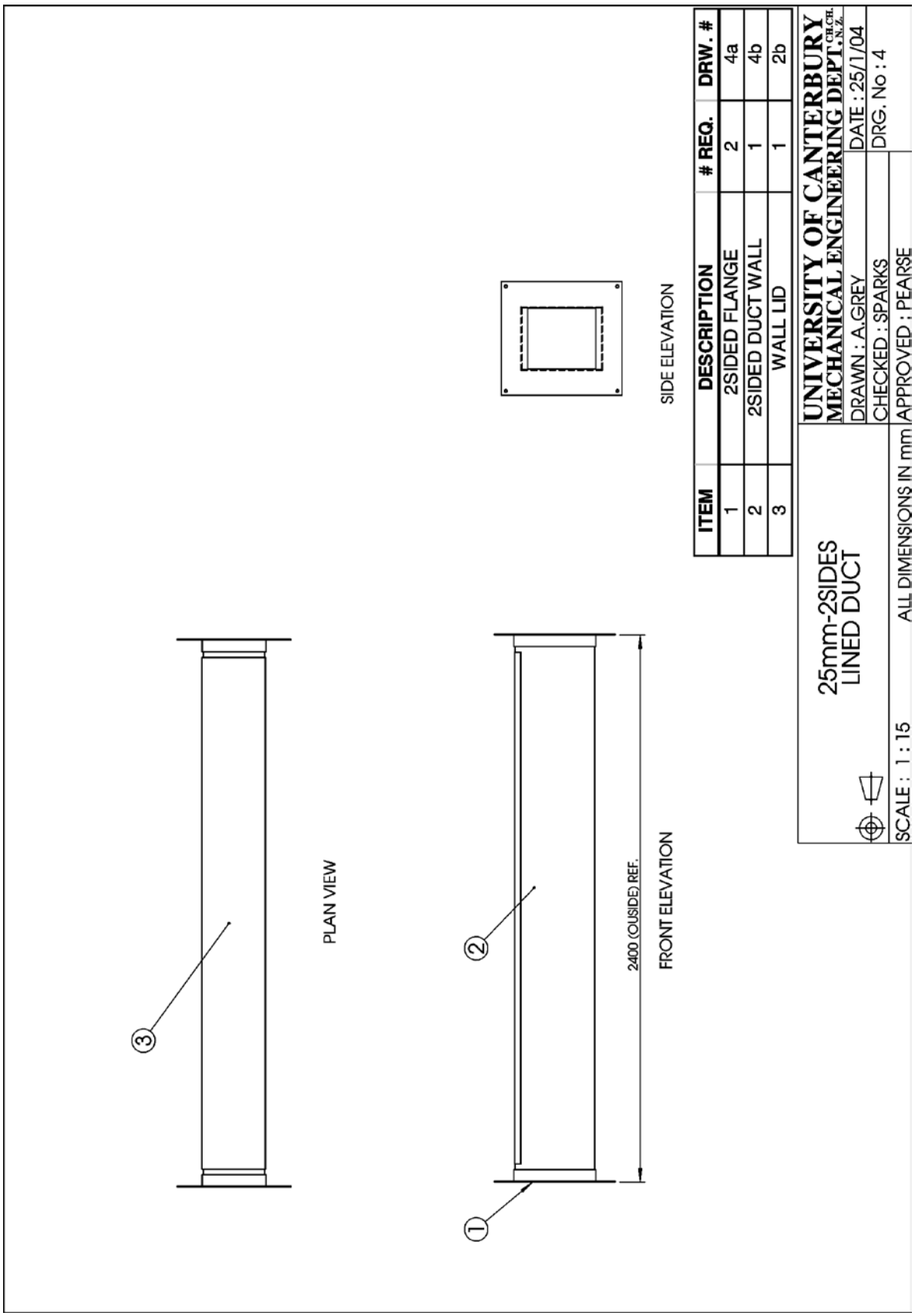
ITEM
DESCRIPTION
REQ.
DRW. #
1
2SIDED FLANGE
2
4a
2
2SIDED DUCT WALL
1
4b
3
WALL LID
1
2b
SIDE ELEVATION
PLAN VIEW
FRONT ELEVATION
2400 (OUSIDE) REF.
25mm-2SIDES LINED DUCT
UNIVERSITY OF CANTERBURY
MECHANICAL ENGINEERING DEPT. CHCH. N.Z.
DRAWN : A.GREY
DATE : 25/1/04
CHECKED : SPARKS
DRG. No : 4
SCALE : 1 : 15
ALL DIMENSIONS IN mm
APPROVED : PEARSE

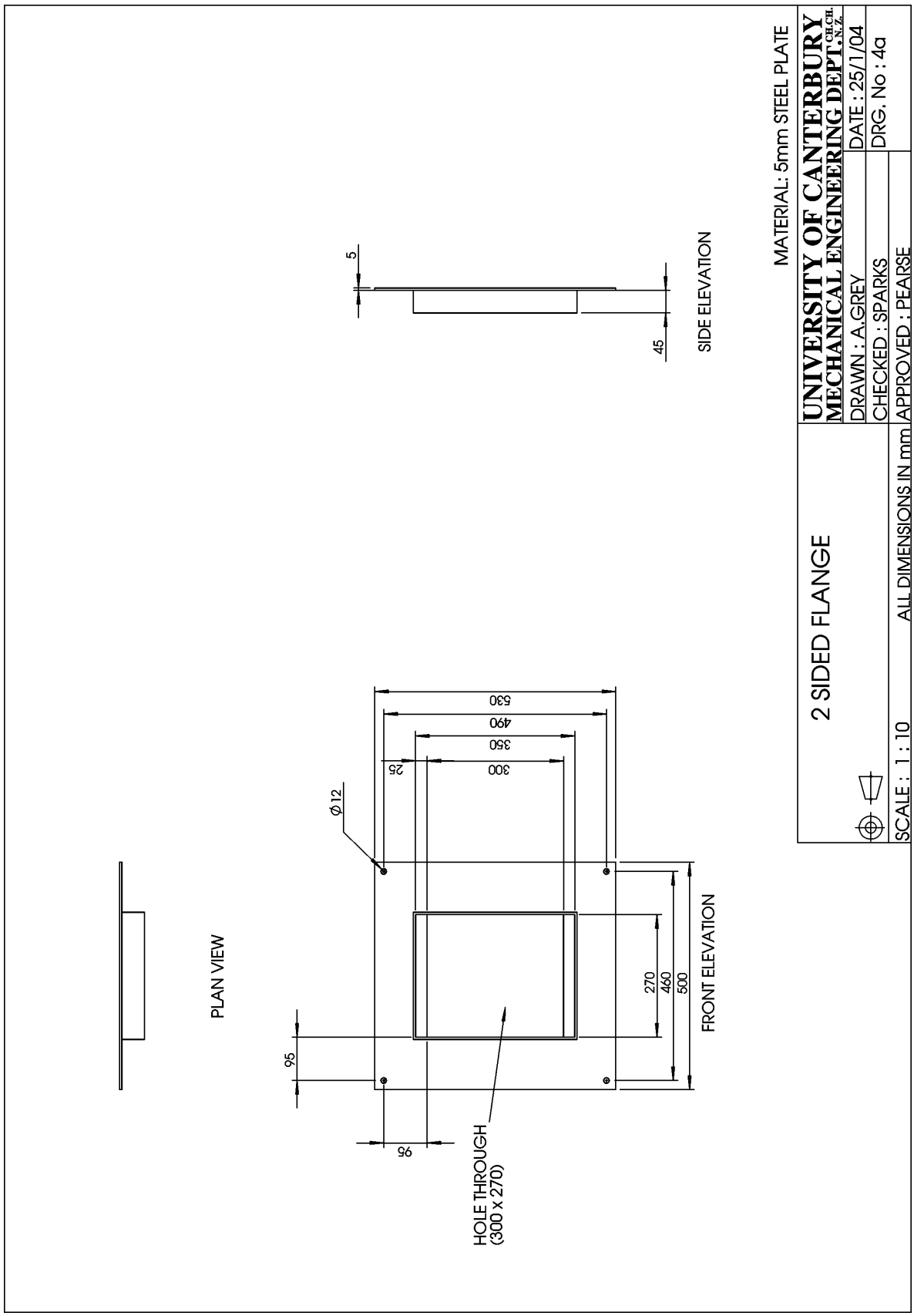
MATERIAL: 5mm STEEL PLATE
UNIVERSITY OF CANTERBURY
MECHANICAL ENGINEERING DEPT. CHCH. N.Z.
2 SIDED FLANGE
DRAWN : A.GREY
DATE : 25/1/04
CHECKED : SPARKS
DRG. No : 4a
SCALE : 1 : 10
ALL DIMENSIONS IN mm
APPROVED : PEARSE
SIDE ELEVATION
5
45
PLAN VIEW
FRONT ELEVATION
530
490
350
300
25
Ø12
270
460
500
95
95
HOLE THROUGH
(300 x 270)

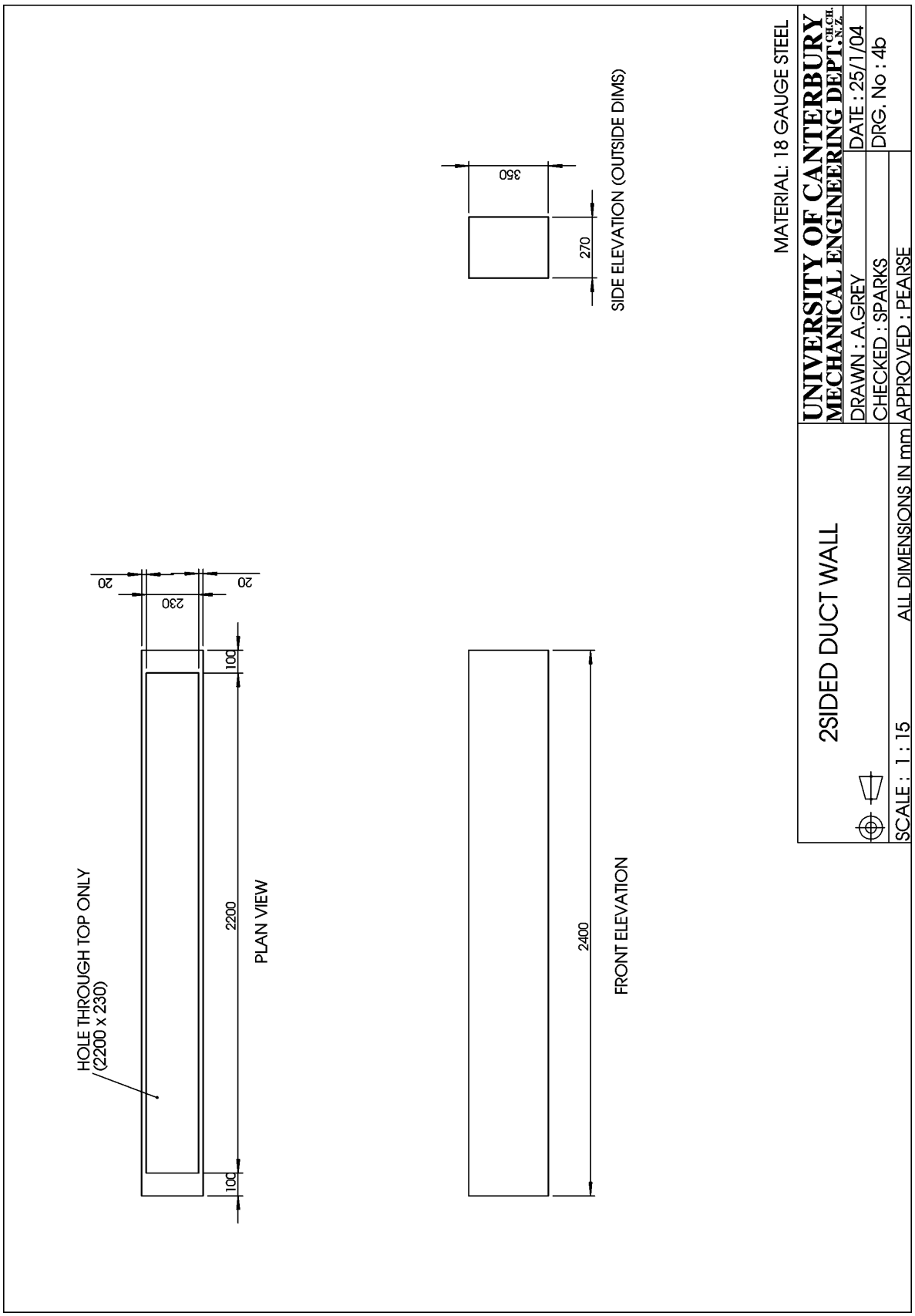
MATERIAL: 18 GAUGE STEEL
UNIVERSITY OF CANTERBURY
MECHANICAL ENGINEERING DEPT. CHCH. N.Z.
2SIDED DUCT WALL
DRAWN : A.GREY
DATE : 25/1/04
CHECKED : SPARKS
DRG. No : 4b
SCALE : 1 : 15
ALL DIMENSIONS IN mm
APPROVED : PEARSE
SIDE ELEVATION (OUTSIDE DIMS)
350
270
FRONT ELEVATION
2400
PLAN VIEW
20
230
20
100
2200
100
HOLE THROUGH TOP ONLY
(2200 x 230)

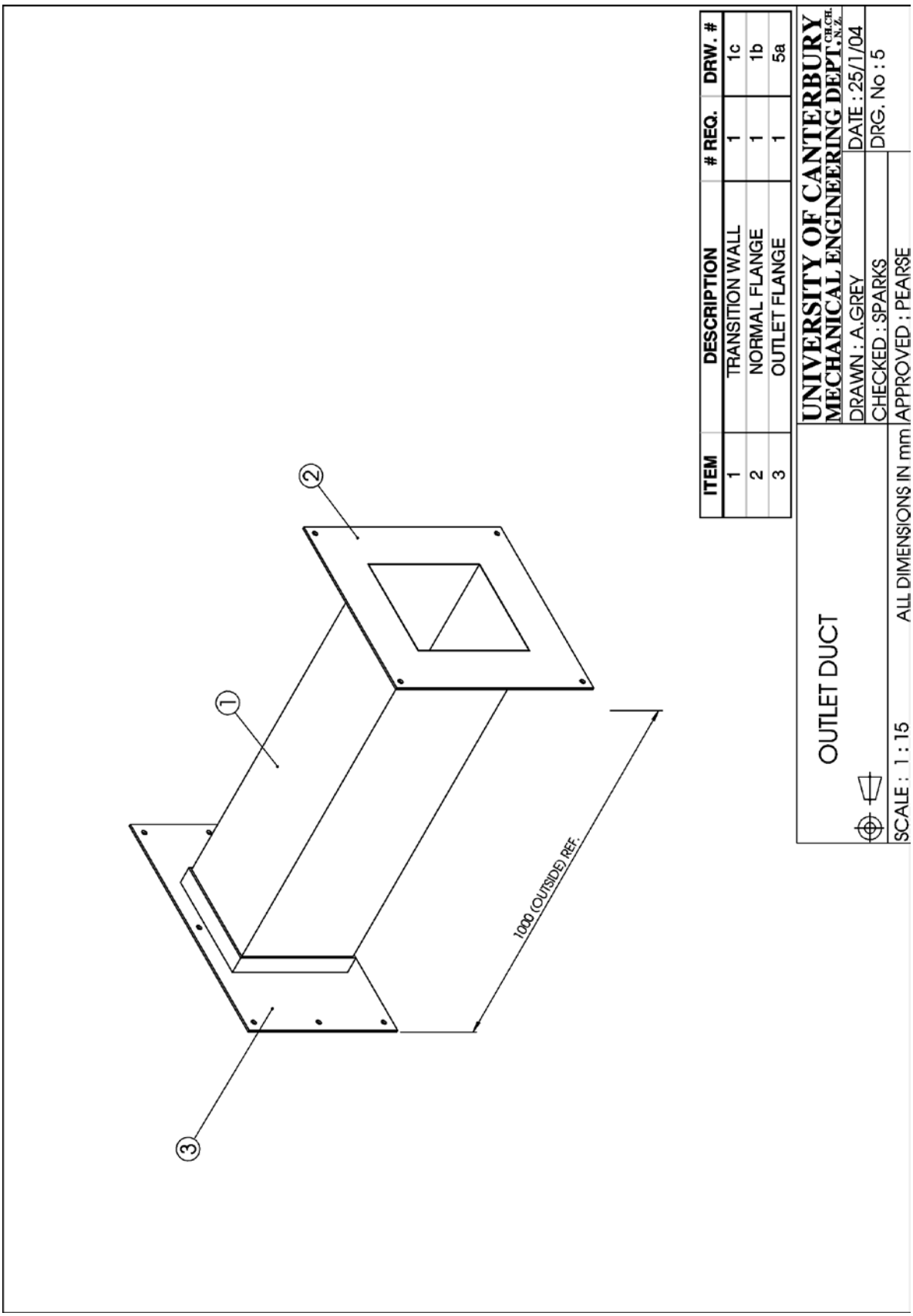
ITEM
DESCRIPTION
REQ.
DRW. #
1
TRANSITION WALL
1
1c
2
NORMAL FLANGE
1
1b
3
OUTLET FLANGE
1
5a
UNIVERSITY OF CANTERBURY
MECHANICAL ENGINEERING DEPT. CHCH. N.Z.
OUTLET DUCT
DRAWN : A.GREY
DATE : 25/1/04
CHECKED : SPARKS
DRG. No : 5
SCALE : 1 : 15
ALL DIMENSIONS IN mm
APPROVED : PEARSE
1000 (OUTSIDE) REF.
1
2
3

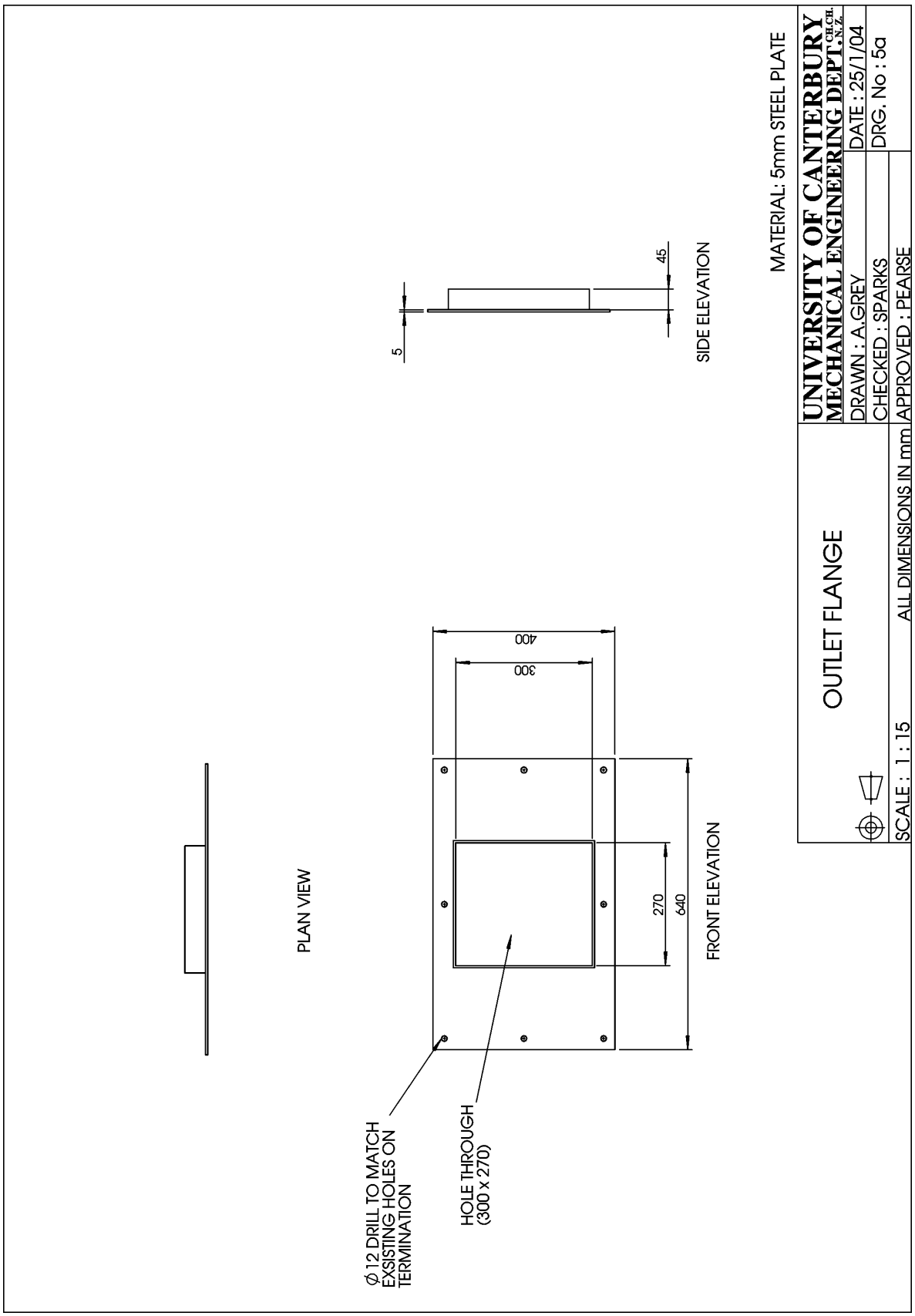
MATERIAL: 5mm STEEL PLATE
UNIVERSITY OF CANTERBURY
MECHANICAL ENGINEERING DEPT. CHRISTCHURCH, N.Z.
OUTLET FLANGE
DRAWN : A.GREY
DATE : 25/1/04
CHECKED : SPARKS
DRG. No : 5a
SCALE : 1 : 15
ALL DIMENSIONS IN mm
APPROVED : PEARSE
SIDE ELEVATION
45
5
PLAN VIEW
FRONT ELEVATION
400
300
270
640
Ø 12 DRILL TO MATCH EXSISTING HOLES ON TERMINATION
HOLE THROUGH (300 x 270)

A4

APPENDIX 4 – NOISE FIELD UNIFORMITY

A.4.1 SUMMARY

The sound field in the substitution duct for both duct sizes was tested to ensure that there was no significant variations in the noise field before the duct silencers were employed. Figure 2.9 and 2.10 (Chapter 2) show the measurement points at reference plane 2. The maximum range at a given frequency with the substitution duct in place was 1.8 dB for the 540 x 300 mm duct and 1.6 dB for the 270 x 300 mm duct.

All values are given in dB for two averaged 10-second measurements.

A.4.2 540 mm x 300 mm DUCT

100 Hz

85.8		86.1
	86.0	
85.1		85.5

Range: 1.0 dB

125 Hz

102.2		102.9
	102.7	
102.4		102.9

Range: 0.7 dB

160 Hz

102.2		102.3
	102.7	
102.3		102.1

Range: 0.6 dB

200 Hz

94.1		93.9
	93.9	
93.7		93.9

Range: 0.4 dB

250 Hz

95.1		94.8
	94.7	
95.0		94.5

Range: 0.6 dB

315 Hz

89.2		89.4
	89.3	
89.3		89.0

Range: 0.4 dB

400 Hz

84.1		83.5
	83.2	
84.2		84.4

Range: 1.2 dB

500 Hz

84.4		83.2
	83.2	
84.4		82.7

Range: 1.7 dB

630 Hz

85.1		85.0
	83.8	
84.5		85.2

Range: 1.4 dB

800 Hz

85.9		85.7
	85.5	
84.8		86.5

Range: 1.7 dB

1000 Hz

82.8		81.9
	83.2	
82.1		81.4

Range: 1.8 dB

1250 Hz

88.0		88.0
	88.4	
87.0		88.3

Range: 1.4 dB

1600 Hz

86.9		85.8
	86.9	
87.2		87.5

Range: 1.7 dB

2000 Hz

86.4		86.2
	86.0	
85.9		85.1

Range: 1.3 dB

2500 Hz

86.9		85.1
	86.1	
85.8		85.9

Range: 1.8 dB

3150 Hz

81.8		80.2
	81.2	
80.2		81.6

Range: 1.6 dB

4000 Hz

73.5		73.2
	74.8	
73.8		74.5

Range: 1.6 dB

5000 Hz

74.4		76.1
	75.7	
74.4		74.7

Range: 1.7 dB

6300 Hz

74.2		74.1
	74.8	
74.5		73.7

Range: 1.1 dB

8000 Hz

66.2		66.9
	66.6	
66.0		65.8

Range: 1.1 dB

A.4.3 270 mm x 300 mm DUCT

100 Hz

90.6	90.65
90.75	90.35

Range: 04 dB

125 Hz

105.7	106.15
106.6	106.65

Range: 0.95 dB

160 Hz

98.6	100.05
98.7	98.55

Range: 1.5 dB

200 Hz

93.9	94.25
94.05	93.85

Range: 0.4 dB

250 Hz

96.8	96.6
96.75	96.75

Range: 0.2 dB

315 Hz

90.4	89.65
90.1	90.05

Range: 0.75 dB

400 Hz

86.6	86.7
87.15	86.85

Range: 0.55 dB

500 Hz

87.5	87.75
87.9	87.85

Range: 0.4 dB

630 Hz

90	91.15
90.75	90.5

Range: 1.15 dB

800 Hz

89.9	91.35
89.95	91.45

Range: 1.55 dB

1000 Hz

86.1	86.55
85.95	86.1

Range: 0.6 dB

1250 Hz

89.6	90.6
90.45	89.8

Range: 1.0 dB

1600 Hz

90.1	90
90.85	89.45

Range: 1.4 dB

2000 Hz

89.4	90.4
90.4	88.8

Range: 1.6 dB

2500 Hz

89.8	89.2
88.85	89.5

Range: 0.95 dB

3150 Hz

82.9	82.7
82.65	82.9

Range: 0.25 dB

4000 Hz

74.4	75.8
75.85	74.8

Range: 1.45 dB

5000 Hz

77.6	78.7
78	78.1

Range: 1.1 dB

6300 Hz

77.1	76.85
76.85	76.85

Range: 0.25 dB

8000 Hz

65	65.6
65.3	64.15

Range: 1.45 dB

A5

APPENDIX 5 – PRC CURVE FITTING

A.5.1 SUMMARY

In assessing the effectiveness of the anechoic termination, the SPL was measured along the test duct. The variation in SPL down the ducting had two components superimposed; the standing wave pattern and the insertion loss due to the substitution duct. The recorded data points for each 1/3 octave band were fitted to Equation 2.8.

The ‘Termination Solver’ was a MATLAB script, which fitted the obtained data points to Equation 2.8 yielding the unknown coefficients. These coefficients gave the amplitude of the standing wave and the insertion loss per metre of the test / substitution duct section.

A.5.2 TERMINATION SOLVER

MATLAB CODE: terminationsolver.m

```
%   Script file: terminationsolver.m
%
%   Objective: Fit  A*sin(B*x + C) + D*x + E
%              To given x and y data points

% Input Data
x=0:0.05:1.95;
y=[112.3 112.8 112.2 113.4 113 112.3 112.3 112.2 111.8 111.4 111 110.8
110.2 109.5 108.8 108.1 107.2 106.1 105 104.3 103.6 103.7 104.1 104.5
105.3 106.4 106.8 108.1 108.9 109.4 109.4 111 111.3 111.3 111.6 111.5
111.6 111.9 110.6 109.2]; %Example data

% Call inputEQ.m given the initial guess values of [1 1 1 1 1]
bestcoeffs = fminsearch('inputEQ',[1 1 1 1 1],[],x,y);

% Repeat solver with previous solution (interations)
while i < 5
   bestcoeffs = fminsearch('inputEQ',[bestcoeffs(1) bestcoeffs(2)
bestcoeffs(3) bestcoeffs(4) bestcoeffs(5)],[],x,y);
   i = i + 1;
end

% Output equation coefficents
fprintf('%2.2f*sin(%2.2f*x + %2.2f) - (%2.2f*x) + %2.2f\n',bestcoeffs(1),
bestcoeffs(2), bestcoeffs(3), bestcoeffs(4), bestcoeffs(5))

% Now compare orginal data with equation solution and plot results
yfit = bestcoeffs(1) *  sin(bestcoeffs(2) .* x + bestcoeffs(3)) -
bestcoeffs(4) .* x + bestcoeffs(5);
plot(x,y,'ro',x,yfit); grid on;
title('\bfCurve Fitted Data')
xlabel('Distance (m)')
ylabel('Sound Pressure Level (dB)')
axis([0 2 100 120])
```

```
disp(' ')
PRC = (10^((2 * bestcoeffs(1))/20)-1) / (10^((2 * bestcoeffs(1))/20)+1);
fprintf('The PRC is: %2.2f\n',PRC)
```

MATLAB CODE: inputEQ.m

```
function out=inputEQ(coeff,X,Y)

% Define the variables
 a = coeff(1);
 b = coeff(2);
 c = coeff(3);
 d = coeff(4);
 e = coeff(5);

% Define the function
 Y_fun = (a *  sin((b .* X) + c)) - (d .* X) + e;

% Output to terminationsolver.m the R^2 values
 DIFF = Y_fun - Y;
 SQ_DIFF = DIFF.^2;
 out = sum(SQ_DIFF);
```

A6

APPENDIX 6 – BAR-SILENCER PROFILES

A.6.1 PROFILES

Circle Bar-Silencer

Cross sectional area: 27,000 mm^2

Perimeter: 0.58 m

OAR (large duct): 0.83

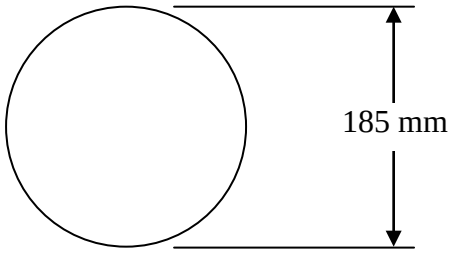

Isosceles Triangle Bar-Silencer

Cross sectional area: 27,000 mm^2

Perimeter: 0.83 m

OAR (large duct): 0.83

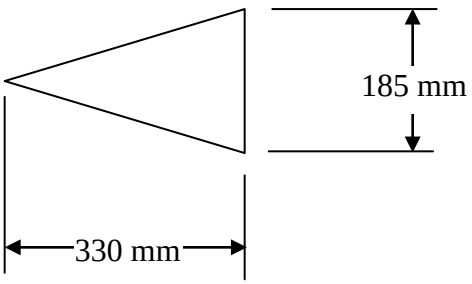

Square Bar-Silencer

Cross sectional area: 27,000 mm^2

Perimeter: 0.66 m

OAR (large duct): 0.83

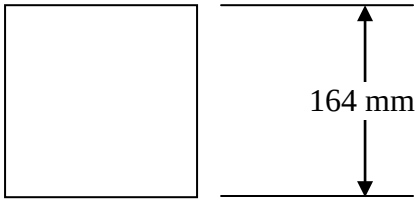

Wedge Bar-Silencers

Cross sectional area: 27,000 mm^2

Perimeter: 1.08 m

OAR (large duct): 0.83

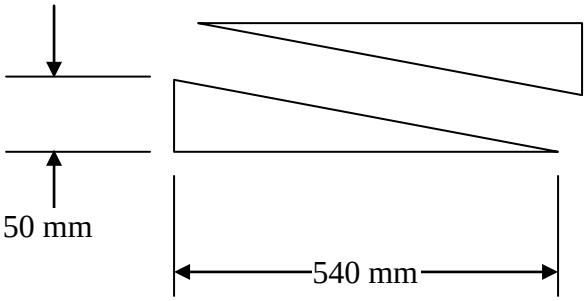

Small Equilateral Triangle Bar-Silencer

Cross sectional area: 13,500 mm^2

Perimeter: 0.51 m

OAR (large duct): 0.92

(small duct): 0.83

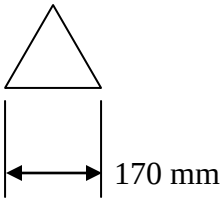

Medium Equilateral Triangle Bar-Silencer

Cross sectional area: 20,250 mm^2

Perimeter: 0.65 m

OAR (large duct): 0.875

(small duct): 0.75

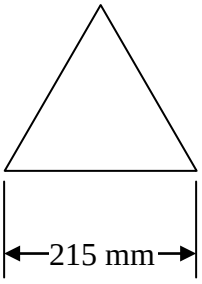

Large Equilateral Triangle Bar-Silencer

Cross sectional area: 27,000 mm^2

Perimeter: 0.81 m

OAR (large duct): 0.83

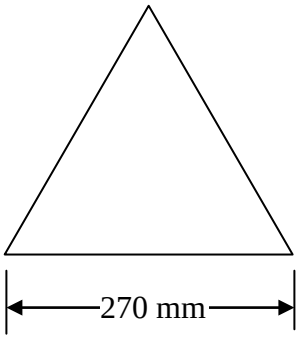

Scaled Equilateral Triangle Bar-Silencer

Cross sectional area: 13,500 mm^2

Perimeter: 0.59 m

OAR (Small duct): 0.83

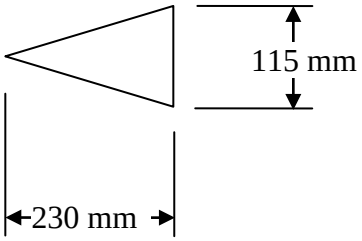

Tiny Equilateral Triangle Bar-Silencer

Cross sectional area: 10,125 mm^2

Perimeter: 0.43 m

OAR (small duct): 0.75

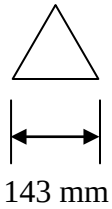

A7

APPENDIX 7 – FACILITY VERIFICATION

A.7.1 SABINE PREDICTION

Sabines method of predicting the attenuation due to linings in a duct, are based on the perimeter of lined section, cross-sectional area and the random incident sound absorption properties of the material.

$$\text{Attenuation} = 1.05\frac{P}{A}\alpha^{1.4} \qquad \text{(A1)}$$

a. Perimeter of Lined Section $P = 1.08$ m

b. Free Cross Section Area $A = 0.16$ m^2

TABLE A.1: SABINE PREDICTED ATTENUATION BASED ON THE ABSORPTION COEFFICIENTS

	1/1 Octave Band Centre Frequency					
	125	250	500	1000	2000	4000
Absorption Coefficient (α)	0.06	0.23	0.61	0.88	0.95	0.9
Attenuation (dB)	0.33	2.15	8.41	14.05	15.64	14.50

A.7.2 WASSILIEFF PREDICTION

Wassilieff prediction scheme utilizes design curves showing the characteristic attenuation of the fundamental mode for any particular frequency.

$$\text{Attenuation} = \frac{1}{2}(C_a \times \frac{l}{d_a}) + \frac{1}{2}(C_b \times \frac{l}{d_b}) + H \qquad \text{(A2)}$$

For any particular frequency from the design curve shown in Figure A7.1, the characteristic attenuation is inputted into Equation A2. Yielding the attenuation at that frequency.

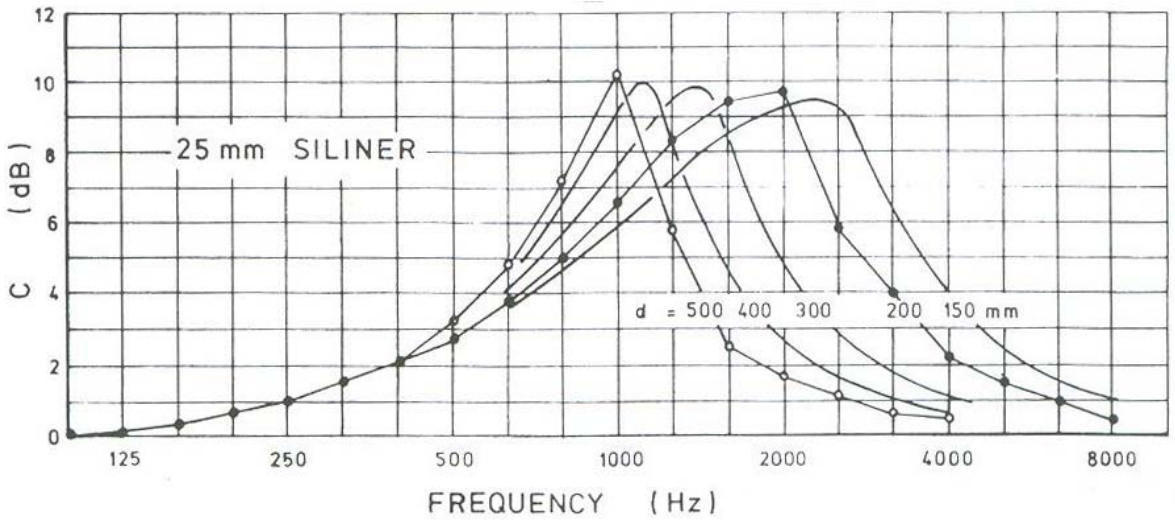

FIGURE A7.1: CHARACTERISTIC ATTENUATION OF THE FUNDAMENTAL MODE (C) VS FREQUENCY OF SQUARE SECTION DUCTS OF AIRWAY WIDTHS D INTERNALLY LINED WITH 25 MM THICK SILINER-MAT FACED

A.7.3 VÉR PREDICTION

Vérs paper (1978) on a review of the attenuation of sound in rectangular duct work recommended a semi-empirical method based on the figure below:

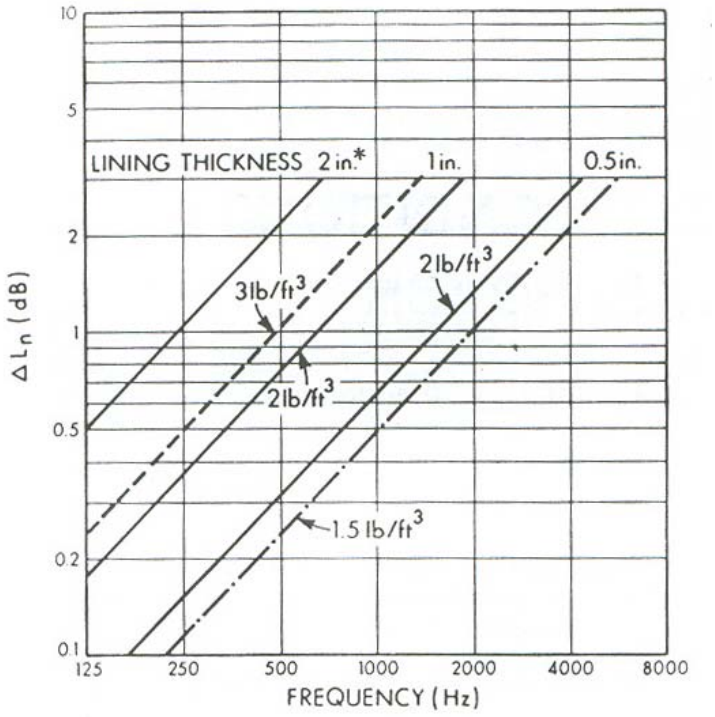

FIGURE A7.2: DESIGN GUIDE CURVES DEPENDANT ON LINING THICKNESS AND DENSITY

The procedure follows the 5 steps outlined in his paper.

Step 1. Collection of Pertinent Information

c.	Length of Lined Section	l = 2.4 m	= 7.87 ft
d.	Lined Perimeter of the Free Cross Section	P = 1.08 m	= 3.54 ft
e.	Free Cross Section Area	A = 0.16 m^2	= 1.74 ft^2
f.	Smallest Free Cross Dimension	2h = 0.3 m	= 0.98 ft
g.	Lining Thickness	d = 0.025 m	= 1 in
h.	Density of Lining Material	ρ_L = 44.8 kg m^{-3}	= 2.8 lb ft^{-3}

Step 2. Auxiliary Parameters

a. $f_u = \dfrac{1130(ft/\sec)}{2h(ft)}$ f_u = 1150 Hz

$2f_u$ = 2300 Hz

b. $\left(\dfrac{P}{A}\right)l$ = 16

Step 3.Creation of Unflanked, No-flow Attenuation ΔL'

a. Selected the low-frequency attenuation-vs-frequency curve in Figure A7.2. For this case it was 1in thick lining with a density of 2.8lb ft^{-3}.

b. This same curve was copied to a double logarithmic paper as in Figure A7.3.

c. Point 'A' is described by, $f = f_u$ and ΔL_n = 3 dB. Point 'B' is described by $f = 2f_u$ and ΔL_n = 0.75 dB. A line is drawn between the two points.

d. The two lines are shifted upwards vertically by the factor $(P/A)l$ as described in step 1.

e. 5 dB is added to all frequencies at and above $2f_u$ to account approximately for entrance losses due to the presence of higher order modes in the incident sound wave.

Parts a – e are indicated on Figure A7.3 in parentheses ( ).

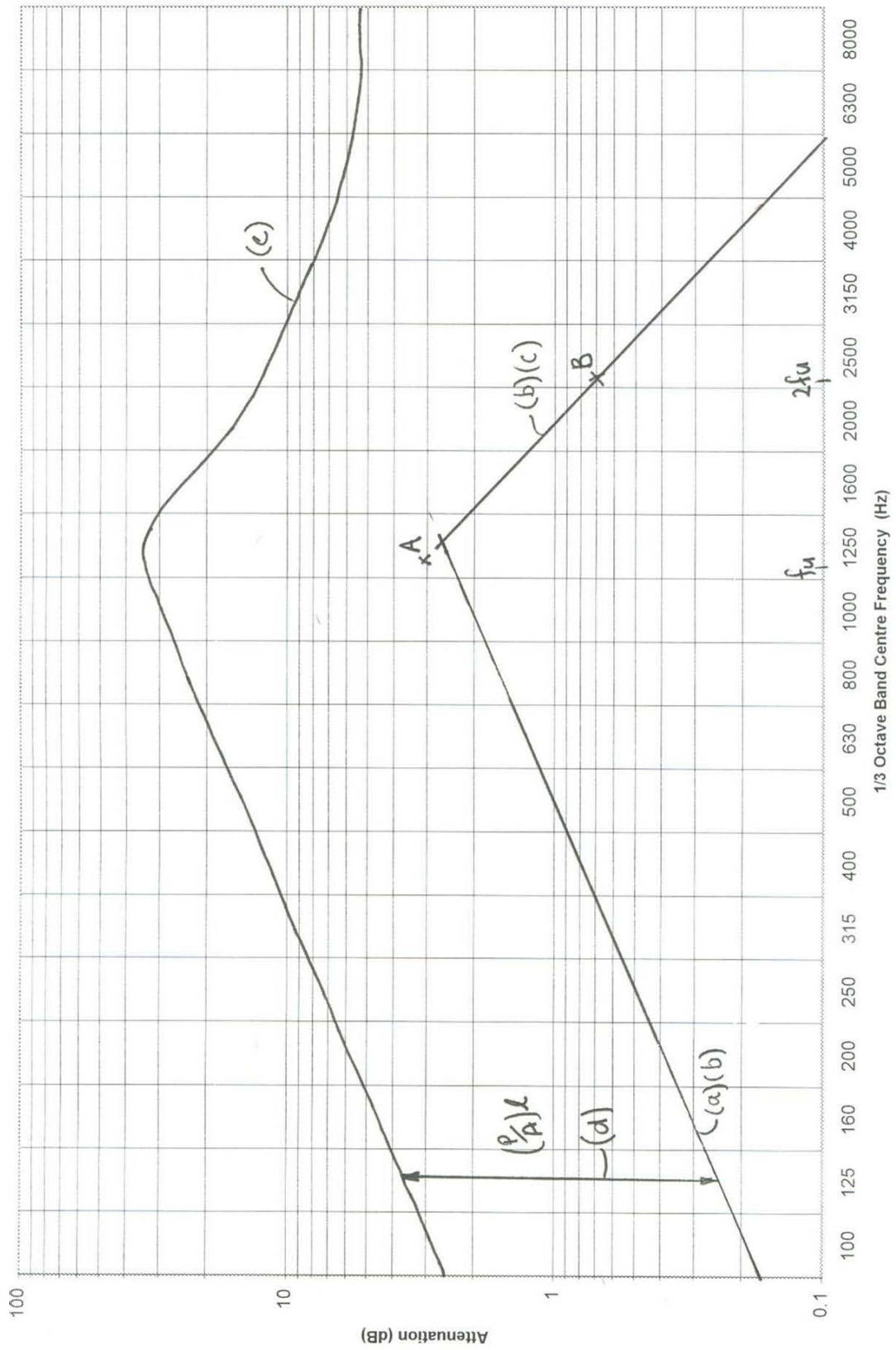

FIGURE A7.3: VER PREDICTED ATTENUATION DUE SILINER LINING

Step 4. Correction for Flow

There is no flow correction as there is no flow.

Step 5. Correction for Flanking

As the resulting attenuation-vs-frequency curve obtained from step 4 did not exceed 40 dB at an frequency range, there is no correction required.

A8

APPENDIX 8 – INSERTION LOSS DATA

A.8.1 SUMMARY

The insertion loss data present was obtained using the test facility described in Chapter 2. The data was recorded in $^{1}/_{3}$ octave band centre frequencies in dB over a 2.4 m test section, unless otherwise stated.

A.8.2 INSERTION LOSS DATA (540 mm x 300 mm DUCT)

1/3 Octave Band Centre Frequency	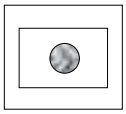	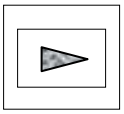	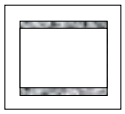
100	1.2	1.7	4.5
125	1.7	1.7	4.3
160	1.9	1.9	3.0
200	2.2	2.1	3.8
250	3.5	3.6	7.8
315	4.8	5.6	7.0
400	8.4	9.0	8.2
500	13.1	13.1	10.7
630	21.7	22.1	18.3
800	23.8	25.3	22.5
1000	20.7	23.0	29.6
1250	19.5	20.9	40.0
1600	16.9	20.0	43.8
2000	12.9	17.1	28.7
2500	13.7	16.5	15.8
3150	13.7	17.4	11.9
4000	13.2	17.1	8.3
5000	11.8	16.2	6.0
6300	10.2	11.1	5.6
8000	10.8	12.5	4.9
Area (mm^2)	27,000	27,000	27,000
Length (m)	2.4	2.4	2.4
Material	Melamine	Melamine	Fibreglass

1/3 Octave Band Centre Frequency	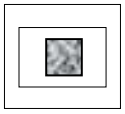	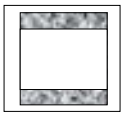	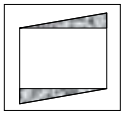
100	0.8	1.1	1.3
125	1.4	1.8	1.4
160	1.2	2.4	0.7
200	1.9	4.5	1.0
250	3.4	8.4	2.2
315	5.3	12.8	4.6
400	8.0	18.9	6.7
500	12.2	29.1	9.8
630	22.2	40.8	20.4
800	22.2	40.9	21.7
1000	21.5	38.9	26.0
1250	19.6	38.3	28.8
1600	16.3	30.2	31.8
2000	11.7	19.7	28.3
2500	12.4	13.6	19.3
3150	12.3	11.8	16.6
4000	13.3	10.5	12.4
5000	12.5	9.9	10.4
6300	10.2	9.5	9.9
8000	9.6	8.3	8.3
Area (mm^2)	27,000	54,000	27,000
Length (m)	2.4	2.4	2.4
Material	Melamine	Melamine	Melamine

1/3 Octave Band Centre Frequency	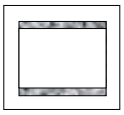	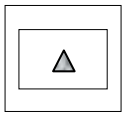	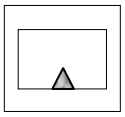
100	0.1	1.4	0.8
125	1.4	0.6	0.3
160	1.2	1.1	0.7
200	2.1	1.6	1
250	2.9	2.1	1.5
315	5.5	2.4	2.3
400	6.5	4.8	5.2
500	6.1	5	6.4
630	15.4	14.2	15.3
800	15.3	14.74	12.5
1000	21.8	13.4	8.7
1250	34.7	15.6	10.6
1600	40.6	13.7	10.1
2000	27.4	10.1	7.5
2500	16.2	10.6	7.5
3150	12.5	10.5	6.7
4000	10	9.9	7.2
5000	9.4	9.6	6.8
6300	9.2	8.3	6.1
8000	8.4	8.7	5.7
Area (mm^2)	27,000	13,500	13,500
Length (m)	2.4	2.4	2.4
Material	Melamine	Melamine	Melamine

1/3 Octave Band Centre Frequency	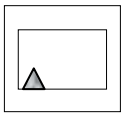	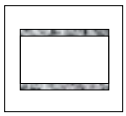	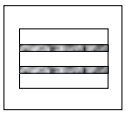
100	0.9	1.9	2.6
125	0	2.1	3.1
160	0.4	2.4	2.9
200	0.9	3	3.2
250	1.2	3.4	4.1
315	2.7	6.8	6.5
400	6.1	7.3	7.6
500	9.6	6.8	6
630	14.8	16.5	14
800	8.7	17.5	13.8
1000	6.2	23.7	18.6
1250	9.3	34.1	28
1600	7.1	41.4	32.5
2000	6.1	39.2	38.9
2500	6	28	34.5
3150	5.8	19.2	30
4000	5.6	15	23.1
5000	5.2	11.2	22.3
6300	4.5	10.6	20.3
8000	4.9	8.8	17.5
Area (mm^2)	13,500	27,000	27,000
Length (m)	2.4	2.4	2.4
Material	Melamine	Melamine	Melamine

1/3 Octave Band Centre Frequency	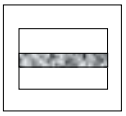	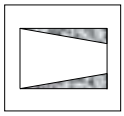	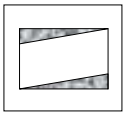
100	2.7	0.6	1.2
125	2.5	1.8	2.0
160	2.6	1.7	1.8
200	3.6	2.1	1.9
250	4	2.8	2.5
315	6.1	5.3	4.4
400	7	8.7	7.3
500	6.4	14.2	10.5
630	16.6	21.6	21.8
800	21.8	20.8	24.6
1000	32.8	24.4	27.8
1250	38.3	26.2	30.3
1600	35.6	29.1	34.7
2000	25.7	29.9	34.3
2500	16.5	23.2	26.1
3150	14.1	22.3	23.2
4000	13.2	15.2	15.4
5000	13.1	12.6	12.4
6300	13.7	12.8	13.0
8000	12.2	10.1	10.3
Area (mm^2)	27,000	27,000	27,000
Length (m)	2.4	2.4	2.4
Material	Melamine	Melamine	Melamine

1/3 Octave Band Centre Frequency	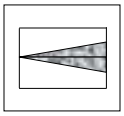		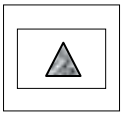
100	0.8	0.4	0.3
125	1.7	1.2	1.1
160	1.6	1.4	1.1
200	2.0	2.3	1.3
250	2.8	3.5	2.4
315	4.6	5.7	4.0
400	7.6	8.7	6.3
500	11.9	14.1	8.6
630	21.6	22.8	17.5
800	23.4	25.7	19.4
1000	25.4	21.6	17.3
1250	27.1	22.4	18.4
1600	25.2	18.7	15.7
2000	21.5	13.9	11.6
2500	19.0	13.1	11.5
3150	15.8	13.6	12.2
4000	13.6	12.8	11.7
5000	14.2	12.5	11.4
6300	13.0	11.6	9.9
8000	12.7	11.0	9.5
Area (mm^2)	27,000	27,000	20,250
Length (m)	2.4	2.4	2.4
Material	Melamine	Melamine	Melamine

1/3 Octave Band Centre Frequency	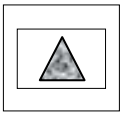	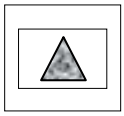	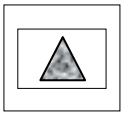
100	0.3	-0.5	0.2
125	0.3	0.5	1.2
160	0.6	0.5	0.9
200	0.8	1.0	1.7
250	0.9	1.6	2.5
315	1.4	2.7	4.2
400	2.4	4.9	7.2
500	3.6	7.6	11.1
630	6.3	13.2	18.8
800	5.7	14.7	20.1
1000	4.7	10.6	16.7
1250	8.1	13.6	17.7
1600	7.0	10.4	14.0
2000	6.6	9.6	10.5
2500	4.7	8.3	9.7
3150	6.0	9.9	11.5
4000	5.3	8.7	11.4
5000	4.9	8.3	10.4
6300	5.1	7.3	9.6
8000	4.1	6.5	9.6
Area (mm^2)	27,000	27,000	27,000
Length (m)	0.6	1.2	1.8
Material	Melamine	Melamine	Melamine

1/3 Octave Band Centre Frequency	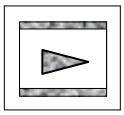	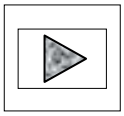	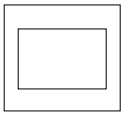
100	1.6	0.4	4.8
125	3.5	1.2	3.1
160	3.5	1.5	2.9
200	5.0	2.6	2.0
250	6.6	3.7	1.4
315	12.6	5.5	1.0
400	16.8	9.0	0.5
500	19.6	14.1	0.5
630	26.8	23.0	1.0
800	31.3	25.1	1.2
1000	36.2	21.9	0.4
1250	42.9	22.1	0.8
1600	48.5	18.2	0.9
2000	47.7	13.6	0.8
2500	39.4	12.9	0.9
3150	34.9	13.8	0.5
4000	31.8	13.0	0.4
5000	29.8	12.6	0.3
6300	28.5	11.9	0.5
8000	28.8	11.3	0.2
Area (mm^2)	54,000	27,000	n/a
Length (m)	2.4	2.4	2.4
Material	Melamine	Melamine	n/a

1/3 Octave Band Centre Frequency	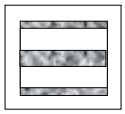	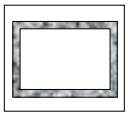	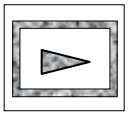
100	2.6	0.0	0.1
125	4.6	0.8	1.9
160	4.3	1.2	2.5
200	5.1	2.5	4.3
250	10.8	5.7	9.3
315	11.3	9.9	14.9
400	12.5	14.7	22.6
500	14.0	16.2	25.2
630	21.9	26.4	34.4
800	23.1	30.2	38.9
1000	31.8	34.7	40.4
1250	41.3	39.9	41.9
1600	47.4	45.1	47.7
2000	46.4	32.3	48.0
2500	44.2	18.1	45.0
3150	48.1	16.7	42.8
4000	42.6	16.3	36.7
5000	39.1	17.0	36.8
6300	34.3	17.1	32.3
8000	25.9	16.7	22.0
Area (mm^2)	54,000	25 mm lining	27,000 25 mm lining
Length (m)	2.4	2.4	2.4
Material	Melamine	Melamine	Melamine

1/3 Octave Band Centre Frequency	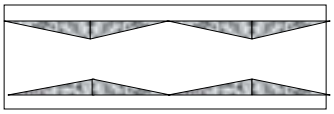	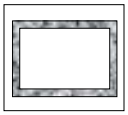	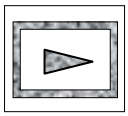
100	1.8	0.0	0.8
125	0.7	0.4	2.0
160	1.4	0.5	2.2
200	1.5	1.5	3.4
250	3.2	3.8	6.6
315	5.1	5.2	11.8
400	8.5	9.5	20.0
500	11.8	15.1	25.5
630	23.3	29.5	37.8
800	23.3	39.8	44.2
1000	29.5	43.0	46.3
1250	29.0	43.6	47.7
1600	19.6	46.5	49.6
2000	18.5	33.8	43.2
2500	13.8	19.6	41.1
3150	12.6	18.2	40.6
4000	13.3	17.8	36.2
5000	13.2	18.3	37.7
6300	12.1	18.6	34.0
8000	12.8	18.7	29.4
Area (mm^2)	54,000	25 mm lining	27,000 25 mm lining
Length (m)	2.4	2.4	2.4
Material	Melamine	Fibreglass	Fibreglass

A.8.2 INSERTION LOSS DATA (270 mm x 300 mm DUCT)

1/3 Octave Band Centre Frequency	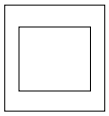		
100	3.2	2.0	0.5
125	2.5	2.3	1.4
160	2.1	2.3	0.6
200	2.6	3.9	1.6
250	2.9	5.4	2.4
315	1.8	7.6	3.5
400	1.4	12.9	5.6
500	1.0	17.5	7.7
630	0.4	28.8	13.2
800	0.5	34.1	19.4
1000	0.8	32.4	20.1
1250	0.8	32.3	22.9
1600	0.6	32.8	24.6
2000	0.7	30.0	23.9
2500	0.5	28.8	24.3
3150	0.4	24.1	21.3
4000	0.3	22.0	20.6
5000	0.1	21.6	22.7
6300	0.2	23.1	21.8
8000	0.1	21.2	17.1
Area (mm^2)	n/a	20,250	13,500
Length (m)	n/a	2.4	2.4
Material	n/a	Melamine	Melamine

1/3 Octave Band Centre Frequency	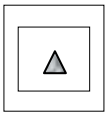	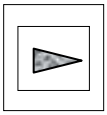	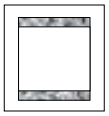
100	0.5	0.4	6.7
125	1.3	1.7	6.8
160	0.3	0.8	6.8
200	1.6	1.6	7.6
250	2.0	2.5	9.3
315	2.8	4.4	9.3
400	4.8	7.1	12.4
500	6.7	10.6	15.0
630	11.8	18.3	21.4
800	17.4	28.2	30.4
1000	18.1	26.5	39.0
1250	21.0	26.2	45.4
1600	22.8	25.9	44.4
2000	23.3	25.7	31.9
2500	22.4	22.2	26.3
3150	19.9	19.3	20.9
4000	19.2	19.4	18.8
5000	20.7	18.4	17.4
6300	20.1	18.7	19.0
8000	18.2	15.6	19.0
Area (mm^2)	10,125	13,500	25 mm lining
Length (m)	2.4	2.4	2.4
Material	Melamine	Melamine	Fibreglass

1/3 Octave Band Centre Frequency	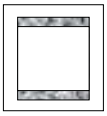	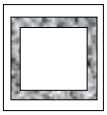	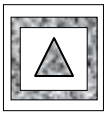
100	5.4	1.7	8.9
125	6.0	1.4	8.2
160	6.2	2.2	9.8
200	7.9	5.3	13.4
250	9.3	7.4	18.5
315	10.7	10.9	18.4
400	11.2	16.8	22.8
500	15.4	26.2	29.9
630	16.9	29.7	35.2
800	21.6	37.7	40.2
1000	29.3	40.8	37.7
1250	44.0	45.0	45.0
1600	42.4	46.4	49.6
2000	29.9	44.8	53.3
2500	25.1	35.4	56.3
3150	20.1	26.0	49.8
4000	19.6	24.1	47.0
5000	17.9	21.3	52.4
6300	19.7	21.0	53.7
8000	20.8	20.0	45.7
Area (mm^2)	25 mm lining	25 mm lining	10,125 25 mm lining
Length (m)	2.4	2.4	2.4
Material	Melamine	Melamine	Melamine

1/3 Octave Band Centre Frequency	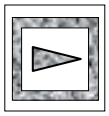	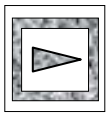	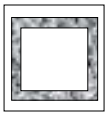
100	9.6	9.5	8.8
125	8.5	8.5	8.2
160	10.4	10.1	8.7
200	13.8	12.3	10.3
250	17.5	14.6	11.8
315	20.3	17.4	13.3
400	24.8	22.3	17.4
500	32.0	29.1	22.8
630	37.1	36.8	31.5
800	41.1	40.4	35.9
1000	44.2	44.0	41.3
1250	45.0	45.5	52.8
1600	49.0	49.9	56.9
2000	53.1	53.5	47.0
2500	55.9	56.8	44.0
3150	50.4	49.9	34.5
4000	46.8	46.9	32.4
5000	51.3	54.8	28.8
6300	51.5	52.3	30.0
8000	44.5	45.6	27.7
Area (mm^2)	13,500 25 mm lining	13,500 25 mm lining	25 mm lining
Length (m)	2.4	2.4	2.4
Material	Melamine	Fibreglass	Fibreglass

A9

APPENDIX 9 – PRESSURE LOSS DATA

A.9.1 SUMMARY

Two methods of investigating the pressure losses in the ducting were used. Firstly, experimentally measured static pressures were measured, at both the upstream and downstream reference planes by use of two water manometers. Secondly, by use of a computation fluid dynamic (CFD) package was used to predict the pressure drops in the ducting system due to blockages.

The pressure losses are presented in Pascals (Pa).

A.9.2 CFD SETUP

The physical shapes of the ducting and the 'bar absorbers' that would be running the length of the ducting were modelled in a CAD package (Solidworks 2001plus). These 3D models were imported into Gambit 2.0.1 where a mesh was applied to each of the 3D models. The computational fluid dynamics (CFD) package, Fluent 6.1, was used to solve the flows and for post-processing of the results.

Grid independence:

To ensure grid independence, grid-adaption was introduced through Fluent until a stable unchanging solution was found. By using solution-adaptive refinement, cells could be added where they were needed in the mesh, thus enabling the features of the flow field to be better resolved.

Convergence:

On a computer with infinite precision, the residuals will go to zero as the solution converges. On an actual computer, the residuals decay to some small value 'round-off' and then stop changing 'level out'. Once the residuals have levelled off the solution has been reached. All solutions were run until the residuals had converged.

Boundary Conditions and Fluid Flow:

The working fluid used was air at 20^{o} Celsius. The flow obtained a developed profile before reaching the test plane.

Inlet: In order to obtain the desired mean fluid velocity through the substitution duct, a constant volume flow rate was required. It was not necessary to use a mass flow inlet which requires more computational effort; instead a *'Velocity inlet'* boundary condition will fix the volume flow.

When the Mach number is less than 1.0, the flow is termed subsonic.

$$M \equiv \frac{u}{c} \tag{A9.1}$$

where *u* is the fluid velocity and c the speed of sound in gas. At Mach numbers much less than 1.0 (M << 0.1), compressibility effects are negligible and the variation of the gas density with pressure can safely be ignored in flow modelling. For all solutions, the flow has been assumed incompressible.

Outlet: An *'Outflow'* boundary condition has been used to model the flow exit as the details of the flow velocity and pressure at exit are not known prior to solution of the flow problem. The CFD package Fluent extrapolates the required information from the interior to find a solution.

Walls: A no-slip velocity specification was used for all solid surfaces. That is, the fluid velocity is zero everywhere on the boundaries except at the inlet and outlet. A log law ('*Law of the wall'*) relationship was used for all wall regions, this is useful to use when the grid is to coarse to calculate the laminar sub-layer on boundary walls.

Turbulence model:

The standard **k-ω** turbulence model was used in the evaluation of the ducting sections and corresponding bar-absorbers. It is an empirical model based on model transport equations for the turbulence kinetic energy (***k***) and the specific dissipation rate (**ω**).

Solver:

Second order upwind schemes were used for the momentum, turbulence kinetic energy and turbulence dissipation rate calculations. A steady state, SIMPLE algorithm was employed as the solver for the models with default settings for the relaxation factors. Single precision solvers were deemed to be sufficiently accurate.

A.9.3 MEASURED PRESSURE LOSSES (540 x 300 mm DUCT)

Average Mean Flow Velocity m/s	**Volume Flow Rate** m^3/s	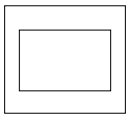	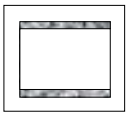	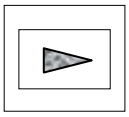
0	0	0.0	0.0	0.0
5	0.81	1.6	2.2	20.9
10	1.62	3.2	4.3	67.6
15	2.43	5.2	7.1	127.5
20	3.24	7.4	10.3	216.8
25	4.05	9.8	13.8	318.8
Volume (mm^2)		0	27,000	27,000
Length (m)		2.4	2.4	2.4
Material		n/a	Melamine	Melamine

Average Mean Flow Velocity m/s	**Volume Flow Rate** m^3/s	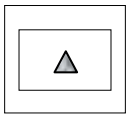	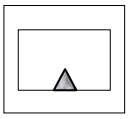	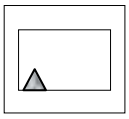
0	0	0.0	0.0	0.0
5	0.81	5.9	6.9	5.8
10	1.62	19.6	17.9	15.4
15	2.43	34.3	32.4	27.7
20	3.24	54.0	47.1	42.2
25	4.05	73.6	66.7	58.9
Volume (mm^2)		13,500	13,500	13,500
Length (m)		2.4	2.4	2.4
Material		Melamine	Melamine	Melamine

Average Mean Flow Velocity m/s	**Volume Flow Rate** m^3/s	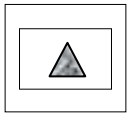	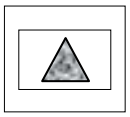
0	0	0.0	0.0
5	0.81	12.8	20.9
10	1.62	34.3	67.6
15	2.43	71.6	127.5
20	3.24	119.7	216.8
25	4.05	176.6	318.8
Volume (mm^2)		20,250	27,000
Length (m)		2.4 m	2.4 m
Material		Melamine	Melamine

A.9.4 CFD PREDICTED PRESSURE LOSSES (540 x 300 DUCT)

Average Mean Flow Velocity m/s	**Volume Flow Rate** m^3/s	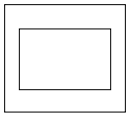	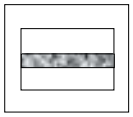	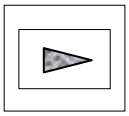
0	0	0.0	0.0	0.0
4	0.65	1.2	18.8	11.9
8	1.3	4.5	64.8	44.9
15	2.43	15.2	221.2	151.5
18	2.92	21.7	318.8	217.2
21	3.4	29.3	431.5	292.7
Volume (mm^2)		0	27,000	27,000
Length (m)		2.4	2.4	2.4
Material		n/a	n/a	n/a

Average Mean Flow Velocity m/s	**Volume Flow Rate** m^3/s	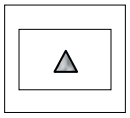	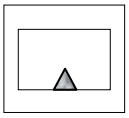	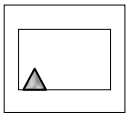
0	0	0.0	0.0	0.0
4	0.65	3.7	2.9	3.0
8	1.3	11.0	11.0	10.3
15	2.43	37.9	37.4	35.2
18	2.92	54.7	53.8	50.5
21	3.4	74.0	72.6	68.1
Volume (mm^2)		13,500	13,500	13,500
Length (m)		2.4	2.4	2.4
Material		n/a	n/a	n/a

Average Mean Flow Velocity m/s	**Volume Flow Rate** m^3/s	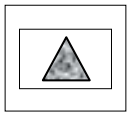	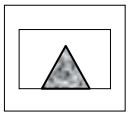	
0	0	0.0	0.0	0.0
4	0.65	5.8	6.4	5.3
8	1.3	22.4	19.9	20.1
15	2.43	77.2	68.9	68.6
18	2.92	112.2	99.4	98.6
21	3.4	150.4	134.6	132.9
Volume (mm^2)		27,000	27,000	27,000
Length (m)		2.4	2.4	2.4
Material		n/a	n/a	n/a

Average Mean Flow Velocity m/s	**Volume Flow Rate** m^3/s	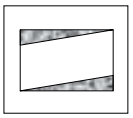	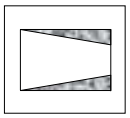
0	0	0.0	0.0
4	0.65	5.9	4.9
8	1.3	22.7	18.9
15	2.43	62.2	64.8
18	2.92	89.5	93.3
21	3.4	120.9	126.0
Volume (mm^2)		27,000	27,000
Length (m)		2.4	2.4
Material		n/a	n/a